INFORMATION TO USERS

This material was produced from a microfilm copy of the original document. While the most advanced technological means to photograph and reproduce this document have been used, the quality is heavily dependent upon the quality of the original submitted.

The following explanation of techniques is provided to help you understand markings or patterns which may appear on this reproduction.

1. The sign or "target" for pages apparently lacking from the document photographed is "Missing Page(s)". If it was possible to obtain the missing page(s) or section, they are spliced into the film along with adjacent pages. This may have necessitated cutting thru an image and duplicating adjacent pages to insure you complete continuity.

2. When an image on the film is obliterated with a large round black mark, it is an indication that the photographer suspected that the copy may have moved during exposure and thus cause a blurred image. You will find a good image of the page in the adjacent frame.

3. When a map, drawing or chart, etc., was part of the material being photographed the photographer followed a definite method in "sectioning" the material. It is customary to begin photoing at the upper left hand corner of a large sheet and to continue photoing from left to right in equal sections with a small overlap. If necessary, sectioning is continued again — beginning below the first row and continuing on until complete.

4. The majority of users indicate that the textual content is of greatest value, however, a somewhat higher quality reproduction could be made from "photographs" if essential to the understanding of the dissertation. Silver prints of "photographs" may be ordered at additional charge by writing the Order Department, giving the catalog number, title, author and specific pages you wish reproduced.

5. PLEASE NOTE: Some pages may have indistinct print. Filmed as received.

76-16,240

SARGENT, Thomas Anthony, 1948-
  SURFACE PHOTOMETRY OF INTERACTING GALAXIES.

  The University of Arizona, Ph.D., 1976
  Physics, astronomy & astrophysics

SURFACE PHOTOMETRY OF INTERACTING GALAXIES

by

Thomas Anthony Sargent

A Dissertation Submitted to the Faculty of the

DEPARTMENT OF ASTRONOMY

In Partial Fulfillment of the Requirements
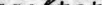For the Degree of

DOCTOR OF PHILOSOPHY

In the Graduate College

THE UNIVERSITY OF ARIZONA

1 9 7 6

THE UNIVERSITY OF ARIZONA

GRADUATE COLLEGE

I hereby recommend that this dissertation prepared under my

direction by ___Thomas Anthony Sargent_____

entitled ___Surface Photometry of Interacting Galaxies_____

_____

be accepted as fulfilling the dissertation requirement of the

degree of ___Doctor of Philosophy_____

_W. G. Tifft_____   _1/26/76_____
Dissertation Director   Date

After inspection of the final copy of the dissertation, the

following members of the Final Examination Committee concur in

its approval and recommend its acceptance:*

_Harlan Gilbert_____   _1/26/-76_____
_W. G. Tifft_____   _1/26/76_____
_P. E. Williams_____   _26 January 1976_
_P. A. Strittmatter_____   _1/26/76_____

_____   _____

*This approval and acceptance is contingent on the candidate's
adequate performance and defense of this dissertation at the
final oral examination. The inclusion of this sheet bound into
the library copy of the dissertation is evidence of satisfactory
performance at the final examination.

STATEMENT BY AUTHOR

This dissertation has been submitted in partial fulfillment of requirements for an advanced degree at The University of Arizona and is depostited in the University Library to be made available to borrowers under rules of the Library.

Brief quotations from this dissertation are allowable without special permission, provided that accurate acknowledgment of source is made. Requests for permission for extended quotation from or reproduction of this manuscript in whole or in part may be granted by the head of the major department or the Dean of the Graduate College when in his judgment the proposed use of the material is in the interests of scholarship. In all other instances, however, permission must be obtained from the author.

SIGNED: _Thomas A. Sargent_

APPROVAL BY DISSERTATION DIRECTOR

This dissertation has been approved on the date shown below:

_____   _Feb 20, 1976_
W. G. TIFFT   Date
Professor of Astronomy

ACKNOWLEDGMENTS

TABLE OF CONTENTS

TABLE OF CONTENTS--<u>Continued</u>

LIST OF ILLUSTRATIONS--<u>Continued</u>

LIST OF ILLUSTRATIONS--<u>Continued</u>

LIST OF TABLES

ABSTRACT

The study of double galaxies may be said to have begun with Holmberg's work in 1937. Since then much evidence has been collected which indicates that normal double galaxies are gravitationally bound and are executing classical dynamical motion. A small fraction of double galaxies are seen to show very distorted morphology and are said to be "strongly interacting." Being rather faint these were very difficult to observe photometrically or spectrographically and their very intriguing appearance gave rise to much speculation about extraordinary phenomena as explanations of their origin. There is still a good case for the presence of non-classical phenomena in at least some double galaxies. About 1970 however, computer models representing interacting galaxies as simple gravitational interaction during a close approach of two galaxies proved to be remarkably successful at mimicking the appearance of many types of interacting galaxies.

Computer simulations performed here attempt to test the models a bit further by adding a true disk potential to the gravitational field and by studying the effects of the addition of varying degrees of velocity dispersion to the stellar component. This reveals the behavior of different dynamical components of the stellar population in a normal spiral galaxy. These experiments showed that true bridges (a "filament" of stars connecting two galaxies) are fairly sensitive to disruption and would have a much reduced density of stars later than F or G. Tails (projections extending away from the system) are more resistant to

disruption simply because they contain more mass than bridges. While the solar type (and later) stars in tails do diffuse over an area 2 or 3 times larger than the zero velocity dispersion population, the major features remain recognizable from most view points.

Analysis of velocity dispersions in formed filaments have shown that the interaction is best characterized as continuous distortion and smooth flow rather than a turbulent or mixing process. Stars which at the end of the simulation are close to each other in space are also close together in velocity space.

It is also shown that within the solar type population it is only those stars which have dispersive velocities which are more energetic than the mean by roughly one sigma or more which are responsible for virtually all the observed diffusion.

Estimates of the change in B-V color of a tail due to the depletion of its red population indicate that it would be less than 0.08 in B-V. Observational confirmation of this effect would require very special conditions.

A simulation of NGC 4676 shows radial velocities in good agreement with the most recent spectroscopic observations of this system.

It is generally concluded that the simple dynamical model has withstood the withdrawal of some of its very idealized conditions very well and is further strengthened.

B-V surface photometry of 3 interacting galaxies (Arp 174, NGC 2648, and NGC 4676) was obtained using the digicon tube developed by Dr. E. Beaver at the University of California at San Diego. The primary common feature of these 3 systems is that they all show some anomalously

red regions. In the case of the two spiral systems it is likely that

this is due to dust. An extremely young blue Population I is probably

not present.

CHAPTER I

INTRODUCTION

Until roughly 5 years ago the mechanism of formation, composition, and evolution of the bridges and tails in interacting galaxies were the subject of much speculation. A good deal of this has recently been dispelled by the results of numerical simulations which will be described below. About the same time very sensitive photon counting devices such as the digicon have become available and provide the opportunity to do photometry and spectroscopy of very faint objects. This thesis was motivated by some doubts about the applicability of the computer models done so far and by the possibility of obtaining photometry of interacting galaxies which might confirm the results of theory.

Each of these two areas is deserving of investigation in its own right. The models done to date are rather simple ones and so the addition of more realistic assumptions is a logical next step; the fine articulated structures seen in interacting galaxies are almost entirely unobserved (quantitatively) and require some basic photometry for their own sake.

Preliminary calculations indicated that if the assumptions defining the computer models were modified by the addition of velocity dispersion, the impressive fine structure seen in earlier model results would break up badly. This implied that models including velocity dispersion would show that any stellar population which had significant

1

velocity dispersion would be seriously depleted in the well delineated
features. Since these stellar populations are also the reddest compo-
nents in a normal galaxy, it was possible that these models would pre-
dict that sharp features of interacting galaxies must be relatively
blue. This possibility is explored in chapter II and the observations
are reported in chapter III. This chapter introduces the history of the
study of double and interacting galaxies and reviews the knowledge on
this subject at the present time.

Early research into double and multiple galaxies was concerned
with statistical information such as frequency of occurrence and distri-
bution of pair separations, and in general the interpretation of double
galaxies as being physically analogous to double stars. The objects in-
volved were selected on the basis of closeness on the sky according to
some rule. Severe interaction is not evident in the majority of such
systems, and it was generally ignored in those systems where it occurred.

Statistics of Double Galaxies

Holmberg's (1937) classic paper began this era of research and
Holmberg (1940, 1956, 1958, 1962, 1969) has carried it forward over the
years, remaining one of the most active investigators of double gal-
axies. His initial criterion for selecting double galaxies was that
their centers be separated by no more than twice the sum of their appar-
ent diameters on a photographic plate. This is a rather conservative
rule which excluded some wide physical pairs but also reduced the like-
lihood of including optical pairs. This criterion indicated that 22% of
all galaxies brighter than 13.0 mag. are members of double or multiple

systems. Holmberg (1940, 1956) later employed the more sophisticated technique of examining the distribution function of pair separations for bright galaxies. Since this distribution has a strictly linear dependence for optical pairs, these can be statistically eliminated. This produced the result that 53% of all the galaxies were members of double or multiple systems. Further, the distribution function for the projected pair separations is evidently very similar to that for binary stars in the Milky Way.

In studying specifically those systems composed of one large spiral and one or more very small companions Holmberg (1969) has shown the remarkable result that virtually all physical companions are contained within 60 degrees of position angle of the minor axis of their primary. Those spirals with the larger numbers of small companions have a tendency to show bluer nuclei, while in double galaxies composed of more nearly morphologically identical components, the two are usually of nearly the same color and surface brightness. The occurrence of tiny companions seems to be independent of total mass of the primary, but does correlate positively with detection of HI inferred from 21 cm observations. This leaves open the question of an extended hydrogen disk selectively retarding (and ultimately eliminating) all companions with orbits coplanar with the disk.

If double galaxies are gravitationally bound, then one would expect the angular momentum vector and the rotational momentum vectors to be fairly well aligned. In spiral-spiral pairs the apparent inclinations are easily measured and the true angle between the planes of a given pair of galaxies is either the sum or the difference of their

individual apparent inclinations. For physical pairs the distribution of their inclination difference should be peaked about zero and that of the sum much less so. For optical pairs the two distributions would be flat, since the inclinations are uncorrelated. Gorbachev (1970) has examined a sample of 1040 such pairs of galaxies selected from the Morphological Catalogue of Galaxies and finds that physical pairs do indeed show a distribution of inclination differences which is nearly gaussian with mean of $0°$ and $\sigma = 27°$. The distribution of inclination sums also has the expected form. It is further noted that if the disks of double galaxies tend to be coplanar, then the position angles of their major axes should also be correllated. A sample of 189 pairs shows a distribution of position angle difference which is narrow and sharply peaked about zero and has somewhat elevated wings as compared to a gaussian distribution with the same standard deviation.

Radial Velocities and Dynamics

Page (1952, 1960, 1961, 1962, 1970) has been the most active investigator of the dynamics of double galaxies as simple binary point mass systems. This technique requires obtaining the difference in radial velocity of the two galaxies and their projected separation. Given a large enough number of systems, the projection effects in radial velocity and separation can be corrected for statistically to give mean true space separations and space velocities. Application of Kepler's third law then gives an estimate of the total system mass. In practice the projected space separation is calculated from the angular separation and the distance which is inferred from the Hubble relation. The mean

masses of systems belonging to various morphological subsets of the sample are then calculated by a least squares method devised by Holmberg (1956). The principal difficulty involved is that the net errors in redshift measurement are often as large as the velocity difference between the two galaxies, especially in some of the older data used by Page (1961). Page has made a very careful analysis of the error propagation and his results, although the probable errors are rather large, are in good agreement with values of M/L and M deduced for nearby galaxies by other methods.

The most recent work of this type is that of Karachentsev (1970) using data on 96 double galaxies with reliable radial velocities selected from the Catalogue of Pairs of Galaxies (Karachentsev, 1972). The velocity difference - separation relation was compared to that expected in three different idealized models: 1) circular orbital motion, 2) gravitationally unbound motion, 3) radial motion. The last was seen to fit the worst, the first two seen to fit equally well. Karachentsev (1974) then proceeded to take almost the same data sample and to analyze it assuming the galaxies to be describing simple circular orbits in order to derive mean masses and M/L ratios. The results are summarized in Table 1 (for a value of H = 55 km/sec/mpc). In contrast to Page, Karachentsev finds very little dependence of mean M/L on morphological type. Only for visibly interacting double galaxies do the calculated M/L values depart significantly from the overall mean of 44.2. That mean is 5 or 6 times the value expected from observations of nearby single galaxies. It is difficult to say how much of this discrepancy is due to the fact that Karachentsev did not use the same reduction

Table 1. Total Masses of Pairs of Galaxies.

Sample	Karachentsev (1974)			Page (1961)		
	Mass $\times 10^{10}$ M$_\text{o}$	M/L	N	Mass $\times 10^{10}$ M$_\text{o}$	M/L	N
All	220	44.2 ± 9.2	101	51.4 ± 19.1	6.7 ± 6.7	52
E–E	261	55.8 ± 23.3	19	–	–	–
E–SO	–	–	–	120 ± 49	55 ± 40	18
S–S	95	32.2 ± 11.2		7.6 ± 7.1	0.36 ± 7.1	17
Interacting	–	9.3 ± 2.2	–	–	–	–
E–S	–	65.1 ± 20.8	25	–	–	–

technique as Page. The former merely calculated M/L for each system individually and then formed simple means for each morphological type. The distribution of M/L values is not one which has a well defined mean. Figure 1 shows the distribution of redshift differences for the data used by Page (1961) and Figure 2 shows the same distribution for Karachentsev's data.

Classical Ideas on the Formation and Evolution of Double Galaxies

Classically, there are two hypotheses of the formation of double galaxies: Either they formed in a chance close approach of two field galaxies resulting in a capture, or the two galaxies formed together out of the same protogalaxy by the same process responsible for formation of single galaxies. Closely connected with this problem is that of stability of double galaxies - once a double galaxy has formed, how long will it remain recognizable as a double galaxy?

If the components of double galaxies initially form together and if their typical lifetime is of the order of the age of the universe, then one would expect double galaxies to represent a constant fraction of all galaxies in any region of the sky. If they are formed by close encounters, then the local density of doubles should increase with the local density of single galaxies. Page, Dahn and Morrison (1961) searched 3 regions on the Palomar Sky Survey - two in the Coma and Virgo clusters and one in an area of low galaxy density - in order to find the dependence of the density of doubles on that of single galaxies. Their results indicate, although not very strongly, that the density of doubles is proportional to the square of the density of single galaxies.
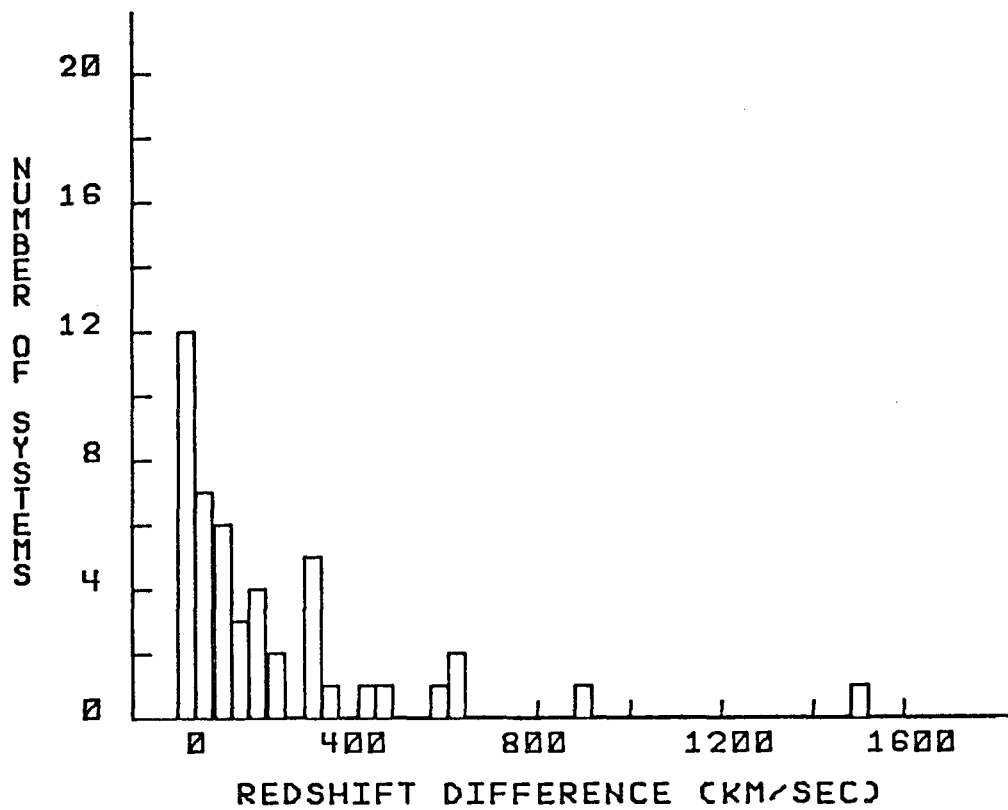
Figure 1. Histogram of radial velocity differences in the double galaxies studied by Page (1961).
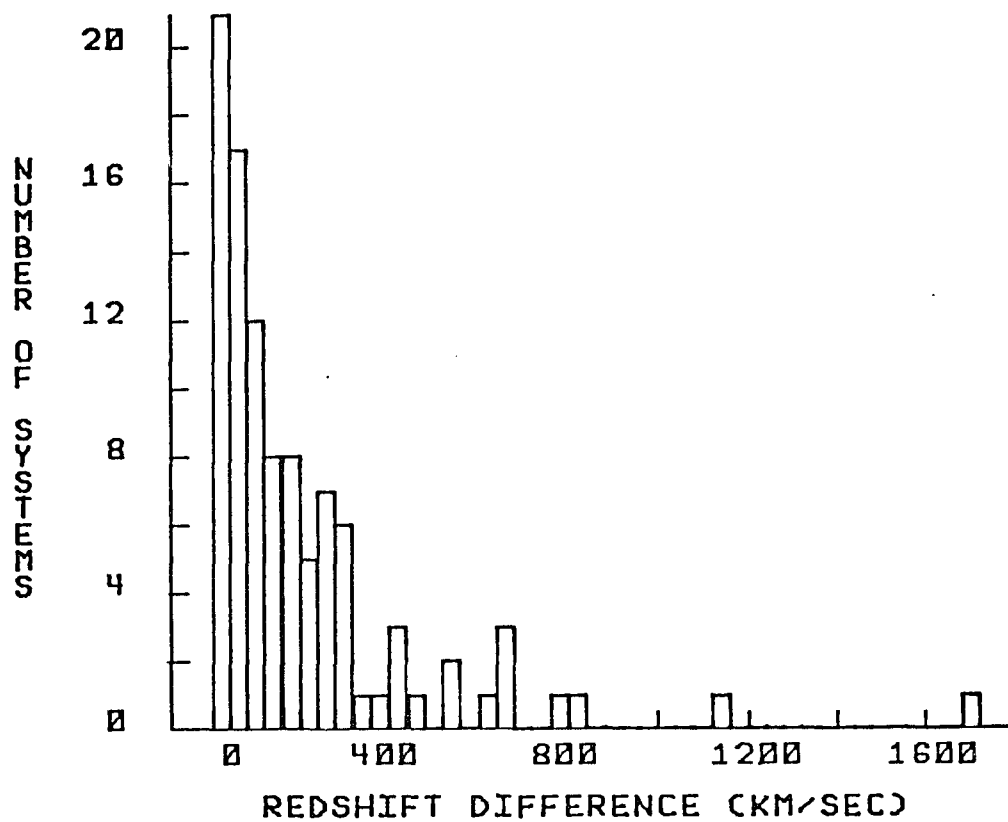
Figure 2. Histogram of radial velocity differences in the double galaxies studied by Karachentsev (1974).

This speaks in favor on the encounter hypothesis. However, all theoretical estimates of the frequency of encounters have indicated it to be too low by orders of magnitude to be able to account for the observed frequency of double galaxies.

Holmberg (1937, 1940) attempted to calculate the age of the universe by estimating how long it would take for the observed density of double galaxies in the near field to arise solely from close encounters. Assuming the universe is not expanding his result was 4×10^{12} years (correcting for changes in the distance scale since 1940 decrease the encounter rate by more than a factor of ten). Page (1961) performed a similar calculation including expansion of the universe and concludes that no more than 10% of the observed number of double galaxies can be accounted for in this way. Pfliederer (1963) has calculated a mean encounter rate of 5×10^{-13}/mpc/yr.

In the classical two body problem there is no possibility of an isolated encounter producing a bound binary system. Galaxies, however, are not mass points, and for a sufficiently close approach, their internal energies may be changed enough to reduce the kinetic energy of each galaxy so that a capture can result. Numerical calculations of a close approach of two spherical galaxies have been performed by Alladin (1965). The gravitational potential of each galaxy is calculated by assuming the stars have a polytropic density distribution. The total galaxy mass was typically 10^{11} M_0 and the perigalactic distance was 10 kpc so that the two galaxies did interpenetrate. Such a galaxy however, has very little of its total mass beyond this radius. The relative velocity at infinity ranged from a few hundred km/sec to a few thousand. As a first

approximation the orbits followed by the two galaxies were forced to be those which two point masses would describe. This model clearly violates energy conservation since any change in the internal energy must be accompanied by a corresponding change in center of mass energy. The point of the simulation is to indicate whether the change in internal energy is large compared to the center of mass energy. If it is, then the approximation is a poor one and it is likely that the center of mass energy would have to change significantly. The most important result of this sort of simulation is that the magnitude of the effects on the two galaxies are fairly sensitive to their relative velocities at perigalacticon. Significant energy changes do not occur at high velocities (greater than 2000 km/sec). A galaxy can suffer tens of such encounters without having its internal energy change by more than a few percent. Contopoulos and Bozis (1964) showed that such encounters result in at most only a few percent of the stars escaping their primary even for very close perigalactic distances, and comment that bridges and tails could not be formed in this way unless the relative velocities were much lower. Low speed encounters where the relative velocities are roughly comparable to the stellar velocities can result in changes in internal energy equal to 10% to 25% of the system center of mass energy (Alladin, 1965, Sastry and Alladin, 1970), although the fraction of escaping stars does not seem to exceed a few percent.

These results lead to the following conclusions.

1. If two galaxies do somehow become a bound pair, then it appears that they could not withstand many perigalactic passages before both have merged into a single loose, kinematically hot system. On the other

hand it is not unreasonable that a double galaxy could have orbital parameters such that its period is of the order of 10^9 years, so that even the oldest double galaxies might persist to the present.

2. If double galaxies form by chance encounters, then galaxies in the inner parts of centrally concentrated clusters like the Coma cluster would probably interact at too high a velocity to form binary systems. In the outer part the velocity is lower, but so is the density, and if the cluster is relaxed, motions in the outer parts will tend to be more radial than random so interaction is not very probably there either. One would expect to find more binaries in the inner parts of loose clusters like the Hercules cluster because the density of galaxies is fairly high, but velocities can be expected to be rather low due to the weak central concentration of mass. This indeed appears to be the case as noted by Zwicky (1956).

3. Evaporation of galaxies from a cluster must be less effective than point mass models of cluster dynamics have indicated because the close encounters which accelerate point masses do not do the same for galaxies.

Strongly Interacting Galaxies and Non-Classical Ideas

Being generally faint and evidently not essential to the understanding of galaxies in general, quantitative observations of interacting galaxies necessarily lagged behind those of bright normal galaxies for many years. For a long time the literature on this subject was composed of predominantly morphological discussions. This dearth of quantitative facts combined with the very intriguing appearance of these

objects provided an ideal environment for speculation and conjecture, some of which is now seen to have been rather wide of the mark. This field is still inescapably influenced by morphology, and one must beware of subjective interpretation; physical processes and visual appearances are not necessarily uniquely related.

Research directed specifically at interacting galaxies did not appear until the 1950's, most notably in papers by Zwicky (1956) and Vorontsov-Velyaminov (1957). These discussed the morphology of interacting galaxies and drew what conclusions they could without photometry or spectra about their origin and evolution. Vorontsov-Velyaminov's work, especially his Catalogue of Interacting Galaxies (Vorontsov-Velyaminov, 1959), was particularly valuable as a stimulus for other research. The generally agreed upon apparent features of interacting galaxies were these.

1. The galaxies to be found in interacting pairs can be of virtually any morphological type.

2. The appearance of interacting systems ranges from that of two or more galaxies showing long, faint filamentary connections or "tails" to two galaxies contained within a common luminous envelope.

3. Where filaments are present, they often appear to be related to distinct structural features of one of the galaxies, usually an extension of a spiral arm. A common form is that of a large spiral with a small satellite situated at the end of an extended spiral arm.

4. The longest and narrowest filaments seem to be associated with systems containing late type spirals, and on any reasonable distance

scale they can reach enormous lengths. The longest known evidently exceed 50 kpc while being only a few kpc in width.

5. Systems containing E and SO galaxies tend to have shorter, broader filaments.

6. Some systems have double bridges.

7. Tails are more common than bridges and are usually directed away from the companion galaxy.

8. Interacting galaxies comprise a small fraction of all galaxies, probably only a few percent.

9. There are some exceptions to the rules; a few galaxies are known which show pronounced tails and which have no visible companion at all.

There was considerable diversity in the interpretation of these observations. Zwicky (1956) (and Zwicky and Humason, 1964) concluded that the faint, narrow filaments were probably made of normal stars with no significant amount of gas present. This was inferred from the fact that spectra of filaments recorded no emission at all. If the observed luminosity of 23 to 25 mag/sec^2 were all due to gas, one would expect emission lines to be detected. The presence of absorption lines was also claimed by Zwicky (1957). The colors inferred from long exposure plates were not in disagreement with this idea. Zwicky proposed that interacting galaxies were the result of gravitational interaction during a close encounter and attributed the great narrowness and length of the filaments to the possibility that the disk material had a considerably higher viscosity than was previously thought. He supposed that there was an important relationship between spiral structure and the

phenomenon of interaction. In those cases where this was not obvious it was probably due to rotation breaking up the connection.

Non-classical interpretations of interacting galaxies have been very seriously considered, most notably by Vorontsov-Velyaminov (1957, 1960, 1962). After long study of the morphology of interaction Vorontsov-Velyaminov concluded that the forces responsible for the distortions were non-gravitational and probably non-magnetic. A major argument against a simple dynamical explanation was that the velocity dispersion which one would naturally expect disk population stars to have should not allow the formation of narrow filaments. Estimating the velocities involved at 100 km/sec, it would take about 4×10^8 years for a filament to grow to 40 kpc. In this length of time a star with a peculiar velocity of just 10 km/sec would move 4 kpc. It appears very likely that filaments would diffuse into space much too rapidly to ever achieve their thread-like appearance. The self-gravitation of a filament is probably too weak to be very significant in containing its diffusion. Hoyle and Harwit (1962) examined the stability of such a structure on the assumption that it was gravitationally bound. It was shown that a small density perturbation near the surface of a filament will grow resulting in disruption in roughly 10^8 years.

Vorontsov-Velyaminov proposed that some hitherto unknown repulsive force was responsible for the interaction. The motivation for this was the observation that tails are usually seen to point away from the companion galaxy and because of a phenomenon he called "frontal disintegration." This was the tendency of a spiral galaxy to show weakened spiral structure on the side of its disk which is nearest to its

companion. Vorontsov-Velyaminov also argued that interaction could have little to do with inducing spiral structure because multi-armed spirals or bifurcated spiral arms could never be produced in this way.

Ambartsumian (1958) proposed the hypothesis that small companions to large galaxies were formed by ejection from the nucleus of their parent galaxy in some sort of violent fissioning process. The filaments observed were evidently a trail of debris left by this fragment of the nucleus. The fragment would in turn eject material from itself and soon appear as a small galaxy next to its parent and attached to it by a "spiral arm." It was not claimed that this phenomenon is responsible for all spiral structure, but merely that it can produce a filamentary structure resembling an elongated spiral arm.

The most serious, that is the best founded, threat to a classical explanation of interacting galaxies is the question of non-doppler redshifts. Halton Arp is a well known advocate of this interpretation of the redshift and the only astronomer to examine specifically the possibility of non-doppler effects in double galaxies. Arp (1970a) claimed that small companions to spiral galaxies tended on the average to be redshifted by a small amount relative to their primaries. Such a systematic redshift cannot be accounted for by orbital motion or disruption and must be intrinsic to the object itself. Arp's result was criticized by Lewis (1971) on the grounds that his data suffered selection effects and comprised too small a sample. Arp (1971) responded rather effectively to these objections. In an attempt to clarify this matter Bottinelli and Gouguenheim (1973) examined 20 galaxies with a total of 52 small companions looking for this effect and found a rather clear

positive result. Selecting their data from the Reference Catalogue of Bright Galaxies (de Vaucouleurs and de Vaucouleurs, 1964), they included only systems having one member at least 50% brighter than the second brightest member, well determined redshifts and a low probability of optical companions. The distribution of velocity difference (companion to primary) shows a gaussian form with mean of 90 km/sec rather than zero as one would expect from a classical interpretation. A chi-square test revealed an 80% probability that the distribution is gaussian with a mean of 90 km/sec and only a 1% probability that it has a mean of zero. There seems to be no plausible explanation of this result in terms of systematic errors in redshift measurement or inclusion of optical companions. In addition to this statistical result, there are many individual cases cited in the literature (Arp, 1971, 1970b, Burbidge and Sargent, 1971) where small companion galaxies seem to have redshift very much greater than their primaries. The literature on the general phenomenon of non-doppler redshifts is extensive and it is likely that some extremely fundamental properties of galaxies or matter lie yet undiscovered.

Computer Simulations of Interacting Galaxies

It is remarkable that so many astronomers were so persuaded that interacting galaxies could not be explained by a gravitational model that it was not until 1970 that one was attempted. When this was finally published by Toomre and Toomre (1972), it was evident that even a very idealized gravitational model could be enormously successful at mimicking the appearance of some of the most extreme examples of

interaction. The history of these computer simulations will be recounted here, while a detailed criticism is deferred to chapter II.

Except for a few variations to be noted, all of the computer simulations described below represent the gravitational field of a disk galaxy with that of a point mass situated at the nucleus of the galaxy with a mass of about 10^{11} M_o. The "stars" in orbit about this mass point are considered to be of negligible mass so that their contribution to the gravitational field is ignored. The initial conditions place the stars in circular, coplanar, direct orbits with zero velocity dispersion. Usually, fewer than 200 stars are used and the initial conditions are established at roughly 10^9 years before perigalacticon. Since the stars do not gravitate, the motion executed by the two mass point galaxies is given exactly by the classical two body problem. This description seems much more that of a solar system suffering a close encounter with a nearby star, than the interaction of two galaxies, but it will be seen to be quite adequate.

The important physical parameters in the simulations are:

1. Mass ratio of the two bodies.

2. Eccentricity of their orbits, e.

3. Minimum separation (separation at perigalacticon), R_{MIN}.

Of secondary importance are:

1. The inclination of the disk of stars to the primary orbit plane, i.

2. W, the argument of pericenter. This is related to the azimuth or longitude of the tilted disk. It is measured in the primary orbit

plane from the ascending node of the disk towards the perigalactic point in the direction of the perturber's motion.

By way of convention, time is reckoned in units of 10^8 years with $T = 0$ being time of perigalactic passage. Distances are measured in terms of R_{MIN}. In virtually all simulations referred to below R_{MIN} = 25 kpc, the mass of the parent galaxy is 10^{11} M_o, and the model was begun at $T = -10$. The mass ratio is always in the sense of perturber/parent.

The earliest computer simulations of interacting galaxies done for the specific purpose of examining the resulting morphology (as opposed to those of Alladin, Sastry, Contopoulos and Bozis mentioned earlier) were done by Pfliederer and Seidentopf (1961) and Pfliederer (1963). These were attempts to induce spiral structure in a disk galaxy via the influence of a close approach of another galaxy. Only one galaxy was given a retinue of stars, the other was simply a point mass perturber. The simulations were restricted to hyperbolic encounters (e = 31), since it was reasoned that this must be a typical encounter of two field galaxies. The experiments were unsuccessful as far as producing any but the most short-lived spiral structure, but they did show transient distortions very similar to the more mild interaction seen in some double galaxies. It is unfortunate that this was not recognized at the time. One important result borne out by later work was also shown; if there is to be any significant interaction at all, the passage must be direct, that is, the perturber must be moving in the same orbital sense as are the stars.

The first simulation to address itself specifically to the formation of bridges and tails was done by Yabushita (1971). These models considered encounters with eccentricity from 1 to 5. It was clearly shown that while in a direct encounter the path executed by a single star was a complex spiral, at any given instant the locus of all stars could look very much like a bridge or tail. Frequently the perturber was able to capture stars from the parent galaxy, rarely was a star lost completely from the system. The effects were diminished if the plane of the disk was inclined much beyond 30 degrees to the plane of the orbit of the primaries. Yabushita also made the very important observation that slower relative velocities produced more violent effects. A moment's reflection shows this fact to be obvious, yet it was largely ignored in previous simulations (and some later ones), probably because encounters were considered in terms of chance passage of two field galaxies rather than a perigalactic passage in a binary system.

Tashpulatov (1970) examined a synchronous close encounter of a point mass with a homogeneous prolate galaxy. This study was done largely analytically and consequently was restricted to calculating the mass outflow from only a single point on the "surface" of the galaxy. Mass drawn out from the vertex of the prolate galaxy was seen to form short bridge-like structures which were very short-lived.

In late 1972 and early 1973 four extensive simulation studies were published almost simultaneously. They were evidently motivated by Toomre's earliest results which were graphically demonstrated at I.A.U. Symposium No. 38 (see Toomre, 1970 and Toomre and Toomre, 1971). The completed study (Toomre and Toomre, 1972) is virtually an instruction

manual for computer simulation of interacting galaxies. A very wide range of orbital parameters were explored showing how to produce the various morphological types of interacting galaxies and successful attempts were made at duplicating certain particular interacting galaxies. These results are the most convincing because they produce strikingly good morphology with all physical parameters (mass, separation, time scale) chosen a priori to be typical for normal spiral galaxies. The Toomres proceed to model M51, ARP 295, NGC 4676 (ARP 242), and NGC 4038/39 (the "antennae"), the last two with impressive results. The simulation of NGC 4676 will be discussed in detail in the next chapter.

Wright (1972) criticized Toomre's models as presented at I.A.U. Symposium No. 38 on the grounds that his initial conditions placed the stars in concentric rings rather than allowing a continuous distribution of stars in radius. Wright performed his own series of simulations using a smooth distribution of stellar radii, but still keeping all initial stellar orbits coplanar and exactly circular. The results of this paper are completely in accord with Toomre and Toomre (1972), although the terminology is a bit different; Wright refers to formation of tails in models with a mass ratio of 1/4. Toomre would call these "tails" counter-arms for they are several times smaller than the well developed tails which result from an equal mass model. Wright also found that an R_{MIN} of about 20 kpc produces good result and that R_{MIN} = 40 kpc has very little effect.

Eenev, Kozlov, and Sunyaev (1973) published a simulation study with models which had stars distributed out to radii as large as 36 kpc and an R_{MIN} of 40 kpc. All models had e > 1.0. These parameters

produced virtually no captures but about 12% of the matter from radius 16 to 36 kpc was lost completely from the system. This range of initial conditions does not yield the dramatic distortions that the Toomre's were able to produce.

Clutton-Brock (1972) performed three series of models. The first used essentially the same scheme as Toomre and Toomre (1972) except for a slightly different gravitational potential for the parent galaxy, and produced similar results. In the second series of models an attempt was made to drop the massless star approximation and to make the gravitational field of the parent galaxy a self-consistent one derived from 600 equal mass points. The great difficulty with this kind of model is well known; in order to avoid a shock relaxation of the type originally described by Lynden-Bell, the velocity dispersion of the mass points must be made very high - much higher than that observed for stars in the Milky Way. Not surprisingly, the interactions resulting from this model were very broad, diffuse clouds of stars rather than well defined features. Consequently a third series of models was done using the very hot self-consistent disk to provide the gravitational field plus a thin disk of massless points with zero velocity dispersion and coplanar, circular orbits to provide the fine structure. This is essentially the same as the other models described above with the addition of a more complex gravitational potential. For all its complexity and computational effort its results were not significantly different from the Toomres'. Clutton-brock's method of potential calculation for the self-consistent disk has been criticized by Schaefer, Lecar, and Rybicki (1973) noting that its error oscillates with a rather large amplitude

compared to other, simpler methods. The problem of the self-consistent disk in regard to interacting galaxy simulations will be discussed in a later chapter.

General Conclusions Drawn from Model Results

One's intuition about the outcome of these interactions is surprisingly poor until a large number of simulations have been studied covering a wide range of initial conditions; many early deductions about tidal interaction are evidently wrong.

Retrograde encounters have very little effect.

All of the violent distortions seen are confined to the outer parts of the disk. Expressed in terms of the Milky Way this would mean radii larger than the sun's distance from the nucleus.

The appearance of an interacting system can be enormously effected by changing one's viewing angle. Bridges and tails which appear long and narrow are often seen to be broad fan-shaped structures which are being viewed edge-on.

Projection effects can make a tail appear to be a bridge (as in the case of M51, according to Toomre).

The degree of development of a filament can be very much enhanced by the choice of initial distribution of stars. Adding stars in the outer parts of the disk at a radius of 70% to 80% of minimum separation of the two galaxies is particularly effective.

To get strong interaction eccentricities should be fairly low, preferably 1.0 or less. Strongly hyperbolic encounters are too impulsive to leave much of a mark.

These systems are not the result of chance encounters. The interacting galaxies are bound binary systems, probably suffering substantial reductions in eccentricity at each perigalactic passage. However, it is difficult to see how so many double galaxies could be in only their first or second orbits unless they initially had very long periods, or are all rather young, less than 10^9 years.

Capture and Escape of Stars

There are generally relatively few stars escaping to infinity unless the perturber has mass greater than the mass of the parent galaxy. Stars placed beyond 16 kpc are much more likely to be lost.

Of those stars extracted from the parent galaxy, proportionately more of them are captured by the perturber (as opposed to escaping the whole system) for slower encounters. Oddly enough, however, the total number of stars extracted from the parent seems to decrease with the relative velocity of the two galaxies.

The more massive the perturber, the more stars it steals from the parent galaxy.

The orbits of the captured stars tend to have high eccentricity – about 0.8.

The Formation and Behavior of Tails

To form a good tail the perturber should be at least as massive as the parent. Good tails are formed with a mass ratio of 1.0.

One can make models producing good tails which endure 10×10^8 years and which increase their length roughly 50% during that time.

The making of a tail is very insensitive to both inclination and argument of pericenter.

Tails formed in models with non-zero i and W are not contained in the primary orbit plane or the plane of the disk. Their form is evidently that of a gently curved and twisted ribbon.

The Formation of Bridges

To make a bridge, the mass of the perturber should be at least 3 or 4 times less than the mass of the parent galaxy. Good bridges can be formed with mass ratios as small as 1/10 if R_{MIN} is reduced sufficiently.

True bridges seem to be not so long lived as tails and seem to involve much less material.

Better bridges seem to result from small but non-zero disk inclinations, say 15 degrees.

Dependence on i and W

Generally, the results are not sensitive to disk inclination unless it exceeds 30 degrees. Good tails seem to be produced even at inclinations as high as 75 degrees. Bridges are more sensitive.

Changing W generally has very little qualitative effect, this is true even for some models with i as high as 75 degrees.

Quantitative Observations of Strongly Interacting Galaxies

The filaments seen in interacting galaxies are generally of such low surface brightness that any sort of observation except a broad band photograph is extremely difficult. Photometry and spectroscopy of faint structures exists only for a very few systems which are particularly

bright. Spectra of the nuclei of interacting galaxies are more common. No systematic radio surveys of interacting galaxies have been done but some scattered observations are available.

Photoelectric photometry of VV117 and VV123 was done by Sandage (1963) in an attempt to infer the ages of the satellite galaxies in these systems from their colors. The colors were rather red indicating ages between 10^9 and 10^{10} years. These are irregular systems however, not showing sharply resolved bridges or tails. There have been several photometric investigations of pairs involving elliptical galaxies (Faber, 1973, Rood, 1965, King and Kiser, 1973) which show the surface brightness distribution of the outer parts to be of the form predicted by King's (1972) model of tidal truncation.

Since magnetic forces have been suggested as being responsible for the support of filaments in interacting galaxies, Arp (1962) photographed ARP 295 through polarizing filters and claimed that these showed strong polarization perpendicular to the very long and narrow bridge in this system. Evidently no other polarization observations of faint sturctures have since been attempted.

Radial velocities are especially interesting in that they can provide a test of the gravitational interaction models. The best radial velocity information available is probably Roberts' and Warrens' (1968) radio data for the M51 system. The Toomres' model of M51 fits the observations well if one assumes that the orbit of the small companion is steeply inclined to the disk of its primary. Spectroscopic information for more distant systems is quite rare. The papers listed in Table 2 are representative. The sample is quite small but it is

Table 2. Spectroscopic Observation of Interacting Galaxies.

Object	Systemic Velocity (km/sec)	Velocity Difference	Lines Observed	Reference
IC 883	1034	229	H_α, [NII]	Burbidge and Burbidge (1964)
VV 254	4588	6	H_α, [NII]	Burbidge and Burbidge (1963)
NGC 3227	1175	175	—	Rubin and Ford (1968)
NGC 4038/39	—	—	H, O, N, He, S	Rubin, Ford, and D'Ordico (1970)
Klemola 30	6560	360	H_α	Graham and Rubin (1973)
NGC 4676	6600	80	Balmer, [NII], H_α	Stockton (1974)
NGC 3345/96	1660	90	H_α, H_β, [OIII], [OII], H_γ, He, [NII], [SII]	D'Ordico (1970)

fairly safe to say that at least some strongly interacting galaxies have rather ordinary spectra. Systems showing many strong emission lines are generally morphologically similar to those single galaxies which show strong emission; emission lines are not necessarily closely related to the phenomenon of interaction. It is interesting to note that Klemola 30, NGC 3227 and M51 all show small companions which at first sight appear to be in retrograde passage, although the interpretation is not unambiguous. Retrograde passage is, of course, incompatible with a dynamical model.

One of the most interesting and most studied systems is NGC 4676 ("The Mice"). It is rather bright and shows two tails, one of which has a length that is easily 2 or 3 times the diameter of its primary. The Toomres' model of this system matches its morphology remarkably well, but the velocity difference between the primaries which it requires is of the opposite sense to that found by Burbidge and Burbidge (1961). Theys, Spiegel, and Toomre (1972) observed only the component with the long tail. Apparently this was the first spectral record of a long, faint filament and it showed a roughly 500 km/sec velocity gradient from the nucleus of the northern galaxy out to the tip of the filament. This very large difference made the case for a dynamical model still weaker. Both of these difficulties were removed by Stockton's (1974) high dispersion (50 Å/mm) image tube spectra. Using H and N emission, Stockton found the velocity difference of the primaries to be only 80 km/sec and a gradient along the tail of the northern galaxy of only 250 km/sec. This is in excellent agreement with the model.

Allen et al. (1973) and Purton and Wright (1972) have made radio observations of a total of 10 interacting systems and found no unusual radio characteristics compared to normal single galaxies. In no case was a bridge or tail observed to emit 21 cm radiation.

Comment

The data discussed above do not easily lead one to an unambiguous understanding of double galaxies. There is much evidence in favor of a simple dynamical explanation: the statistical results of Gorbachev (1970), Holmberg (1940, 1956), and Page (1961), and the evidence of tidal truncation in elliptical doubles. The computer models of interaction are especially strong circumstantial evidence. Yet, there are conflicting results that are difficult to ignore. Concerning the small companions to large spiral galaxies, the combination of Holmberg's (1969) observation of their peculiar distribution about their primaries and Bottinelli and Gouguenheim (1973) evidence of non-doppler redshifts for these same systems is very difficult to dismiss. Arp's very high redshift difference systems are another puzzle. It is interesting that Karachentsev's (1974) analysis of velocity differences in pairs conflicts with that of Page (1961), although the former's data are much more recent and presumably more precise. Especially intriguing is that Karachentsev's results were dynamically normal only for those systems showing strong interaction -- exactly the type which are most certainly demonstrating simple gravitational interaction.

If all these observations are to be taken as valid, then one must concede that some double galaxies are normal (that is,

understandable), while others are exhibiting phenomena beyond our ex-
perience. The logical conjecture is that some sort of evolutionary se-
quence is involved wherein the operative physical laws in a system
change fundamentally with time; we understand only the set we happen to
be dealing with in the laboratory and any others are visible to us only
in distant galaxies.

The following chapters will try to shed some light on the gravi-
tational interpretation of interaction, attempting to observationally
test some of its ramifications and to critically discuss the application
of the computer to this problem.

CHAPTER II

COMPUTER SIMULATION OF INTERACTING GALAXIES

The computer simulations described in the last chapter are impressive in their ability to mimic the appearance of interacting galaxies, but a more quantitative test of the hypothesis would be desirable. This chapter attempts to carefully criticize this very idealized modeling technique and to make models which are a little less idealized and which provide a more thorough test of the hypothesis.

Approximations and Assumptions in Computer Models

A brief recounting of the particulars of the models reported in the literature is in order:

1. All the gravitational potential in the model derives from the two mass points representing the two galaxies.

2. The "stars" referred to are massless. Their contribution to the gravitational field is completely neglected. Thus the model is not "self-consistent".

3. The stars are initially placed in exactly circular and coplanar orbits. The "disk" referred to has no gravitational significance. It is purely an artifact of the programmer's chosen initial conditions of position.

4. The initial conditions for a model are established some 10^9 years before perigalactic passage.

5. The actual computation is only that of the restricted three body problem. The two mass point galaxies and any one of the stars comprise the three bodies. The calculation is run through from start to finish separately for each star. Since the stars do not gravitate, there is no inconsistency in this method.

6. These particles probably represent stars much better than they represent interstellar material. They exhibit not the slightest bit of viscosity or inelasticity.

The approximations listed above are dictated largely by the impracticability of more realistic models. Computing time increases very rapidly as one attempts to include more realistic potentials or especially if the model is made self-consistent.

The approximation of a galaxy as a mass point is a poor one in only two respects:

1. It ignores gravitational acceleration perpendicular to the plane.

2. It is a bad approximation close to the nucleus, say within 6 kpc. However, the mass density in the disk of a spiral galaxy is such a sharply decreasing function of radius, that a star at a radius of more than 5 or 6 kpc sees a gravitational field which (for $Z = 0$) is an excellent approximation to that of a mass point and which asymptotically approaches that of a mass point as a function of radius (this ignores contribution from the halo). Since it is the outer parts of a galaxy disk ($R > 10$ kpc) that seem to be involved in bridges and tails, this representation is not at all a bad one.

Neglecting the gravitation of the individual stars is perfectly acceptable as far as star-star interactions are concerned. The

relaxation time of stars in the solar neighborhood exceeds 10^{13} years. The only disadvantage incurred by this approximation is that the gravitational field of the galaxies is wholly unaffected by the apparent distortions in the disk. Indeed, the disk itself is rather fictitious. The energy of the system is also completely insensitive to the effects of the interaction; since the stars are massless test particles, their motions do not affect the energy of the system. Energetically these simulations are nothing more than the two body problem.

The initial conditions of position are usually chosen to distribute the stars in concentric, coplanar rings. Wright (1972) performed simulations with stars initially distributed smoothly in radius but retained the exactly circular and coplanar orbits. One would expect this to interpolate, albeit spottily, the results obtained from the ring models, which it in fact did. The surface density of stars as a function of radius in the models of Toomre and Toomre (1972) and those to be reported here, is very nearly constant. This is quite contrary to the true distribution in a spiral galaxy, which is approximately inversely proportional to radius. The uniform distribution is used because of the observation that the outer parts of the galaxies are more prominently involved in forming fine structure, while the stars in the inner parts (R < 8 kpc) are affected very little by an encounter. A realistic density distribution would at least double or triple the cost of a simulation without materially affecting the final appearance. This has been verified by Wright's (1972) simulations. The reader must bear in mind this departure from the facts however, and also the fact that

the degree of development of sharp features can be fairly strongly affected by manipulation of the initial density distribution.

The distribution of stars in radius is not extremely important as long as the circular and coplanar orbits are retained. The total absence of velocity dispersion in the velocity initial conditions is a much more serious excursion from the truth. A star with a peculiar velocity typical of old Population I will travel roughly 2 or 3 kpc in 10^8 years. Since most simulations cover about 10^9 years, it is to be expected that solar type stars would diffuse very badly, producing no fine structure at all. This point will be specifically examined below.

Modeling that has been done so far has shown results that are fairly insensitive to the beginning time of the model, that is, how long before perigalacticon the initial conditions are established. As long as the simulation is begun with the perturber far enough away so that the acceleration of a star due to the perturber is only a few percent or less of that due to its primary, the results are unaffected. The simulations described here were always begun 10×10^8 years before perigalacticon, with the two galaxies usually separated by more than 100 kpc.

It is important to emphasize point number 5 above. It is a natural consequence of point number 2, but is often overlooked by the casual reader. No "star" is affected in any way by any other star in the simulation. More importantly, the interaction of the two mass point galaxies is completely elastic - there is no accounting for collision losses of the sort described by Alladin (1965). While this deficiency probably does not significantly affect the qualitative results, it probably is serious in regard to studying a system's dynamical evolution

as it suffers successive perigalactic passages. These simulations can only be expected to give a crude first order indication of energy changes in a close passage.

The question of the behavior of the interstellar medium in the course of an encounter is very important. These models probably do not represent it all. It must surely undergo at least some sort of compression, but it is difficult to say how conservative the processes are. It has often been suggested that this process might produce showers of star formation. The particles that comprise these models show the behavior of the interstellar matter to the extent that it is not viscous or does not have highly dissipative mechanisms.

Velocity Dispersion in the Computer Simulations

The objectives of the computer simulations described below are to investigate the effects of inclusion of a disk potential and the sensitivity of the results to varying degrees of velocity dispersion in the initial conditions. The velocity dispersion of stars is closely associated with stellar population, so this should shed light on the degree of diffusion of various population types which may be detectable photometrically.

Ideally to calculate initial conditions including velocity dispersion one would have a relation giving the velocity ellipsoid as a function of radius in the outer parts of a spiral galaxy. Such a result is not the objective of most theoretical work on galactic dynamics, and very little is known observationally about stellar motions in the plane beyond about 1 kpc from the sun. Only a very approximate estimate of

this function is required here however, and suitable relations can be inferred from the work of Oort (1965). Assuming an axisymmetric system and no time dependence Oort found (for Z = 0)

$$\frac{1}{\sigma_x^2} = C_1 \qquad\qquad \frac{1}{\sigma_y^2} = C_1 + C_2 r^2 \qquad\qquad \theta = \frac{C_3 r}{C_1 + C_2 r^2}$$

where θ = mean orbital velocity and r = radial distance from the center of the galaxy. The X-axis is directed radially outward from the center and the Y-axis is in the direction of rotation. For reasonable values of C_1, C_2, and C_3 these relations imply that the ratio

$$\frac{\sigma_y}{\theta} = \frac{\sqrt{C_1 + C_2 r^2}}{C_3 r}$$

is a very slowly varying function of r, changing only by about 10% over the region of interest (r = 10 to 17.5 kpc). For purposes of calculating initial conditions here, it will be assumed that this ratio is constant in the outer parts of a normal spiral galaxy.

Further, Oort (1928) showed that

$$\frac{\sigma_x^2}{\sigma_y^2} = \frac{A - B}{-B}$$

where A and B are the Oort constants. A and B of course are not globally constant but are defined locally as

$$A = \frac{1}{2}\left[\frac{\theta(r)}{r} - \frac{d\theta(r)}{dr}\right] \qquad\qquad B = \frac{-1}{2}\left[\frac{\theta(r)}{r} + \frac{d\theta(r)}{dr}\right]$$

Thus if $\theta(r)$ (the rotation curve) is known, A and B can be calculated

for any point in the galaxy. For these models the radial component of acceleration is virtually identical to that due to a mass point at all times, so

$$\theta(r) = \sqrt{GM/r}$$

can be taken as the rotation curve. In this special case one finds

$$A = \frac{3}{4} \sqrt{GM/r} \qquad\qquad B = \frac{-1}{4} \sqrt{GM/r}$$

so that $\sigma_x^2/\sigma_y^2 = 4$ or $\sigma_y = \sigma_x/2$.

Observations in the solar neighborhood give $\sigma_y = \sigma_x/1.6$ for dwarf stars, so $\sigma_y = \sigma_x/2$ is a reasonable rule to use and it is consistent with the potential used in the models studied here, so it will be assumed that $\sigma_y = \frac{1}{2} \sigma_x$ everywhere in the outer parts of the galaxy.

One can now proceed to calculate σ_x and σ_y as a function of r for the initial conditions of a computer simulation by calculating orbital velocity from

$$\theta(r) = \sqrt{GM/r}$$

and then choosing a value of σ_x/θ to represent a desired degree of velocity dispersion. Thus $\sigma_x(r)$ is determined and then $\sigma_y(r) = \frac{1}{2} \sigma_x(r)$. In the solar neighborhood $\sigma_x/\theta = 1/6$ for solar type stars. The velocity dispersion of the models described below will be discussed in terms of this ratio.

The Z velocity dispersion, σ_z, as a function of r (for $Z = 0$) is somewhat more difficult to ascertain because it depends on the mass

surface density distribution and on the distribution of kinetic energy

perpendicular to the plane. Estimating the Z velocity dispersion re-

quires first finding the surface density distribution in the plane of

the disk. Given this and some simple assumption about the thickness of

the disk or the random energy of the stars, an operational rule can be

obtained. Freeman (1970) has studied disks with a surface density dis-

tribution of the form

(1) $$S(r) = M_d \, S_0 \, e^{-r/a}$$

where M_d is the total mass of the disk and S_0 is a normalization constant.

Such a disk has a reasonable rotation curve when in centrifugal equi-

librium. Freeman showed that surface photometry of 36 face-on nearby

spirals (collected primarily from the work of de Vaucouleurs and the

work of Liller) seems to fit very well the model of an exponential disk

with a spherical nuclear component, assuming that M/L is roughly con-

stant everywhere in the disk. The data from these 36 galaxies (exclud-

ing SO's) indicates a median value for a of about 1.5 kpc and the Milky

Way is estimated to have a = 1.6 kpc. From the plots of log I(r) versus

log r the contribution due to the disk and spherical components are

easily resolved and imply that the major part of the mass of a spiral

galaxy is in the "disk" as it is defined by equation 1.

To estimate σ_z as a function of radius once S(r) is known re-

quires some assumption about the Z energy of the stars as a function of

radius. The simplest such relation requires the typical star (that is

one whose Z velocity is σ_z exactly) will rise to a height above the

plane which is constant with r. This makes the plane have constant

thickness. This height was generally chosen to be slightly under 1 kpc and produced Z velocities of the size observed in the solar neighborhood.

There has been some controversy about the apportionment of mass in spiral galaxies between the spherical component and the disk. The halo mass is very difficult to determine observationally because it is composed of very faint stars and may possibly have large numbers of white dwarfs. Ostriker and Peebles (1973) suggested that the halo is the dominant mass component by some factors of ten. This conclusion was reached as a result of self-consistent computer simulations of a disk galaxy. The simulations showed that such a disk heats up very rapidly giving the stars a very large velocity dispersion and tends slowly towards a more spherical form. This heating process could be suppressed by drastically increasing the mass of the spherical component. Since the disk of the Milky Way is seen to be "cold", that is to show much less velocity dispersion than the computer model did, it was suggested that the Milky Way's spherical component is extremely massive. This was attractive in that it seemed to solve the missing mass problem in galaxy clusters and to explain the recently observed behavior of spiral galaxy rotation curves to be rather flat in the extreme outer parts of the disk. However, it relegates the disk to the status of an insignificant wisp of material distinguished only in that it radiates detectable amounts of light. Further, it is very difficult to imagine what form the extra mass could be in so that it would not be observable.

A brief look at the computer model used casts severe doubt on its similarity with real galaxies. These models had at most 500 mass points initially distributed according to a reasonable density law

throughout the disk. Each was given an orbital velocity appropriate to its position plus sufficient velocity dispersion to support the disk against collapse according to the criteria determined by Toomre (1964). If one scales this model to the order of size and mass of the Milky Way then it is obvious that these initial conditions must lead rapidly to a very hot system simply because the total mass of the disk is concentrated in such a small number of mass points. Each "star" represents at least 10^8 M_o. In the outer parts, analogous to the sun's position in the disk, one of these massive stars feels roughly 1/4 as strong a gravitational attraction from its mean nearest neighbor as it does from the rest of the galaxy. The corresponding figure for the sun is roughly 5×10^{-5}. This obviously will promote rapid relaxation. Using Chandrasekhar's (1948) expression for calculating relaxation time one obtains roughly one thousand years for the outer parts of the Ostriker and Peebles model, whereas the same expression applied to the solar neighborhood gives 10^{13} years. Adding a very large spherical mass component obviously would tend to stabilize the model because it increases the strength of the general field compared to the perturbations of neighboring stars which are the mechanism of relaxation.

The problem of extremely short relaxation times due to too small a number of mass points is a very well known one and is very difficult to avoid. It is clearly impossible with the present or foreseeable state of the art of computing machinery to ever to able to do a truly self-consistent simulation of a galaxy. Some sort of approximations are necessary such as Hohl's (1971) methods, and then one must be very

cautious in interpreting the results; the effects of the approximations must be carefully examined.

The Computing Algorithm

About half of the simulations to be described below include a true disk potential. In those cases where a disk is present it is assumed to contain 75% of the total galaxy mass, the rest being contained in a mass point at the center, and a value of 1.5 kpc was chosen for a in equation 1. Only the galaxy with the satellites is given a disk potential and the shape and orientation of the disk remains constant throughout the simulation -- it is completely insensitive to the encounter. The paths followed by the two primaries are identical to the orbits described by the two point mass models, in other words simple conic sections. This is not a bad approximation considering that 95% of the disk mass is contained within 4.5 kpc of the center of the disk. The smallest orbital radius at which stars are placed was 10 kpc which encloses 99% of the disk mass. The presence of the disk affects the radial acceleration of the stars very little, but it does produce a significant restoring force in the Z direction. It is important to emphasize that this disk potential is forced on the model and is in no way sensitive to the positions, or for that matter even the existence, of the stars. This is a first order approximation. If the stars are observed to move far from the plane of the disk, then it would be seen to be a bad approximation. Comparison with models having no disk at all will allow some intelligent judgment of this point.

Having found a rule for estimating $\sigma_z(r)$ it remains to implement the disk potential calculation economically. Since the calculation of acceleration at any arbitrary point due to the disk is a very time consuming one and since the disk is not changing in time in these models, it was decided that the best method of implementing the disk was via a table look-up scheme. A two dimensional table of acceleration tabulated at intervals in radius in one coordinate and altitude in the other coordinate was calculated and punched on cards. This table served for all simulations involving the disk. The table was calculated with rather simple and inefficient methods because it need be done only once, but the best method for performing this calculation is probably that described by Schaefer, Lecar, and Rybicki (1973) involving elliptical integrals. The table extended from 0 to 22.5 kpc in radius and from 0 to 18.5 kpc in Z. Any star that fell outside this range was treated with a point mass potential because at distances that large, the difference between the acceleration due to a point mass and that due to a disk is less than 1%.

The plane which has been discussed so far is implicitly two dimensional. The Z component of force due to a truly two dimensional plane has a maximum at Z = 0 and is nearly constant for small Z. This is definitely not the case for an extended disk, that is, one which has some thickness. In the latter case the Z component of force is zero at Z = 0 and increases as a function of Z until a maximum is reached some distance above the plane. Thereafter it decreases monotonically with increasing Z. At larger Z there is little difference between the two types of disk. The desired effect was achieved in the table by simply

forcing the Z component of force to be zero at Z = 0. The program cal-
culates the acceleration due to the disk for a given point in space by
interpolating linearly between rows in the Z direction and via a La
Grange interpolation in radius. Thus the tabulation interval in Z de-
termines the altitude and magnitude of the maximum referred to above.
This interval was chosen to be 0.9375 kpc. This produces a Z dependence
for Z direction acceleration which approximates the form and magnitude
of Oort's (1965) curve deduced from observations of high latitude stars
in the solar neighborhood.

The calculation of initial conditions is sufficiently complex a
task so that it is desirable to have it done by a separate program.
This program allowed for the specification of all orbital parameters of
the two primary masses and for placing the stars in any specified plane
with or without a disk potential and with various amounts of velocity
dispersion. Velocity dispersion in all models where it was present was
introduced by first calculating the velocity vectors necessary to pro-
duce exactly circular orbits and then velocity perturbations were added
on, being calculated by a random number generator which populates a
specified gaussian distribution. One important exception to this method
of perturbing velocities will be noted below.

The simulator program accepts the initial conditions from the
above program along with some other parameters such as a time step size
changing criterion, the times at which a "snapshot" of the interacting
system should be taken by recording all position and velocity vectors,
and a criterion for deciding when to drop a star from the calculation

because it requires too many time steps to follow it through to the end of the simulation.

The calculations were performed on the CDC 6400 of The University of Arizona. This machine is particularly well suited to calculations of this nature. Having a 60 bit word, the single precision floating point format has nearly 15 significant digits and a total dynamic range of $10^{\pm320}$, so it is quite practical to perform the calculations in cgs units. For reasons of economy the major part of the program was written in assembly language with considerable care given to efficiency. The simplest models required about 3 CP minutes and the most complex ones about 10.

The crux of the calculation is the solution of a linear second order differential equation. Several different differential equation solving algorithms were experimented with including 3 and 4 point predictors and predictor correctors and Runge-Kutta methods. For a given step size the second order Runge-Kutta method was the most accurate, but involved a rather large amount of calculation at each step. The best overall efficiency in terms of achieving the desired accuracy in a minimum amount of computer time was found for the 4 point predictor. This algorithm was finally chosen for the simulation program and was used in conjunction with a second order Runge-Kutta starter. Since the positions of the two primaries are known analytically, they were not solved for as part of the three body calculation but were tabled at equal intervals in time. During the calculation they were obtained via a three point La Grange interpolation.

The motion of a given star is checked at every other time step
to see if the size of the time step should be changed. This is decided
on the basis of the distance the star moves per time step expressed as a
fraction of its distance from whichever galaxy attracts it more strongly.
The step size changing criterion was usually chosen so that this frac-
tional displacement was between one and two percent. Some experiments
with widely differing step sizes implied that the accuracy at this level
was more than adequate. To run a model from T = -10 to T = +5 required
500 to 1000 time steps for a typical star (recall that time is measured
in units of 10^8 years).

The appraisal of the results obtained from these calculations
depends strongly on their visual appearance. This makes flexibility in
graphic display extremely important. The simulation program writes the
three dimensional velocity and position vectors of all the stars on a
magnetic tape at the specified model times. The data on this tape were
then analyzed on a minicomputer with a highly interactive CRT display.
This allowed projection of the stars onto any desired plane, observing
the radial velocity of all the stars viewed from any arbitrary angle,
measuring the velocity dispersion within a specified volume of space,
and even viewing the galaxies in stereo. A hard copy device connected to
the CRT display provides permanent copies of anything drawn or written
on its screen.

Simulation Results

In order to provide a clear comparison with previous work the
simulations were done in two separate groups; the first without and the

second with a disk potential. In those simulations without a disk potential σ_z was set to zero because in the absence of a disk there is no restoring force in the Z direction. Having nonzero Z velocities in this case would only confuse the results and would not provide a fair test of the model's stability in the presence of velocity dispersion.

The first concern was verifying that the program worked correctly. A completely separate and distinct program which does a self-consistent N-body calculation using an entirely different algorithm was used. The agreement between the two programs was excellent. The next step was to duplicate some of the results of Toomre and Toomre (1972). Figures 3a and 3b show the first such comparison. Figure 3a is from Toomre and Toomre (1972), Figure 3b was produced by the author's program. The initial conditions and viewing angle are virtually identical except that here the stars were concentrated more in the outer parts of the disk which accounts for the enhanced fine structure. In this and all succeeding figures the three crosses represent the center of mass of the system and the centers of the two galaxies. The viewing angles are given as the apparent altitude and azimuth of the observer as seen from the center of mass and relative to the primary orbit plane. All simulations are arranged so that at perigalacticon the two primaries are exactly on the X-axis.

The model in Figures 3a and 3b is intended to produce a well developed bridge. The mass ratio is 1/4 ($M_1 = 1.0 \times 10^{11}$ M_o and $M_2 = 0.25 \times 10^{11}$ M_o) and the passage is parabolic. There is no disk potential present and the apparent disk is coplanar with the orbit plane of the two primaries. The length of the bridge at this time is about
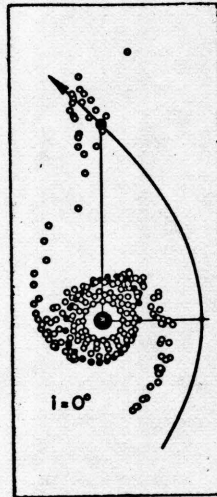
a. From Toomre and Toomre (1972).
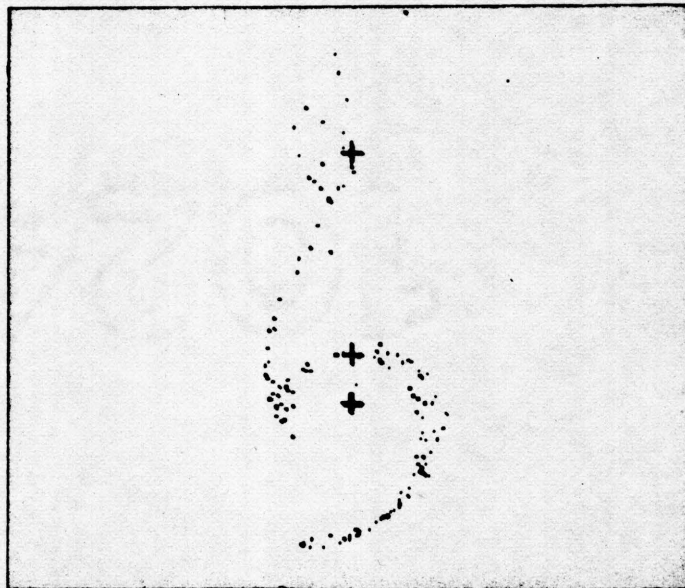
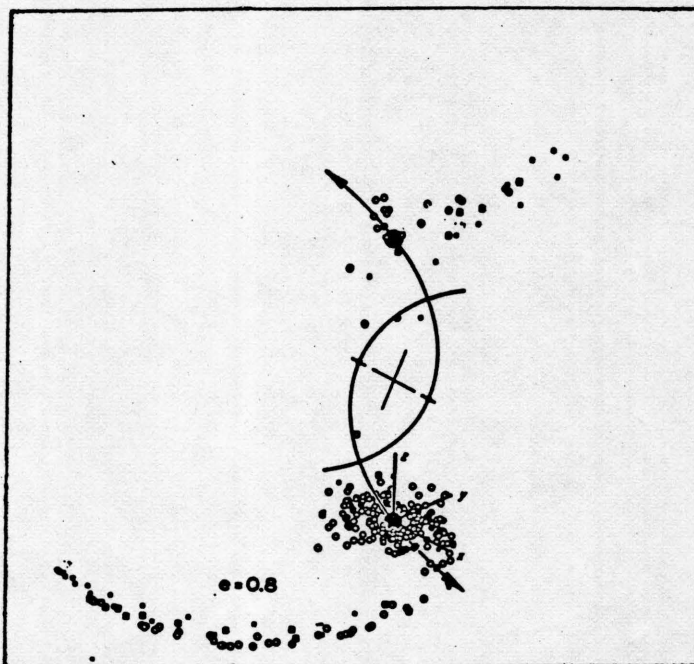
b. From the author's simulation program.

Figure 3. 1/4 mass model at T = 3.143 with no disk potential and no velocity dispersion, face-on view.

38 kpc. The apparent tail is more properly called a counter arm. Well formed tails are much longer as is shown in Figures 4a and 4b.

The equal mass models (each galaxy 1.0×10^{11} M_o) show much more strongly developed tails and virtually no bridge. Figure 4a is Toomre and Toomre's (1972) simulation of this system. Again, the two models shown in Figures 4a and 4b are identical except that the model done here has, in the interests of economy, a different total number and slightly different initial distribution of stars. The eccentricity of the orbit of the primaries is 0.8 and the view shown is chosen to emphasize the length and sharpness of the tail. Its projected length is about 60 kpc. There is no disk potential in the model in Figures 4a and 4b and the apparent disk in this model is initially inclined at 60 degrees to the primary orbit plane. It is seen fairly close to edge-on in this view. Figure 5 shows the same system at the same time in a face-on view and Figure 6 shows another view point intended to maximize the sharpness of the tail. This demonstrates how sensitive the appearance of the system is to viewing angle. There are many such examples possible.

The two models described above, the "1/4 mass model" and the "equal mass model" are here taken as the standard ones by which the effects of the addition of disk potential and velocity dispersion shown below are to be appraised. The figures showing the results of these models also contain a reproduction of Figure 3b or 4b in order to aid comparison with the standard models.

The effects of the addition of a disk potential to the standard models are shown in Figures 7, 8, and 9. Qualitatively no significant difference is produced. The disk has a slight tendency to reduce the

a. From Toomre and Toomre (1972).

b. From the author's simulation program.

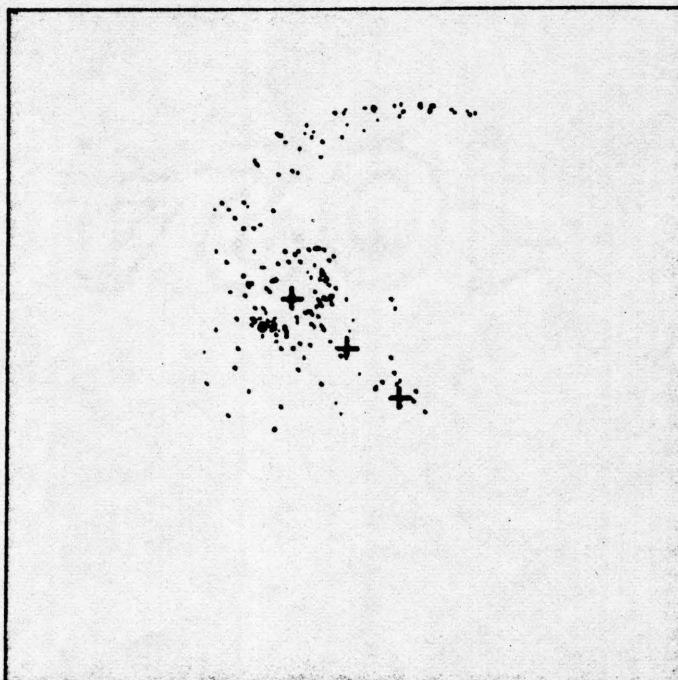Figure 4. Equal mass model at T = 5 with no disk potential and no velocity dispersion, viewed from $(0^0, 45^0)$.

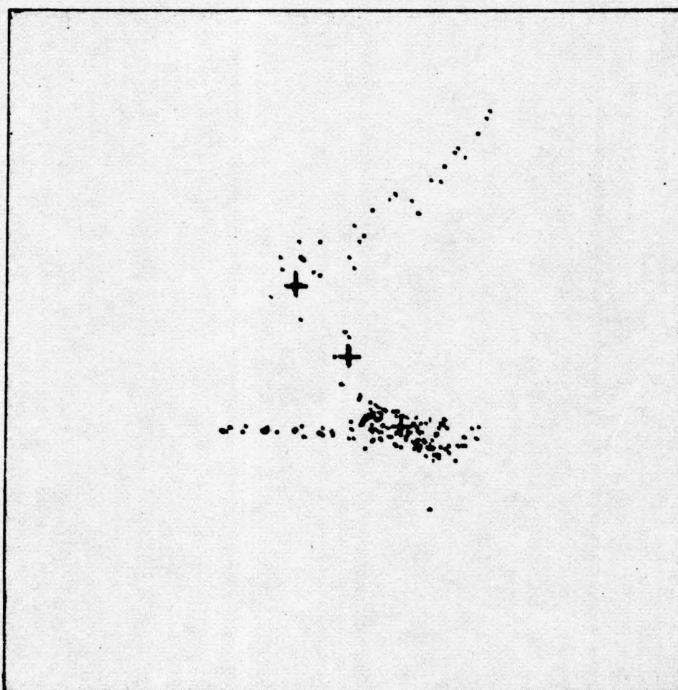Figure 5. Equal mass model at T = 5 with no disk potential and no velocity dispersion, face-on view (90°, 30°).

Figure 6. Equal mass model at T = 5 with no disk potential and no velocity dispersion, edge-on view (270°, 45°).
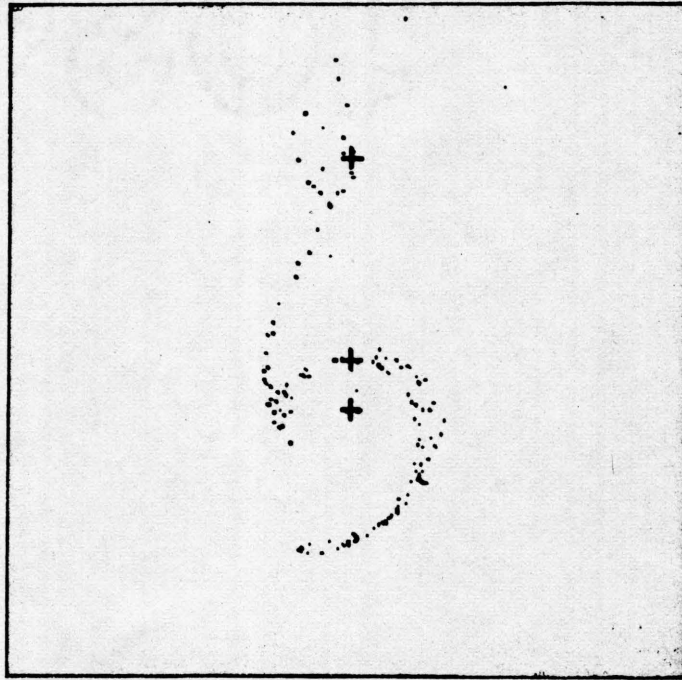
Figure 7.   1/4 mass model at T = 3.143, disk potential is present
but there is no velocity dispersion.   Face-on view.
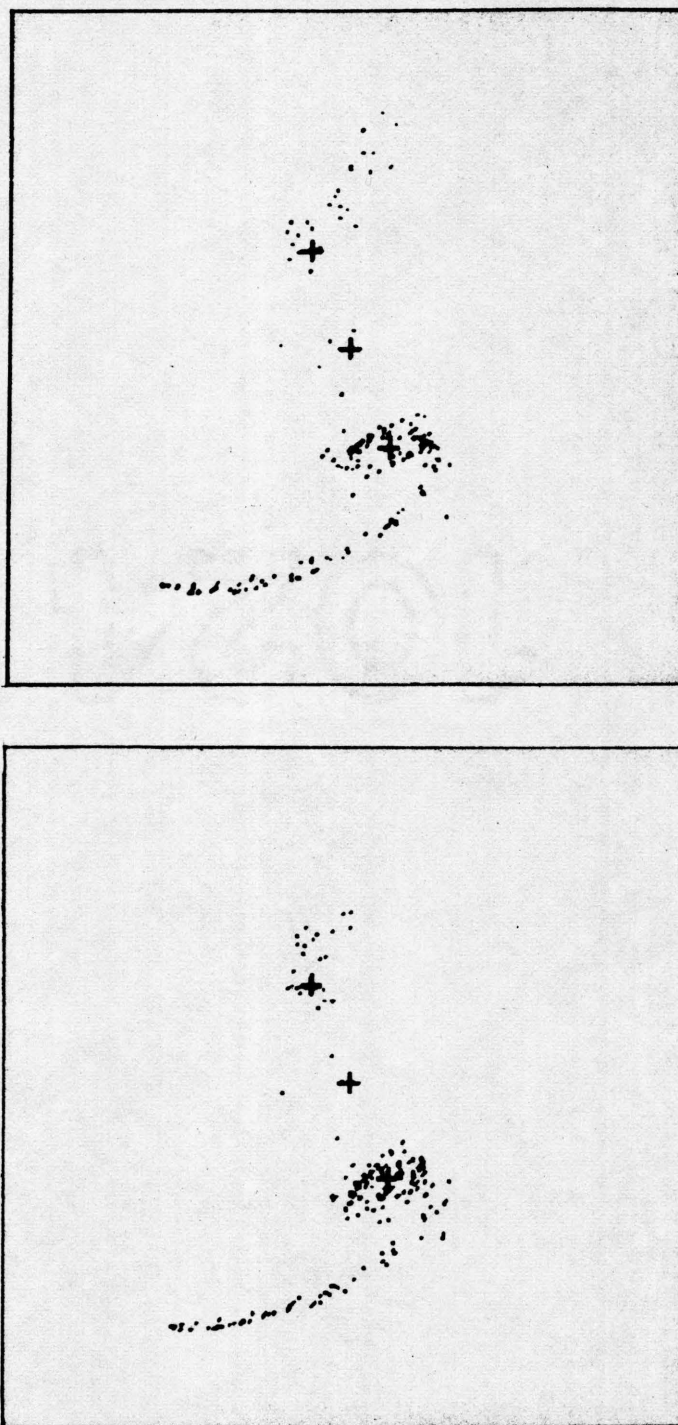
Top picture is the same as Figure 3b.

Figure 8. Equal mass model at T = 5, disk potential is present
but there is no velocity dispersion. Viewed from
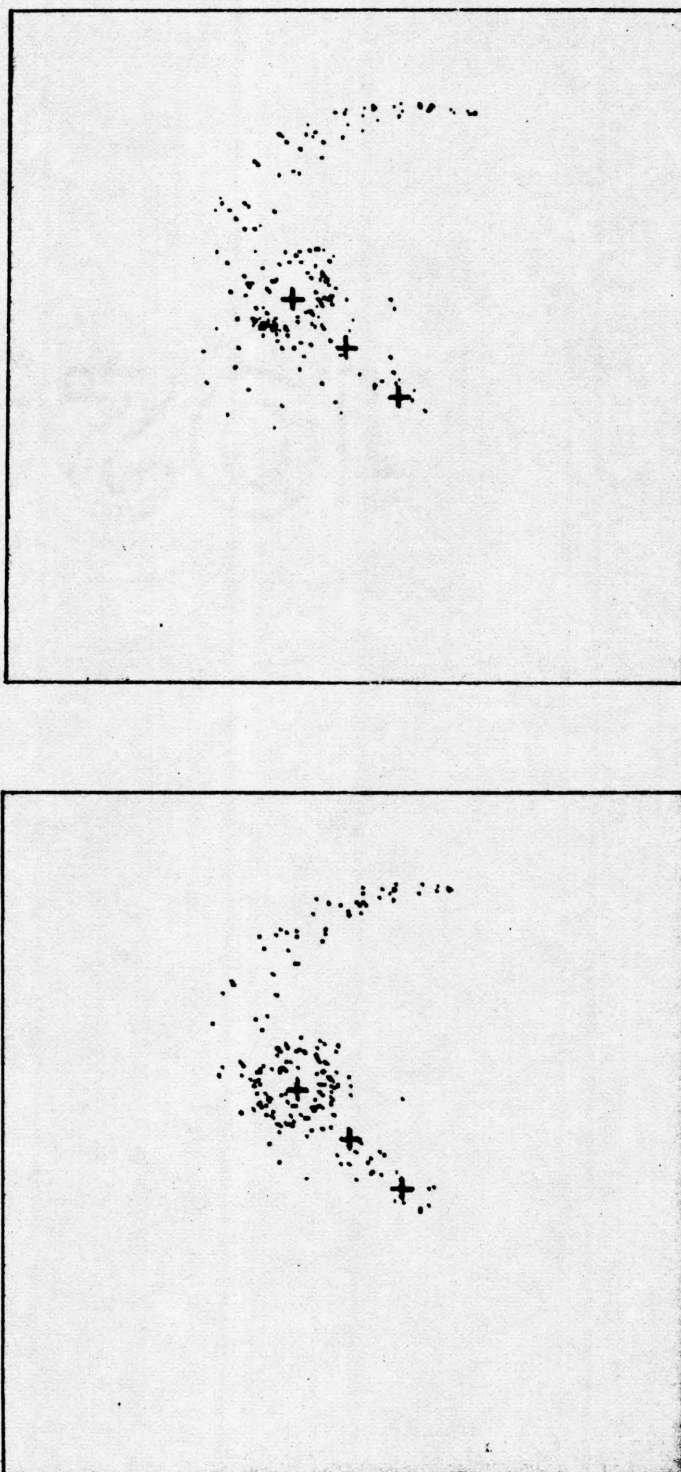(0°, 45°).

Top picture is the same as Figure 4b.

Figure 9.   Equal mass model at T = 5, disk potential is present
but there is no velocity dispersion. Face-on view.

area over which the stars are spread, to keep them a bit more closely coiled about their parent, but the overall result is essentially the same.

Figure 8 shows the equal mass model with the addition of a disk potential. The accompanying illustration of the standard model shows that the two models are, again, virtually identical except for the slight tendency of the disk to keep the stars from spreading as much.

These results are to be expected. All of the stars in the models discussed above have no component of velocity perpendicular to the plane by merit of the initial conditions and at their distance from the nucleus of their parent galaxy, the disk potential's radial component differs only negligibly from that of a point source. The major purpose of these models was to verify that the disk potential was working properly by showing the same results as the previous models.

A moment's thought gives a plausible explanation of the tendency of the disk to suppress the scattering of stars. First the stars have slightly less kinetic energy in the presence of a disk to start with simply because they are in orbit about an extended body. Second, and far more important, is the fact that a star passing near a point mass nucleus is accelerated much more strongly than one passing near the nucleus of an extended galaxy. Given the intervention of the perturbing mass at the proper time, a star can easily retain the velocity it gained as a result of this passage. Failing that intervention, it is at least deflected through a smaller angle by the disk than by the point mass. This is verified by watching the progress of the model.

The next series of models show the addition of velocity dispersion to the 1/4 mass model. Figures 10a and 10b show this model with $\sigma_x/\theta = 1/12$ and $\sigma_x/\theta = 1/6$ respectively. As explained earlier, $\sigma_y = \frac{1}{2}\sigma_x$ $\sigma_z = 0$ because no disk is present. Typical values of velocity dispersion are $\sigma_x = 15$ km/sec in Figure 10a and $\sigma_x = 29$ km/sec in Figure 10b. Even in Figure 10b the basic pattern is still visible, although quite blurred. It is clear that typical old Population I velocity dispersion is close to critically high values beyond which well defined bridges are not produced.

Figure 10c shows the same model with a disk potential present. Here velocity dispersion is present in all three coordinates. Values of σ_z run from 12 km/sec in the innermost ring to 7.8 km/sec at the edge. This extra bit of random energy was evidently enough to disperse the bridge completely.

In Figure 3b, the bridge, although well defined, is made up of only about a dozen stars (about 7% of the total). It is quite difficult to make a realistic model which has a much more substantial bridge. So it is plausible that true bridges would be sensitive to this sort of disruption. However, it should be remembered that a system with a long tail can often be mistaken for one with a true bridge if it is viewed at the right angle. The equal mass system of Figure 4b is such a model and the tail contains some 60 stars or about 30% of the total. One would expect it to be somewhat more difficult to disrupt.

Figures 11a, 12a, and 13a show the standard equal mass model from three different viewpoints with $\sigma_x/\theta = 1/12$. Figures 11b, 12b, and 13b show the same model with $\sigma_x/\theta = 1/6$. The face-on view in Figure 12b
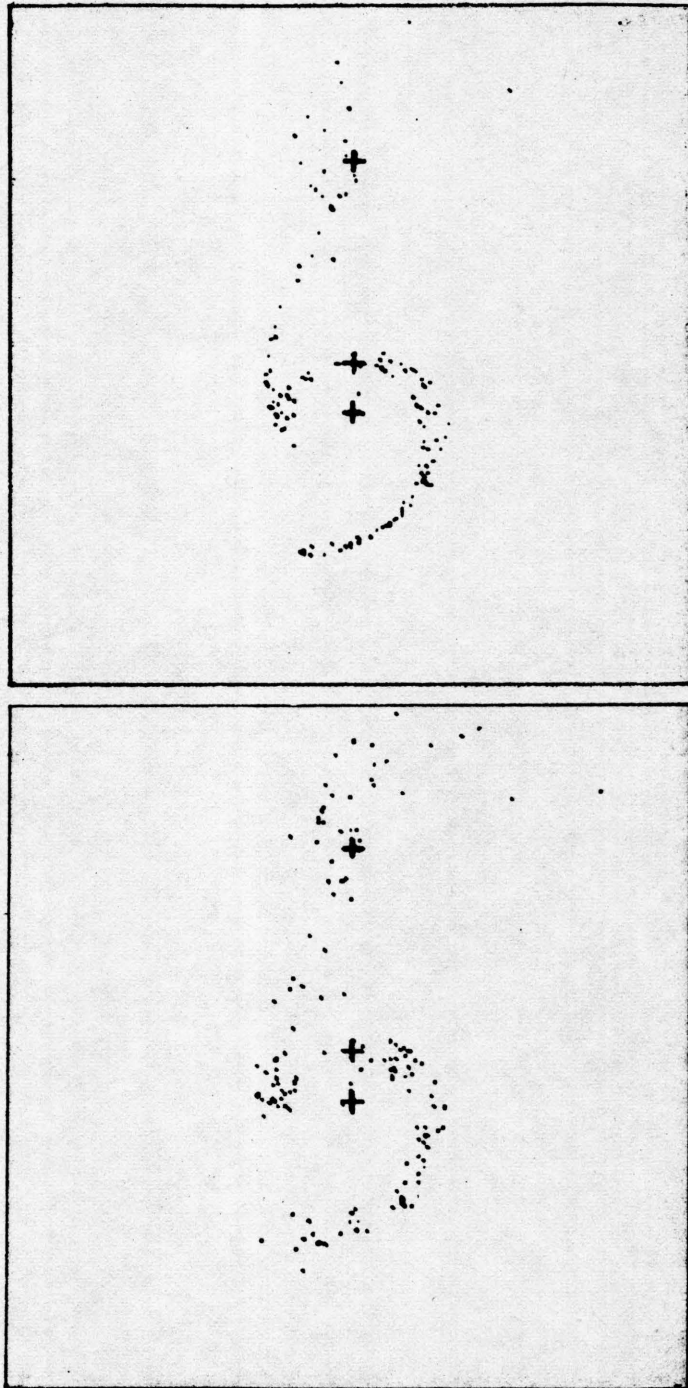
Figure 10.   1/4 mass model at T = 3.143, face-on view.

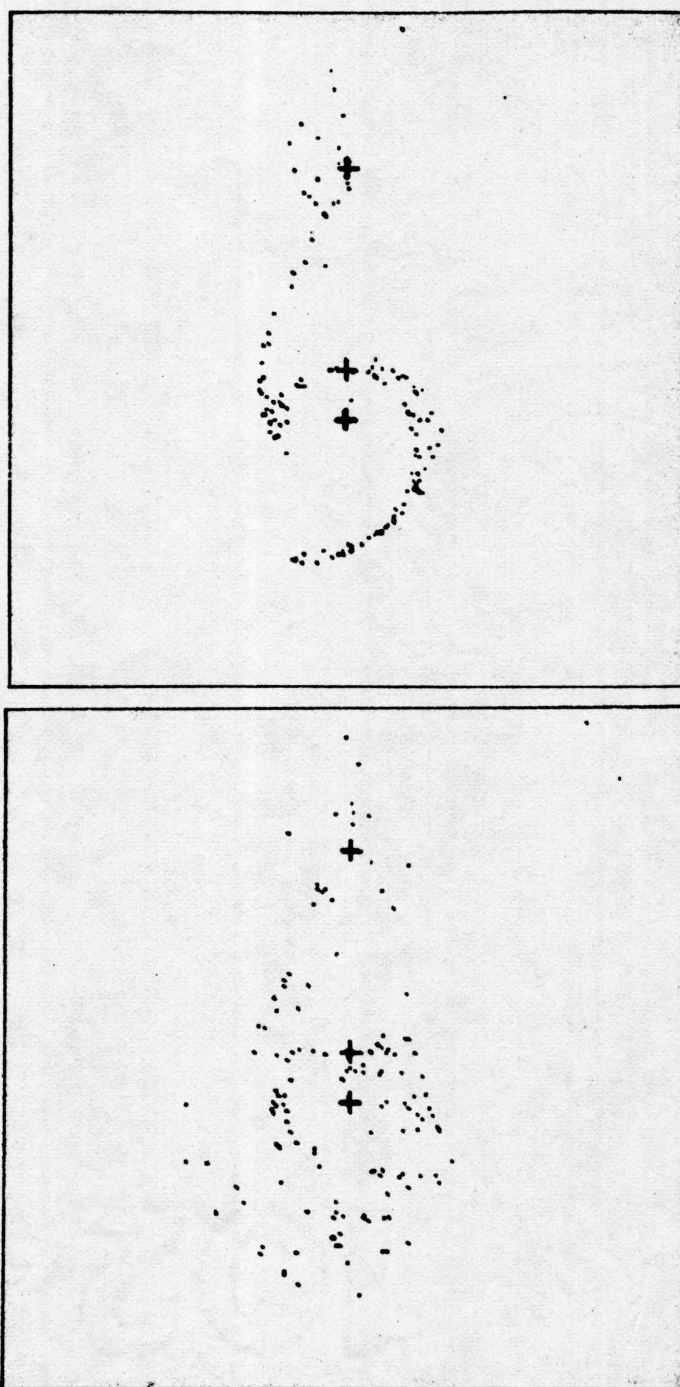a. $\sigma_x/\theta = 1/12$, $\sigma_y = \frac{1}{2}\sigma_x$ and $\sigma_z = 0$ with no disk potential.

Figure 10.   1/4 mass model, continued.

   b. $\sigma_x/\theta = 1/6$, $\sigma_y = \frac{1}{2}\sigma_x$ and $\sigma_z = 0$ with no disk potential.

Figure 10. 1/4 mass model, continued.

c. $\sigma_x/\theta = 1/6$, $\sigma_y = \frac{1}{2} \sigma_x$ and $\sigma_z \neq 0$. A disk potential is present.

Figure 11.   Equal mass model at T = 5, viewed from (0°, 45°).

a. $\sigma_x/\theta = 1/12$, $\sigma_y = \frac{1}{2}\sigma_x$, and $\sigma_z = 0$ with no disk potential.

Figure 11. Equal mass model, continued.

b. $\sigma_x/\theta = 1/6$, $\sigma_y = \frac{1}{2}\sigma_x$ and $\sigma_z = 0$ with no disk potential.
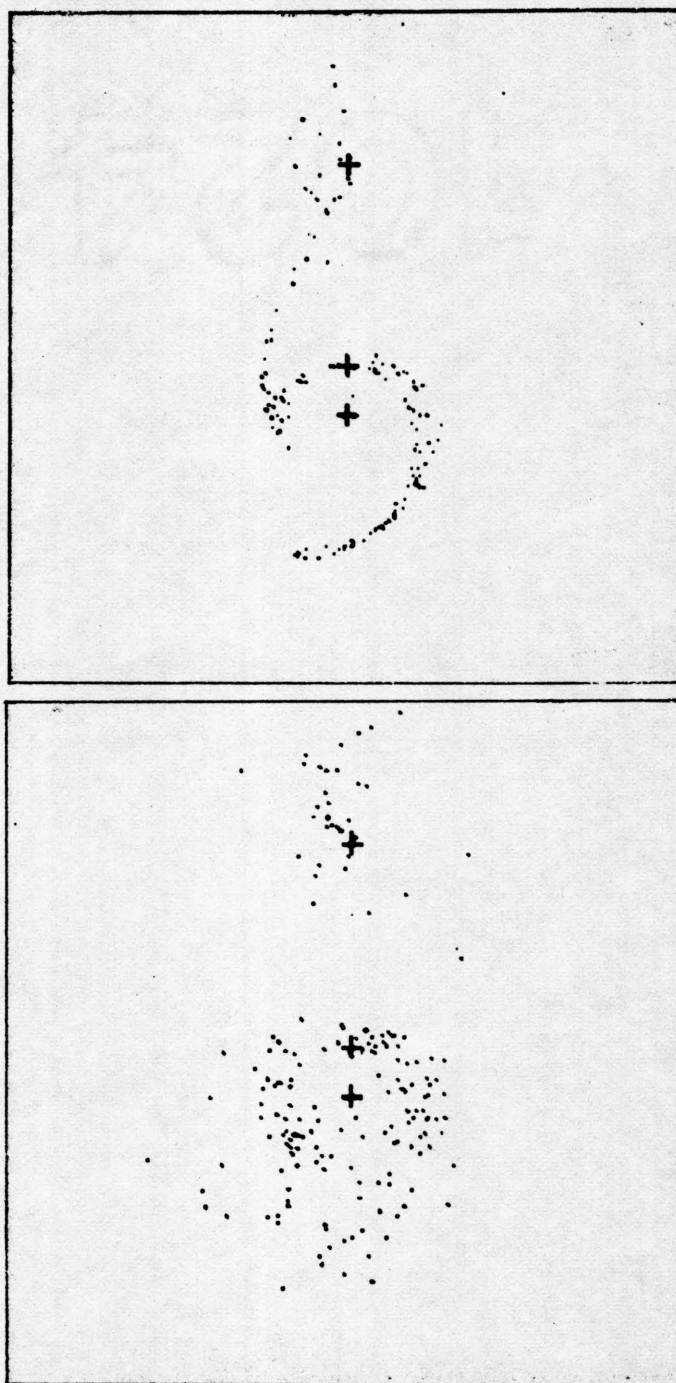
Figure 11. Equal mass model, continued.

c. $\sigma_x/\theta = 1/6$, $\sigma_y = \frac{1}{2}\sigma_x$ and $\sigma_z \neq 0$. A disk potential is present.

Figure 12.   Equal mass model at T = 5 in a face-on view.

a. $\sigma_x/\theta = 1/12$, $\sigma_y = \frac{1}{2}\sigma_x$ and $\sigma_z = 0$ with no disk potential.
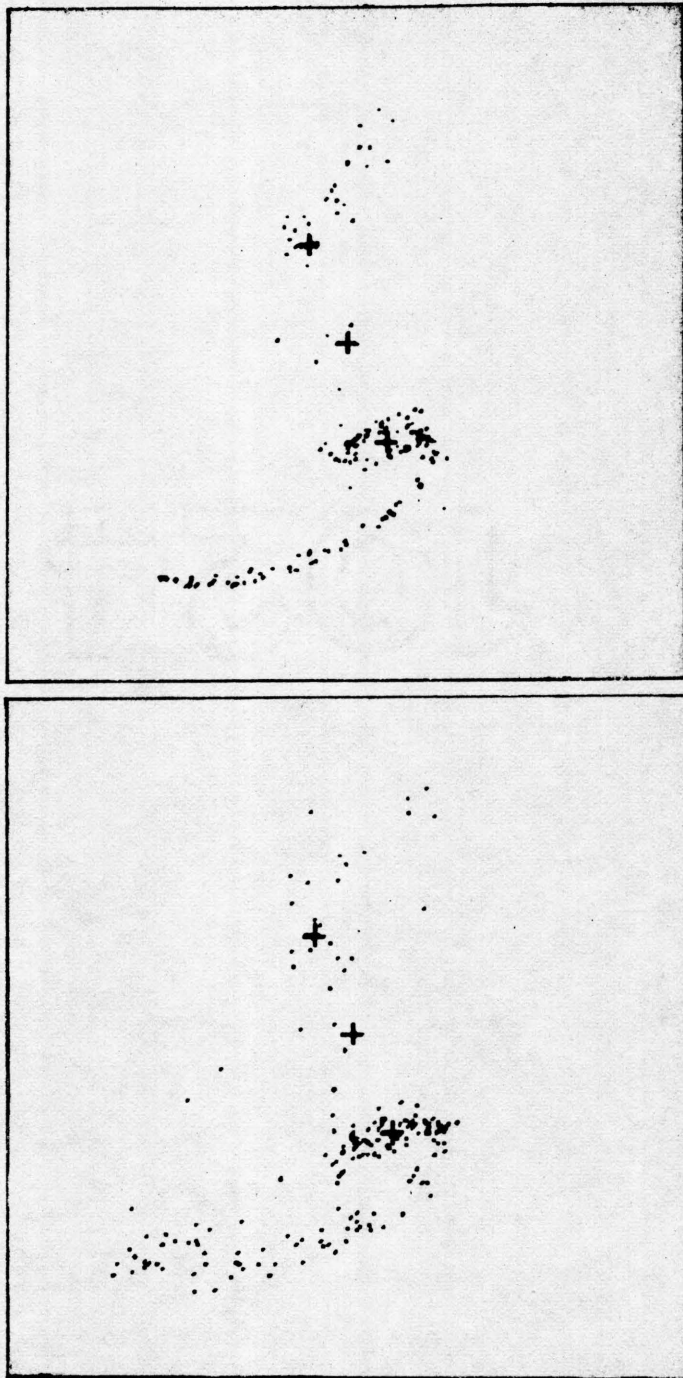
Figure 12.   Equal mass model face-on, continued.

b. $\sigma_x/\theta = 1/6$, $\sigma_y = \frac{1}{2}\sigma_x$ and $\sigma_z = 0$ with no disk potential.

Figure 12.   Equal mass model face-on, continued.

c. $\sigma_x/\theta = 1/6$, $\sigma_y = \frac{1}{2}\sigma_x$ and $\sigma_z \neq 0$.   A disk potential is
present.

Figure 13. Equal mass model at T = 5 viewed from (270°, 45°).

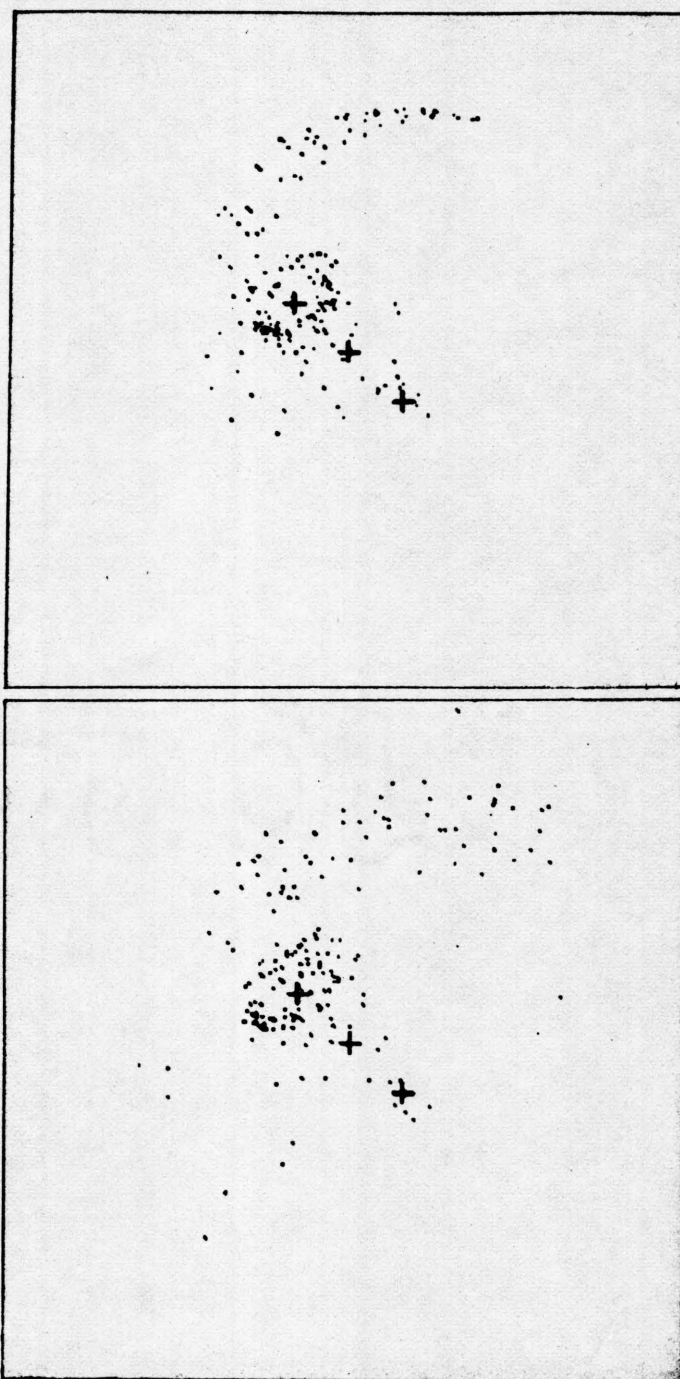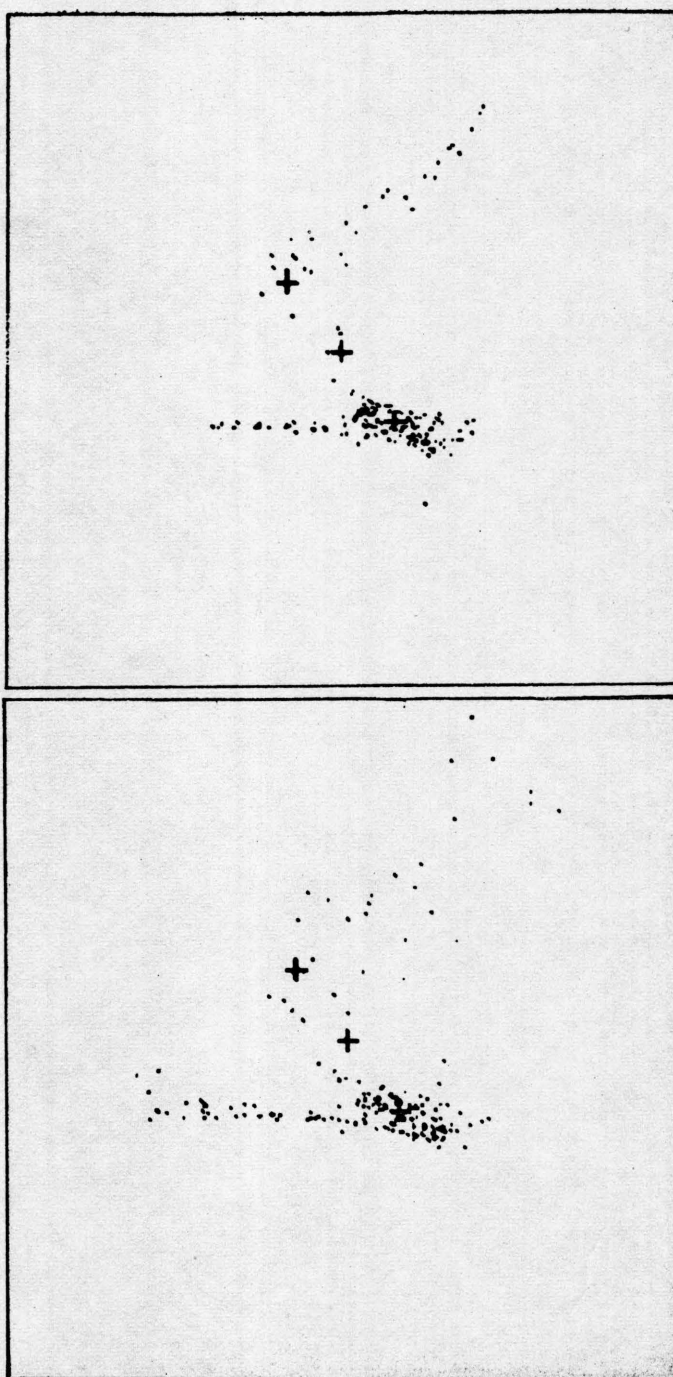a. $\sigma_x/\theta = 1/12$, $\sigma_y = \frac{1}{2}\sigma_x$ and $\sigma_z = 0$ with no disk potential.

Figure 13. Equal mass model, continued.

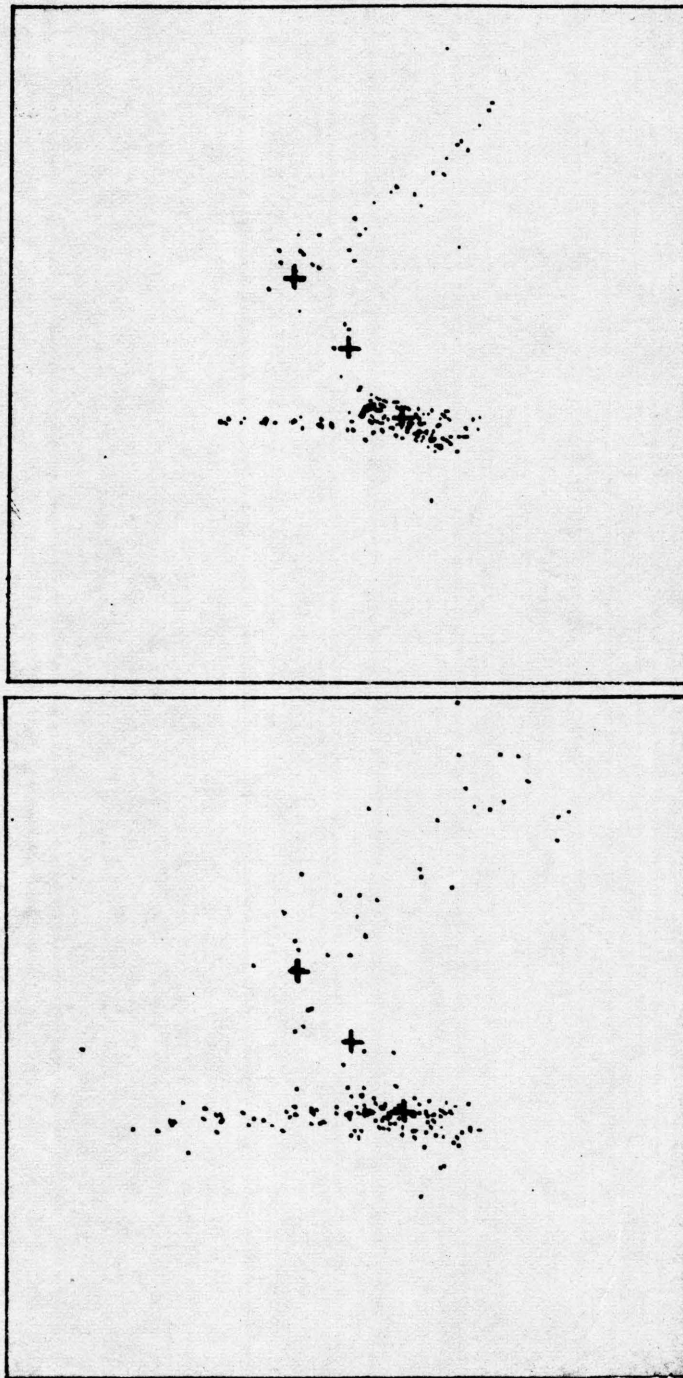b. $\sigma_x/\theta = 1/6$, $\sigma_y = \frac{1}{2}\sigma_x$ and $\sigma_z = 0$ with no disk potential.

Figure 13. Equal mass model, continued.

c. $\sigma_x/\theta = 1/6$, $\sigma_y = \frac{1}{2}\sigma_x$ and $\sigma_z \neq 0$. A disk potential is present.

reveals the most violent disruption but the structure seen in the standard model is still recognizable. More edge-on views seem remarkably unaffected. This is surprising since the plane of the disk was sharply inclined (60 degrees) to that of the primary orbit plane, so strong forces perpendicular to the plane were present. It is evidently due to the absence of Z velocity dispersion.

Figures 11c, 12c, and 13c show the same model with the addition of a disk and hence $\sigma_Z \neq 0$. The face-on view is quite badly disrupted, almost beyond recognition, but the more edge-on views are still recognizable as tails, although at least two times wider than in the zero velocity dispersion case.

A careful look at the sequence of equal mass models shows that the total number of stars involved in the tail remains very nearly the same regardless of initial velocity conditions. Only in the worst case and only from a particular range of viewing angles (Figure 12c) may the tail be said to have been destroyed by the dispersion. An analysis of the velocities of all the stars in the tail relative to their primary shows that those in the tip of the tail are very energetic – many exceed escape velocity. Those closer to the primary are tightly bound. When the local velocity dispersion was measured in the tip of the tail for various models, it was found to have no significant dependence on initial velocity conditions. The stars are more widely dispersed in the models with more velocity dispersion but the measured velocity dispersion among neighboring stars in the tail always remains low. Evidently, travelling so great a distance very carefully segregates the stars in

space; if two stars are close together in space at the end of such a journey, they are also close together in velocity.

To reveal the effects of velocity dispersion more clearly three models were run with a very non-gaussian initial velocity distribution. This distribution had all odd numbered stars with exactly circular velocities and all even numbered stars with circular velocity plus (or minus) a constant velocity perturbation. This constant velocity vector was exactly $\theta/6$ in the radial coordinate and $\theta/12$ in the tangential (orbital) coordinate. Thus the distribution consists of two spikes. Half the stars are grouped at exactly circular velocities and the other half are all at circular velocity (in one model) plus or (in another model) minus $(\theta/6, \theta/12, 0)$. This is to represent the behavior of only those stars whose dispersive velocity is exactly one standard deviation from the mean.

In Figure 14 the 1/4 mass model is shown with the extra constant velocity vector added to every other star. The large dots are the stars with circular initial velocities, and the small dots are those with the extra bit of energy. It is very interesting to note that while both subsets of the stars have very strongly patterned initial conditions, only those with the circular velocities yield strongly patterned results. The other half of the stars are responsible for all of the diffusion seen in the model.

Figure 15a shows the equal mass model with the constant velocity vector added to every other star and Figure 15b shows the same model with that same constant velocity vector subtracted from every other star. Figures 16a and 16b are the same two models seen from a more edge-on

Figure 14. 1/4 mass model at T = 3.143 with no disk potential and a non-gaussian velocity dispersion, viewed face-on.

Large dots had initially circular velocities. Small dots had a constant positive velocity perturbation added to them.

Figure 15.   Equal mass model at T = 5 with no disk potential and a
             non-gaussian velocity dispersion, viewed face-on.

             Large dots had initially circular velocities.

        a.   Small dots had a constant positive velocity perturbation
             added to them.

Figure 15, continued.

       Large dots had initially circular velocities.

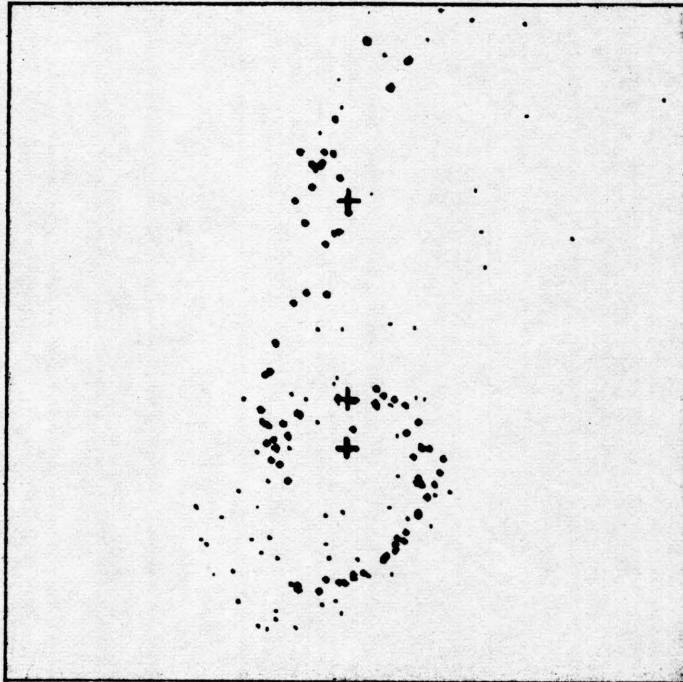b. Small dots had constant velocity perturbation subtracted from them.
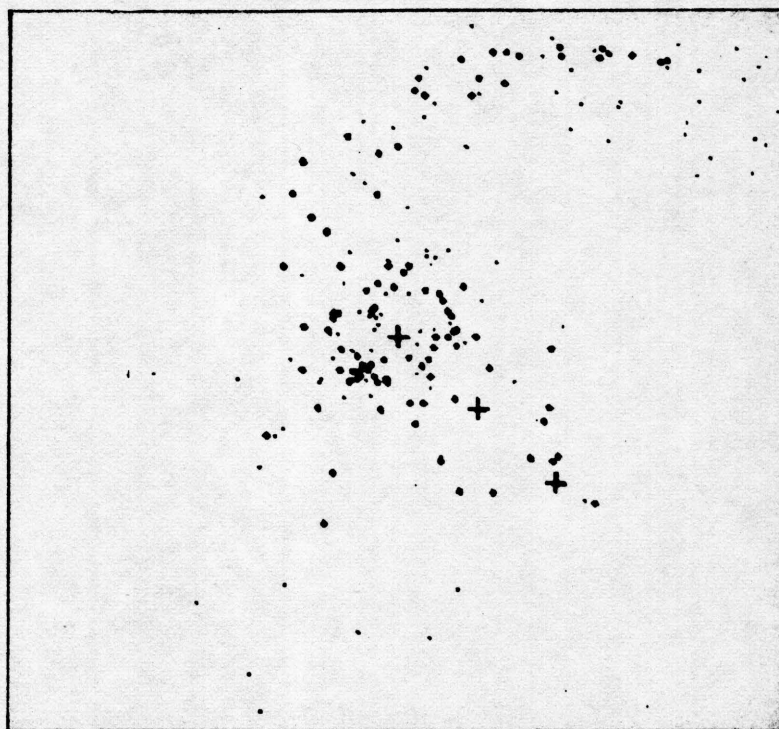
Figure 16.　Equal mass model at T = 5 with no disk potential and a
　　　　　　 non-gaussian velocity dispersion viewed from (0°, 45°).

　　　　　　 Large dots had initially circular velocities.

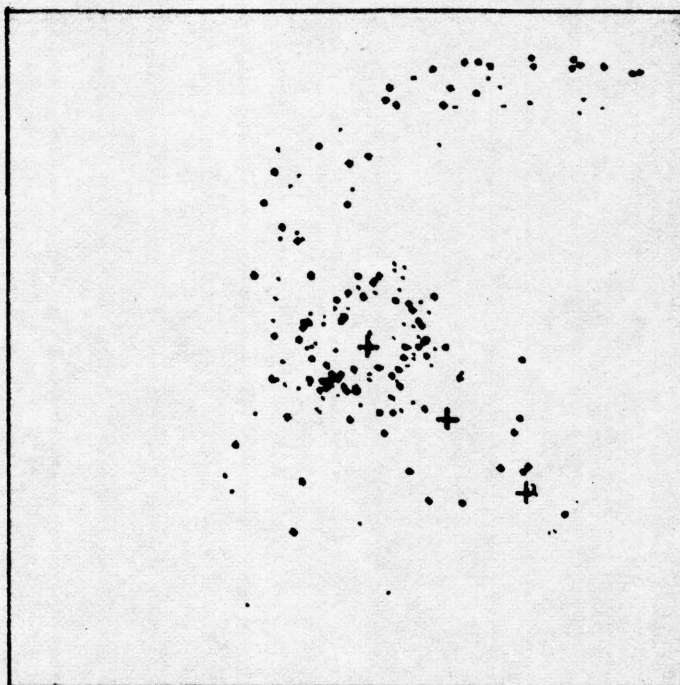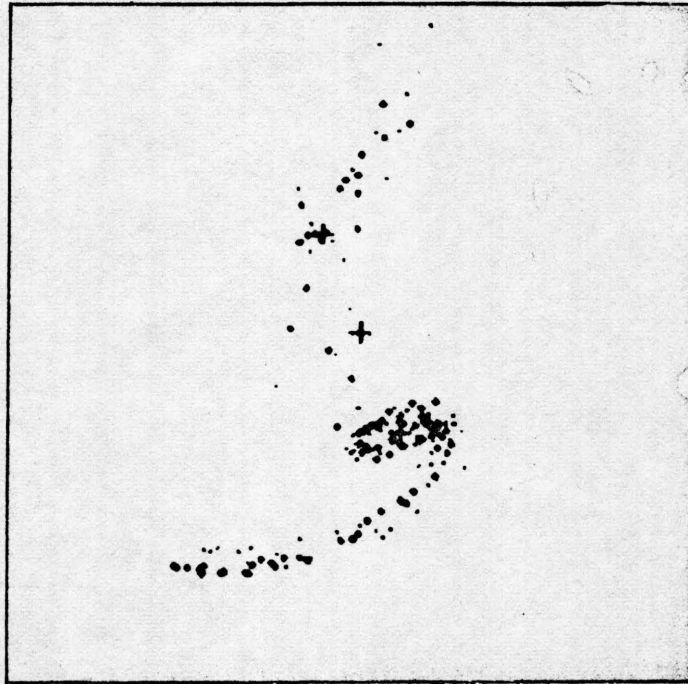　　a.　Small dots had constant velocity perturbation added to them.

Figure 16, continued.

Large dots had initially circular velocities.

b. Small dots had constant velocity perturbation subtracted
from them.

view point. The more energetic model shows the same result as above, but the less energetic stars in Figures 15b and 16b show virtually no diffusion. They are almost completely contained within the pattern of the zero velocity dispersion stars. This is very important. It means that roughly one third of a stellar population which has a high velocity dispersion -- the fraction that has positive dispersive velocity about equal to or larger than one standard deviation -- will appear physically dispersed. The rest of that population will follow very well the pattern of the zero velocity dispersion population.

Simulation of NGC 4676

One of the more striking results of the Toomre's work was their success at simulating several particular interacting systems, among them NGC 4676 (ARP 242, "The Mice"). With some experimentation they found that a model with two 1×10^{11} M_o galaxies in an orbit of eccentricity 0.6 with i = 15 degrees worked quite well. The model was begun at T = -16.0 and it is viewed at T = +6.1. Figures 17 and 18 show the author's rendition of this system in a face-on view and an edge-on view, the latter intended to duplicate the appearance of NGC 4676. This model attempts to reproduce only the long, narrow tail of NGC 4676A and only galaxy A was initially given satellites. The small number of stars around the other galaxy were captured from galaxy A.

It is impressive that one can mimic the appearance of such galaxies so well, but some quantitative evidence would be very welcome. One obvious way to do this is to observe the radial velocity distribution across the model and to compare it to that observed in the

Figure 17. Simulation of NGC 4676 at T = 6.1 with no disk potential and no velocity dispersion. Viewed face-on.
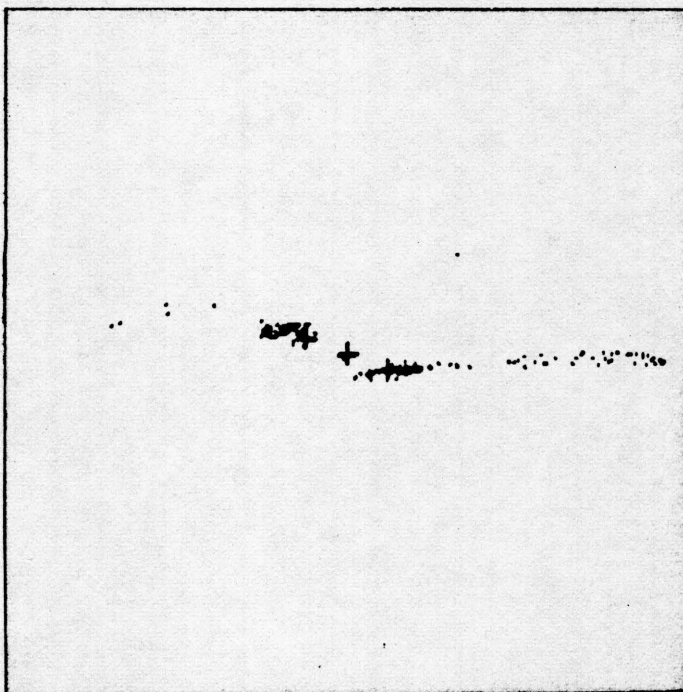

Figure 18. Simulation of NGC 4676 at T = 6.1 with no disk potential and no velocity dispersion. Viewed edge-on (166°, -14°).

interacting system. Very few galaxies are bright enough to allow this observation. The tail of NGC 4676A is unusually bright and Stockton (1974) has obtained image tube spectra of the tail. Figure 19 shows a sketch of the system and Figure 20 shows the observed radial velocity as a function of position along the tail.

The radial velocity of each star in the tail and body of galaxy A as seen from the viewing angle of Figure 18 is shown in Figure 21. It must be emphasized that this result is by no means unique. Variations of viewing angle and initial conditions can change the detailed appearance of this graph, but its essential characteristics remain: a very steep rise ending in a sharp discontinuity, then a region of much lower slope. Presuming that Stockton's observations simply do not extend far enough along the tail to show the turnover seen in the simulation, the agreement here is remarkably good.

It is interesting to note that if one associates the rightmost point of Stockton's graph with the maximum of the broad hump in Figure 21, then the distance from that point to the tip of the very steep portion gives a yardstick for measuring the distance to this system. This is observed to be 80 arcseconds on the sky and is about 55 kpc in the model. This implies a distance of 1.4 mpc. Since the mean redshift of this system is 6600 km/sec, a value of about 47 km/sec/mpc is implied for the Hubble constant.

The model of NGC 4676 was also investigated for the velocity dispersion effects that may be important in interpreting the observations of the next chapter. Figure 22a shows the same model as that of Figures 17 and 18 from a viewing position minimizing the thickness of
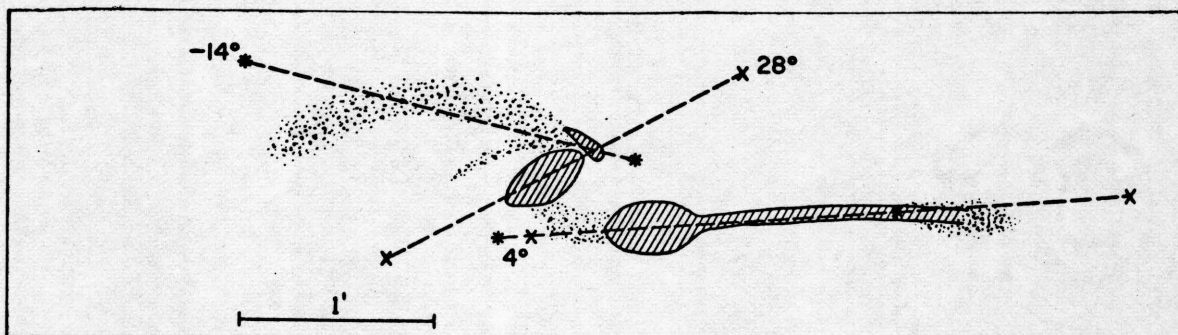
Figure 19. Sketch of NGC 4676 showing slit positions for image tube spectra taken by Stockton (1974).
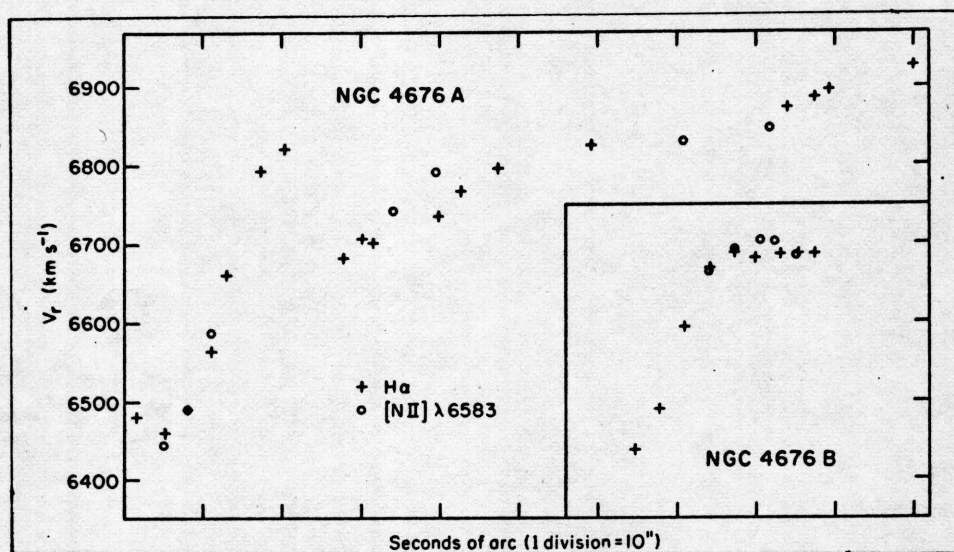
Figure 20. Plot of radial velocity versus distance along the tail of NGC 4676A. From Stockton's (1974) observations.
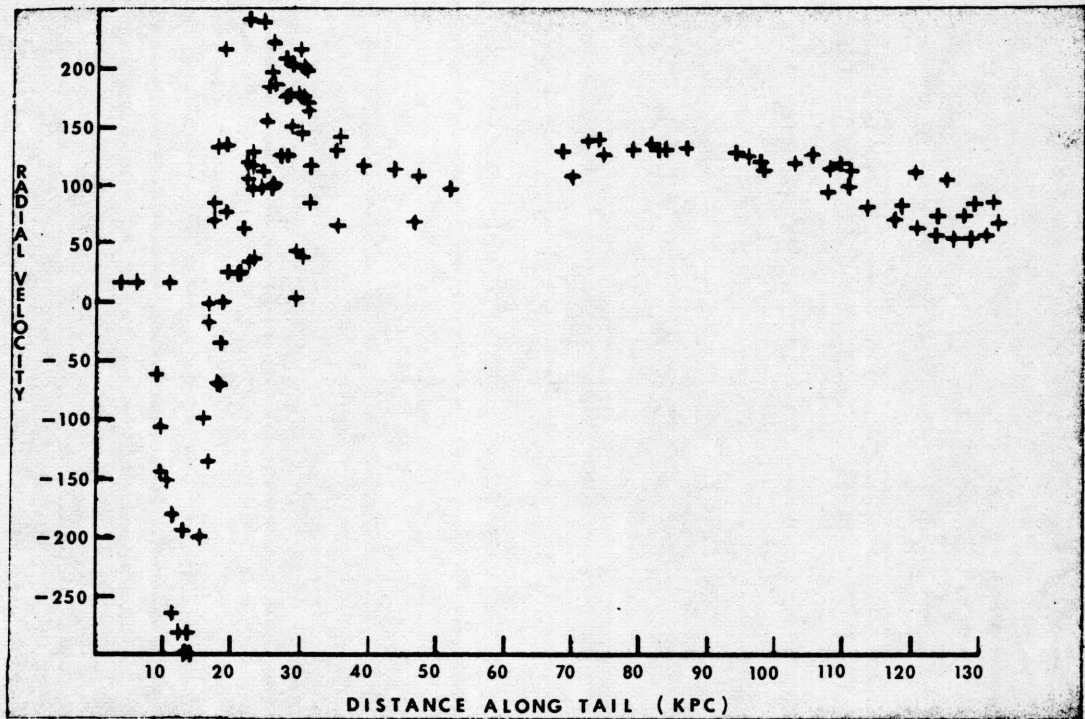
Figure 21. Plot of radial velocity versus distance along the tail in simulation of NGC 4676.
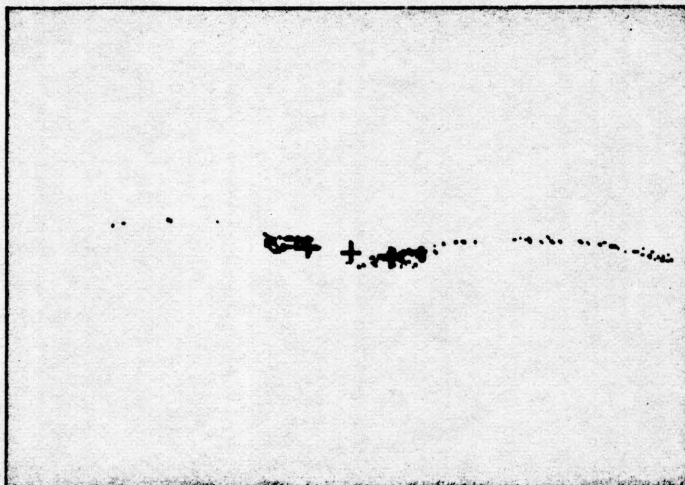
a. $\sigma_x = \sigma_y = \sigma_z = 0$ with no disk potential.
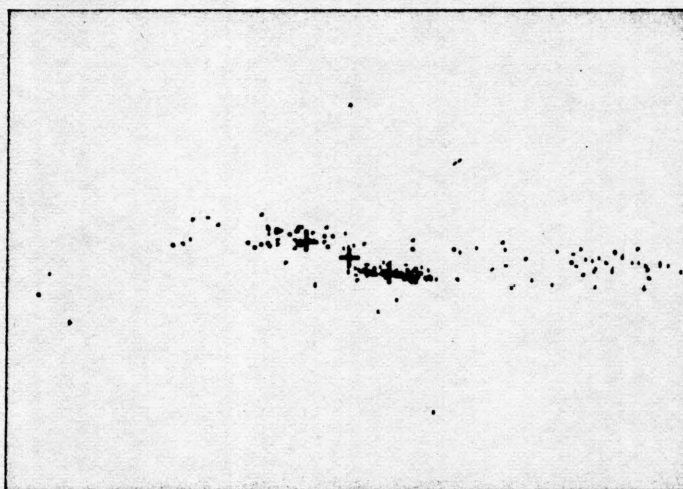
b. $\sigma_x/\theta = 1/6$, $\sigma_y = \frac{1}{2}\sigma_x$ and $\sigma_z = 0$ with no disk potential.

Figure 22. Simulation of NGC 4676 at T = 6.1 viewed from $(166^0, -5^0)$.
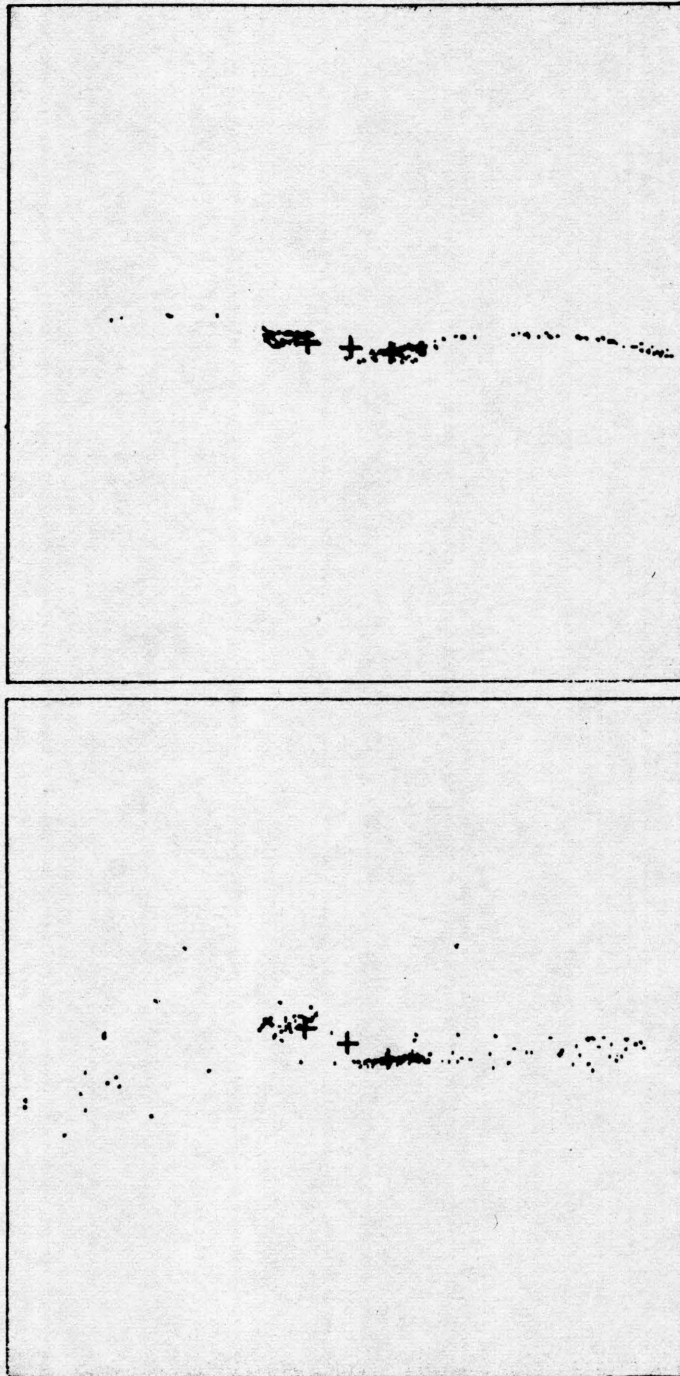
Figure 22, continued.

    c. $\sigma_x/\theta = 1/6$, $\sigma_y = \frac{1}{2}\sigma_x$ and $\sigma_z \neq 0$. A disk potential is present.

Figure 23.   Simulation of NGC 4676 at T = 6.1 in a face-on view.

a. $\sigma_x/\theta = 1/6$, $\sigma_y = \frac{1}{2}\sigma_x$, $\sigma_z = 0$ with no disk potential.
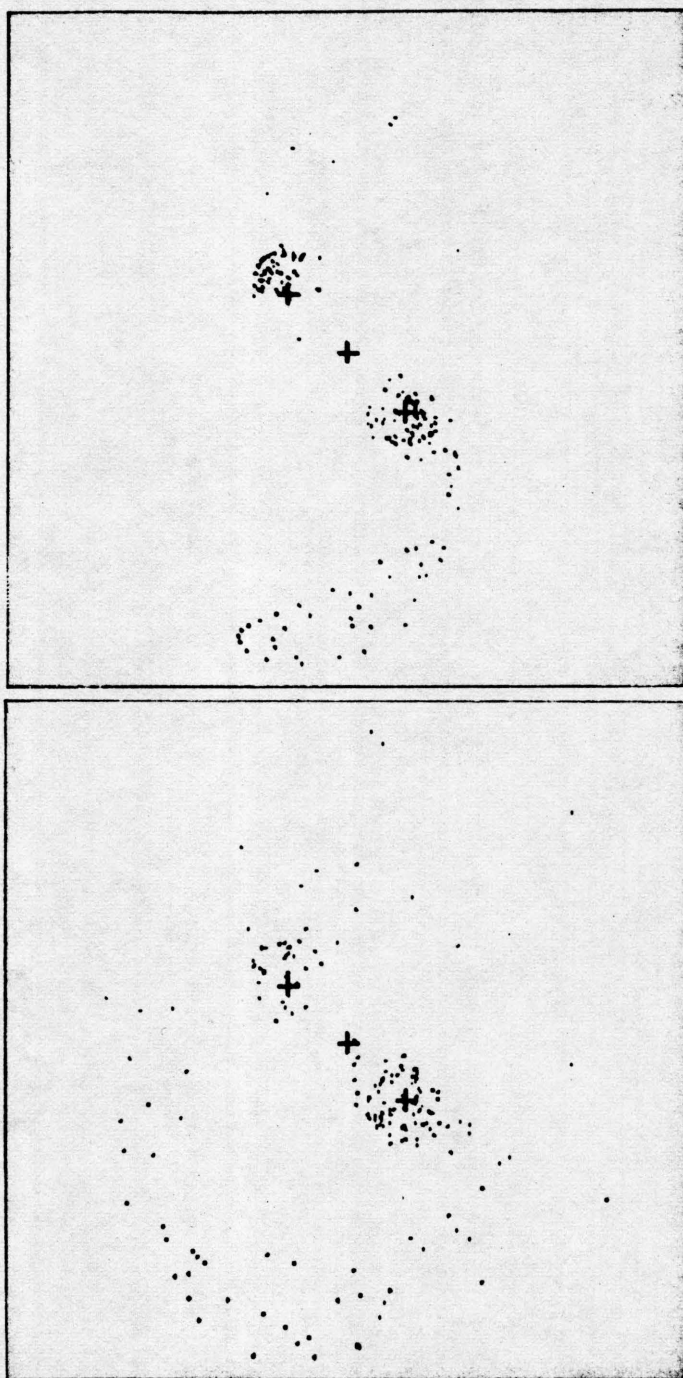
Figure 23, continued.

b. $\sigma_x/\theta = 1/6$, $\sigma_y = \frac{1}{2} \sigma_x$, $\sigma_z \neq 0$. A disk potential is present.

the tail. Figure 22b is identical to 22a except that a $\sigma_x/\theta = 1/6$ velocity dispersion has been added as with earlier models. Figure 22c has a disk potential and velocity dispersion. Figure 22a is reproduced in 22b and 22c for comparison. Figures 23a and 23b show the same two models from a face-on view.

This system is a striking example of both the dramatic effects of altering viewing angle and also the blurring effects of velocity dispersion. The sharpness of the filament is quite seriously degraded in Figure 22c, the model with the maximum random energy.

Conclusion

The approximations involved in the computer simulation of interacting galaxies are severe limitations on the models' generality, but clearly contain the essential physics necessary to describe the motions of stars during a single, long range encounter. Any analysis of detailed energetics, long term evolution, or short range encounters must use a different scheme.

The results of the models performed here are as follows.

1. The addition of a disk potential to the models reported in the literature to date in itself does not qualitatively affect the results. The disk is essential to any logical study of velocity dispersion, however.

2. The velocity dispersion used in these models was not excessive, yet models can be found whose acclaimed fine structure suffers very badly in its presence. The major fraction by mass of all the stars in the disk of the Milky Way belong to a population whose velocity dispersion

is $\sigma_x/\theta = 1/6$. These models then are quite representative and probably a bit conservative in implying the degree of diffusion of mass in an interaction. The major portion of the observed light from a galaxy does not come from this mass component however. See point 6 below.

3. Bridges are more sensitive to disruption largely because they are quite insubstantial. The results here indicate that any bridge observed must either be made of extreme Population I material or it is not a true bridge, but actually a tail seen in the appropriate projection. In light of this observation ARP 295, a system with an enormously long, narrow bridge, is very puzzling. The bridge is not only several galaxy diameters long but Beaver, Harms, Tifft and Sargent (1974) have shown it to have (B-V) of 1.0. Toomre and Toomre (1972) attempted a simulation of this system which was not entirely successful. The bridge, as usual, was composed of very few particles. Given the results obtained here, one must conclude that the bridge in this system either is not a true bridge but a tail seen in projection, or it was produced by a completely different mechanism. The former possibility is favored by the fact that the bridge is seen to extend beyond the smaller galaxy.

4. Tails are a good deal more resistant to disruption from velocity dispersion provided the viewing angle is correct. Tails are much more massive than true bridges. If a large tail were seen face-on, it might show a color gradient from the center to the edge, the bluest elements forming a bright core and the older red population diffusing over an area several times larger. This would probably be quite difficult to observe, however.

5. There has often been speculation that during an interaction strong compression or collision of interstellar clouds might produce regions of rapid star formation. The results found here indicate that the period of maximum compression is at perigalactic passage. That is the time when the distribution of material is pinched most strongly. This may not be very significant however, because, a) neighboring clouds of material have very low relative velocities, b) the behavior of the particles in these models indicates that the more two particles differ in initial energy, the less likely it is that they will find themselves close together in space. In other words, there is little chance for high energy collisions. The process is reminiscent of a mass spectrometer or centrifuge, tending to sort out the material rather than mix it up. But these are speculative statements. The particles in these models may behave very differently than does the interstellar medium.

6. The results obtained here have clearly shown that of the old disk population (main sequence stars of type G or later) those stars whose peculiar velocities are about one sigma greater than the mean are responsible for the observed diffusion. The stars with smaller velocity dispersions (the bluer stars) are scattered much less. How much can the observed color be expected to change because of the depletion of the red population? In order to estimate this the number density of stars of various spectral types in the solar neighborhood were taken from McCuskey (1965). The range from 0 to K6 along the main sequence was represented by 14 spectral intervals. Stars later than K6 were ignored because of their very low contribution to the net luminosity. Data on G8 to K6 giants were taken from Weistrop (1972). Only the main sequence

and the late type giants were considered. The absolute B and V luminosities for each type star were weighted by their number densities and summed. The ratio of the net B and V luminosities gives a B-V color of 0.63, which is a very plausible value. The color was then recalculated after decreasing the number density of main sequence stars of type G or later by one third and a value of B-V = 0.62 was obtained. The faint red stars evidently do not significantly affect the observed color. The late type giants are responsible for most of the red contribution, but their velocity dispersion is only one half to two thirds that of the solar type stars and they would be dispersed much less than the disk population. Nevertheless, if the numbers of these giants are also reduced by one third, which is excessive, the net color obtained in B-V = 0.54. This indicates that the change in color resulting from the dispersion of stars due to gravitational interaction is quite small-- smaller than the normal variations in color among galaxies of a given type or for that matter smaller than normal variations in color in the outer parts of a single galaxy.

CHAPTER III

OBSERVATIONS OF INTERACTING GALAXIES

Surface photometry was obtained for three different interacting

systems using the 229 cm (90 inch) telescope of Steward Observatory and

the 40 element digicon designed and built by Dr. E. Beaver at the

University of California at San Diego.

The Digicon Tube

The digicon is a conventional single stage magnetically focused

image tube whose target phosphor has been replaced with a silicon wafer

supporting 40 PN diodes. The diodes are each 0.089 mm square and are

deposited in a line on 0.101 mm centers. The actual sensitive area is

almost completely restricted to the area of the diodes themselves. A

photoelectron from the cathode is accelerated through approximately 20

kv and impacts on a diode typically producing a pulse of 4000 or 5000

electrons. Each diode has its own discriminator and pulse amplifier

easily capable of generating one digital output pulse for each incident

20 kv photoelectron. The pulses are counted in 16 bit accumulators

which are read out on a roughly 60 second time scale, the counts being

recorded on magnetic tape. This recording scheme produces a large vol-

ume of data, but allows for rejecting the occasional record which shows

a noise burst. In practice steering coils around the tube are driven so

that the electron image is stepped along the length of the line of

diodes in steps equal to one eighth of the diode spacing. This allows

the maximum possible resolution for the diode size. A detailed description of the tube is given by Beaver and McIlwain (1971).

The digicon was first used with a cassegrain spectrograph for recording spectra. Fortunately this same configuration with a slight modification proved almost ideal for doing direct surface photometry as well. The grating in the spectrograph is replaced with a flat mirror and the digicon tube is rotated ninety degrees so that the slit of the spectrograph is accurately parallel and in registration with the line of diodes in the tube. By moving the entire telescope and rotating its base ring which supports the spectrograph, the slit may be oriented to isolate any desired portion of a galaxy. Using the spectrograph also has the benefit of demagnifying the 10 arcsecond/mm plate scale of the cassegrain focus down to 57.3 arcseconds/mm. This gives each diode a width of 5.79 arcseconds or 0.72 arcseconds per one eighth step and increases the total length of the diode array to 231 arcseconds. This is a very good balance between resolution and field width. The oversampling due to the one eighth stepping allows in theory achieving an effective resolution of about 5.79/2 = 2.90 arcseconds which is about the size of the telescope's resolution element under typical observing conditions.

The digicon has an S11 cathode and is therefore easily applied to photometry using the UBV system. Only observations in B and V were made. The transformation problem is slightly complicated by the fact that two different sets of B and V filters were used. This was almost unavoidable. The first set was used for about one half of the data. It had a V filter with a peak transmission of 59% at 5300 Å and a full

width at half maximum of 590 Å. The B filter had a peak transmission of 72% at 4000 Å and a full width at half maximum of 1200 Å. These are both about 250 Å bluer than standard UBV. The V is a bit narrow and the B is a bit wide, but they can be expected to transform well enough to the standard system. One would expect this combination to work quite well as long as it is not applied to very cool stars with complex spectra. The second set of filters had a V filter of Schott OG4 and a blue filter of Schott GG13 and BG12. These are the filters recommended by Hardie (1962).

The overall sensitivity of the entire system was sufficient to produce between 1 and 2 counts per second per diode from a moonless sky through the B filter. Integration times of less than an hour usually produce sufficiently high counts to allow measurement of objects with surface brightness 2 or 3% above sky with 10 or 15% accuracy (counts from one diode only). The relative diode to diode sensitivity is quite stable within a given night, usually changing much less than 1%. The data also imply good long term absolute stability, although this is not essential for the measurements made here.

<u>Observing Method</u>

At the beginning and end of each night's observations the relative diode to diode calibration was obtained by observing the bright sky during twilight. This provides an ideal uniformly illuminated source which is at optical infinity. The calibration light therefore follows exactly the same path through the system as does the light from the galaxies. Figure 24 shows a typical calibration plot. This is formed by
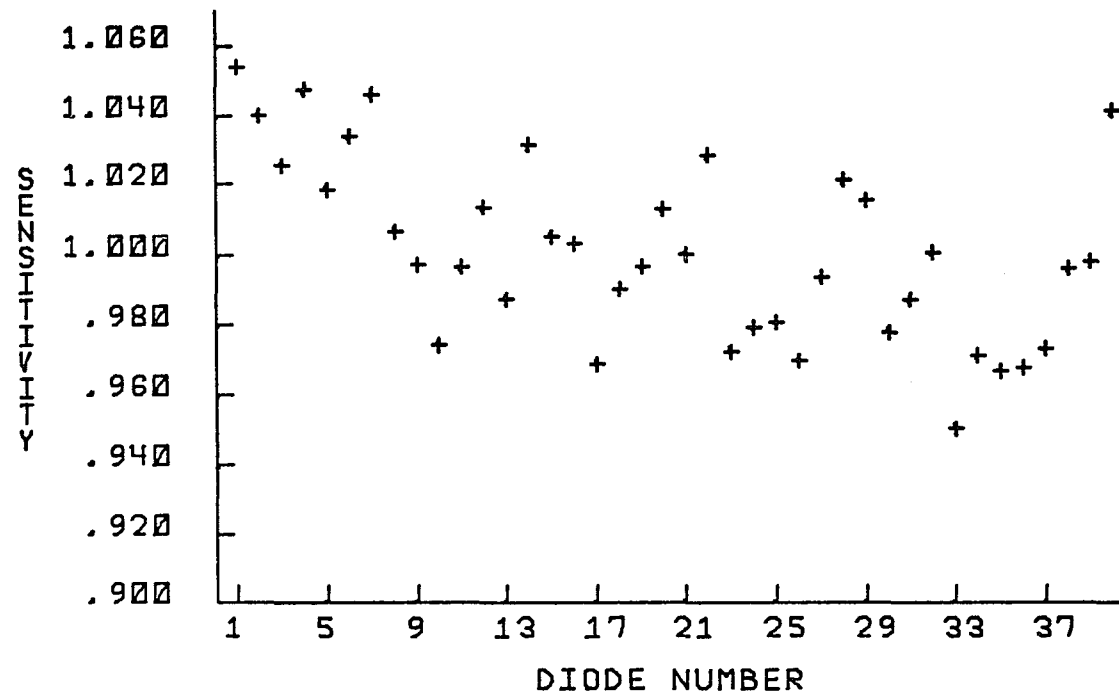
Figure 24. Relative diode calibration.

taking the average of the counts for all 40 diodes and displaying the counts for each diode as a fraction of this mean. The raw data are then multiplied by these ratios to correct them to the values that would have been obtained if all 40 diode-discriminator-amplifier units were exactly identical.

The position angle of the spectrograph slit for each desired scan was determined beforehand from a photograph of the object. These position angles appear to have an accuracy of about one degree as does the position angle adjustment of the base ring of the telescope. The slit was usually adjusted so that its projected image on the face of the tube was slightly larger than the width of the diodes. Thus, it had a length to width ratio of about 40 to 1 making a one degree error tolerable. In practice however, error in position angle is usually not important because the position of the faint object is directly visible by means of a sensitive TV camera. The camera is mounted to view the highly polished surface of the spectrograph slit jaws. The observer watching a TV monitor sees the image of the galaxy on the slit jaws cut by the black line of the slit opening itself. This usually makes it easy to verify that a given position angle does indeed include the desired features of the image and simplifies guiding as well, especially if there is a stellar object in the field of view.

The scans were to be calibrated in an absolute sense by including in the slit one of the brighter foreground stars which would later be observed with a conventional stellar photometer to determine its magnitude and color. Since one of the diodes is over 5 arcseconds on a side, it could be expected to hold the entire star image fairly well

even allowing for some seeing problems and small guiding errors. The
choice of position angle for the slit then, was usually constrained to
include a calibration star. It was also necessary to choose slit posi-
tions which had enough of the diode array measuring pure sky background,
preferably some at each end of the slit. A scan which contains no por-
tion which is clearly only sky is of little quantitative value.

Data Reduction and Calibration

Figure 25 shows a typical scan across NGC 2648. These are raw
counts corrected only for relative diode sensitivity. Recall that since
the electron image is one eighth stepped along the diode array, the data
displayed in Figure 25 are equivalent to what would be observed if there
were only one diode which was scanned along the slit with samples being
taken at intervals on one eighth of its width for a total of 320 steps.
The individual points are therefore not independent. Adjacent points
measure substantially the same area on the image -- about 6/7 of the area
of a single diode. This suggests a simple smoothing algorithm. Each
point in Figure 25 is averaged with the 3 points on either side of it
using weighting factors proportional to the amount of overlapping diode
area which the points have in common. It is easily shown that this
method is analytically exact as long as there are no gradients higher
than first order in the scan. This is equivalent to saying that on a
distance scale of 7/8 of the diode separation the scan can be well
represented by a straight line. This is an excellent approximation
almost everywhere in the scan. The technique is only necessary in areas
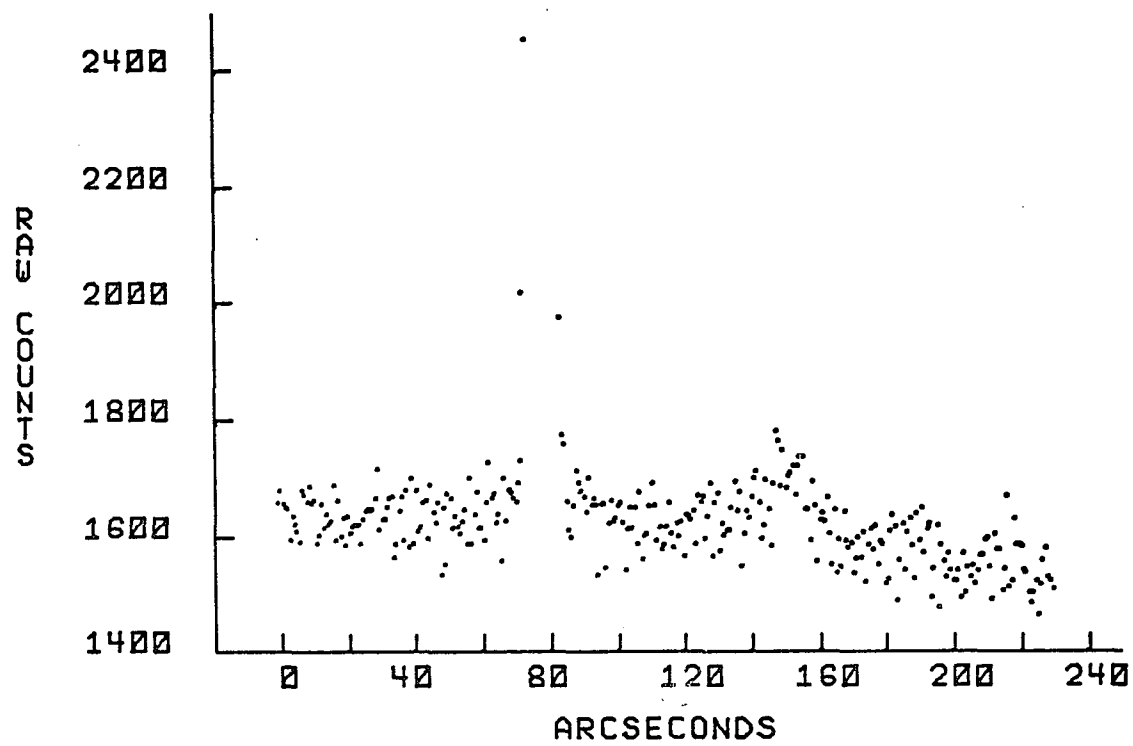where the counts are close to the sky level and these areas do not show

Figure 25.   Raw data.

steep slopes. The results of applying this smoothing algorithm to the scan in Figure 25 are shown in Figure 26. The smoothing clearly brings out the faint tail in NGC 2648.

Trying to determine a meaningful sky level for Figure 26 is rather confusing. One would expect the major source of noise in the counts to be simple square root noise from the counting statistics. The scatter in the unsmoothed data support this idea. Yet, there are several features present in Figure 26 which are rather large compared to the square root of the counts and which extend over many consecutive steps. These are found in virtually all smoothed scans, occasionally being quite large. The possibility was considered that these are real and that they are faint foreground stars, background galaxies, or perhaps until now undiscovered bits of flotsam which are always produced by the galaxy interaction itself. They are so faint as to be virtually undetectable on most photographs. However, intercomparison of scans taken at the same slit positions showed poor correlation of these features. It also showed that particular diodes are not chronically noisier than others and that true background objects are relatively rare. A chi-square test revealed no correlation of maxima or minima with a particular one eighth step within a given diode. It seems much more likely that these features are an effect of the smoothing algorithm applied to an essentially flat sky background which has square root noise present. To test this idea data with these characteristics were synthesized and smoothed. Figure 27 shows the unsmoothed data produced by selecting a sky level of 1000 counts and adding noise to it. The noise was derived from a random number generator which populates a specified gaussian
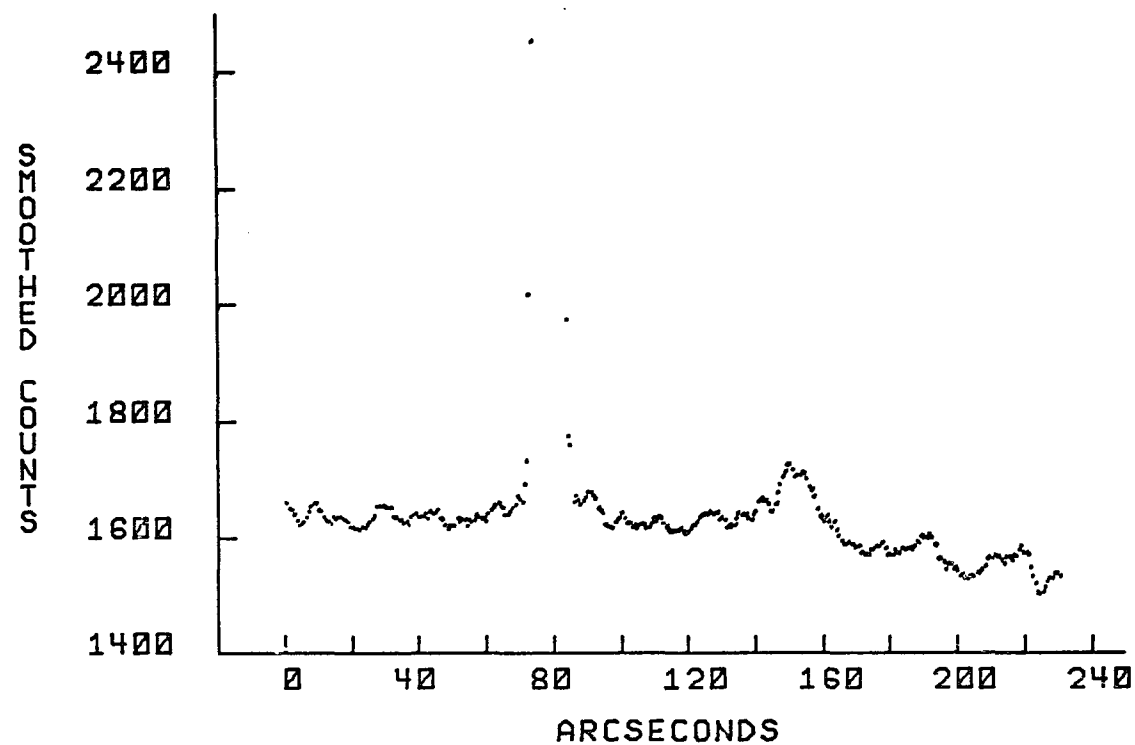
Figure 26.   Smoothed data.

Same data as in Figure 25 after
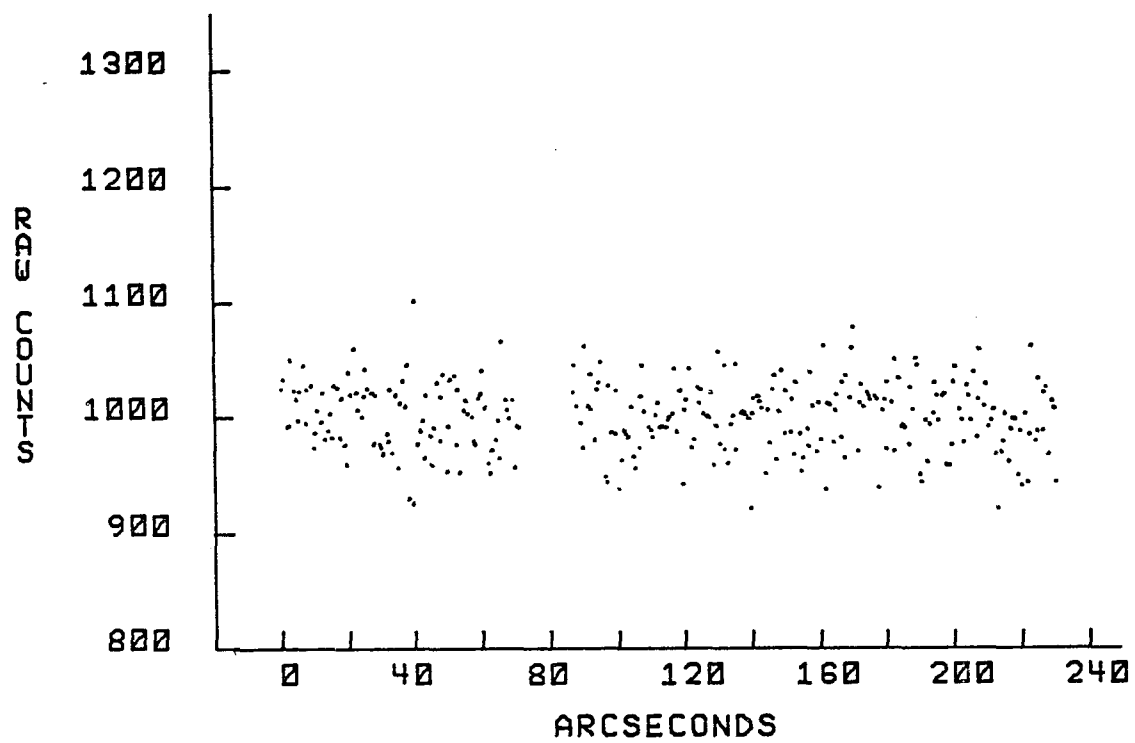application of smoothing algorithm.

Figure 27.   Synthetic data.

distribution. The result of smoothing this scan is shown in Figure 28 and are remarkably similar to the sky background seen in the smoothed scans. It is concluded that the small features are almost entirely due to counting statistics.

The sky levels for all scans were easily drawn in by hand using the knowledge gained from the noise experiment described above. They sometimes show a slight but real slope as is evident in Figure 26. The slope is usually less than 0.1% of the mean sky level per diode. Both positive and negative slopes are found. It is difficult to imagine a cause for this which would not be corrected for by the relative diode calibration. Possibly it can be attributed to a vignetting or a slight wedging of the slit jaws during the calibration scans which was not identical to the form it had during the actual observations.

After the sky level is determined and subtracted from the smoothed counts, they are converted to magnitudes using the relation

$$m = K - 2.5 \ Log(counts)$$

There are several ways to proceed from this point depending on the nature of the calibration data. In this case, as will be explained below, only the standard colors of the calibration objects were available, not their standard apparent magnitudes. Natural system external atmosphere magnitudes were calculated for each calibration star and a color transformation was determined from these. Then the values for the constant K for each scan were determined by forcing the above equation to give the external atmosphere natural system magnitude for the calibration star in the scan. Note that by using the external atmosphere magnitude of the
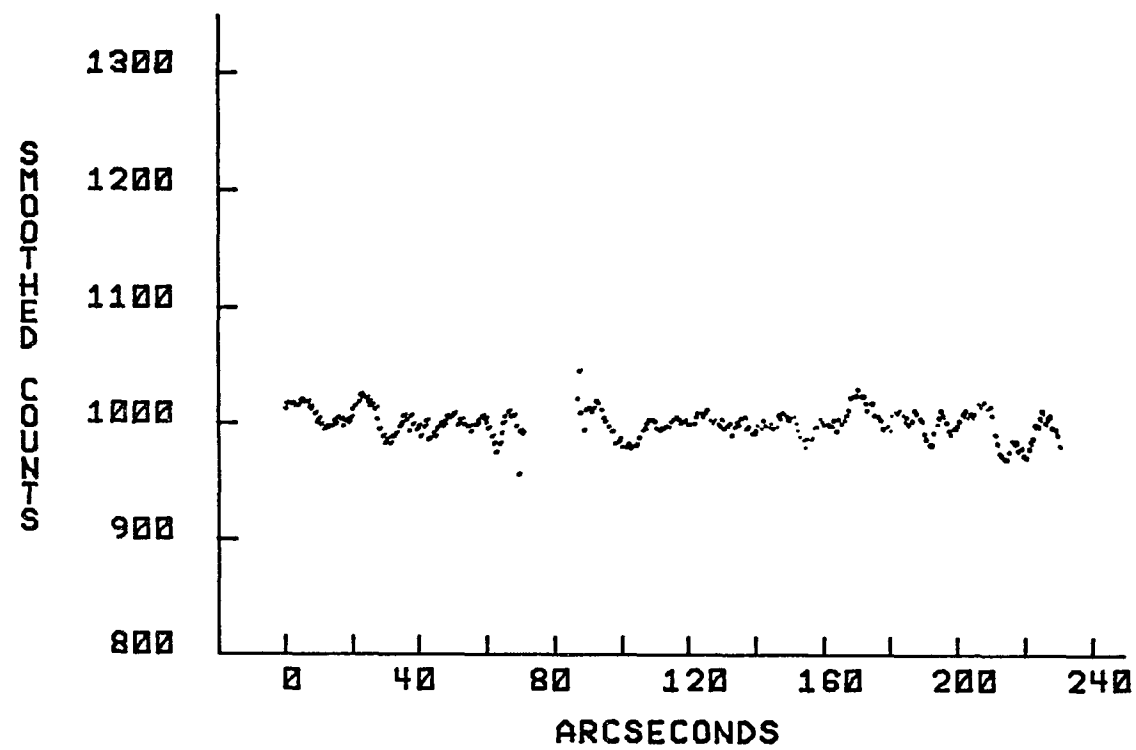
Figure 28. Smoothed synthetic data.

star this method also corrects for the effects of extinction. As long as the observations are not made at large airmasses color effects in this process will not be significant (no scan was taken at an airmass larger than 1.55 airmasses). In fact, since the star is calibrated it does not matter how long the integration time is or whether light clouds were present during the observation.

Once the data are in the form of natural system magnitudes, prominent features (such as the calibration star profile) are used to determine the necessary shift (usually 1 or 2 points) necessary to put the two scans in a B and V pair into proper registration. They are then subtracted producing natural system colors. Knowing the transformation coefficient and the standard color of the calibration star, the color of the galaxy is obtained relative to the color of the calibration star.

The plotted and tabulated colors to be discussed below are corrected for redshift effects and galactic absorption. The former is derived from the results of de Vaucouleur (1961) who found the correction in B-V due to redshift to be

$$\Delta(B-V) = 1.25 \times 10^{-5} \, v$$

The galactic absorption was estimated using the method of Sandage (1972). It is taken to be zero above galactic latitude 50 degrees. All of these corrections are summarized in Table 3. Since these are morphologically peculiar systems no attempt to correct the color for tilt effects has been made.

To summarize, the observing and reduction process consists of the following steps.

Table 3. Photometric Corrections.

Object	Gal. Lat.	Gal. Abs. Correction	Redshift km/sec	Redshift Correction
NGC 2648	32.5°	0.05	?	0.05 ?
NGC 4676	86.7°	0.00	6550	0.079
Arp 174	53.7°	0.00	?	0.05 ?

1. Observe the galaxies using a slit position which includes a calibration star and some clear sky area.

2. Obtain a relative diode to diode calibration from observing the twilight sky and use it to correct the counts from each diode to that which would have been observed if all the diodes were exactly identical.

3. Smooth the data to better allow determining the sky level, and subtract the sky level from the counts.

4. Using the known natural system magnitudes for the calibration star calibrate each scan by determining K in the expression

$$\text{Known mag.} = K = 2.5 \, \text{Log(peak star counts)}.$$

Apply this to the rest of the scan thus obtaining the luminosity of the galaxy in natural system magnitudes per unit area on the sky.

5. Shift the B and V pair of scans until they are in registration and subtract them producing natural system color.

6. Using the known standard colors of the calibration objects and the digicon's transformation coefficient, determine the color of the galaxy relative to the calibration star.

7. Corrections for redshift reddening and galactic absorption are then applied to the apparent colors.

Calibration Photometry

The three pairs of interacting galaxies which were observed had a total of 5 calibration objects which required conventional stellar photometry. Unfortunately, only one usable night's observing time was available and that with light cirrus clouds present. Fortunately

however, the photometer which was used is a high speed computer con-
trolled instrument. This allows for alternate star/sky measures about
10 times per second and changing from one filter to the next in one or
two seconds. With such an instrument it is possible to obtain good
color data under poor observing conditions, although apparent magnitudes
are of course unmeasurable. (This has since been verified by other
observers.) The observing program was altered to move as rapidly as
possible from one color to the next and as many faint standards as pos-
sible were measured; a good linear color transformation curve would
indicate reliable data. The B-V transformation obtained from the
night's observations is shown in Figure 29 and is very encouraging.

The slope of the digicon's transformation relation was calculat-
ed by using the integration time of the scans to determine a natural
system magnitude for the calibration stars. The natural system colors
derived from these yielded the slope of the transformation relation.
This process can only be applied to about 40% of the data (one night's
observations) and this produces only 3 points with which to determine
the transformation. The 3 points define a straight line with virtually
no scatter and give a slope of 0.933. Every possible comparison with
objects observed on the other two nights has been made and no systematic
difference can be found. In other words, the standard colors of the
same galaxies measured on the other two nights show no systematic devia-
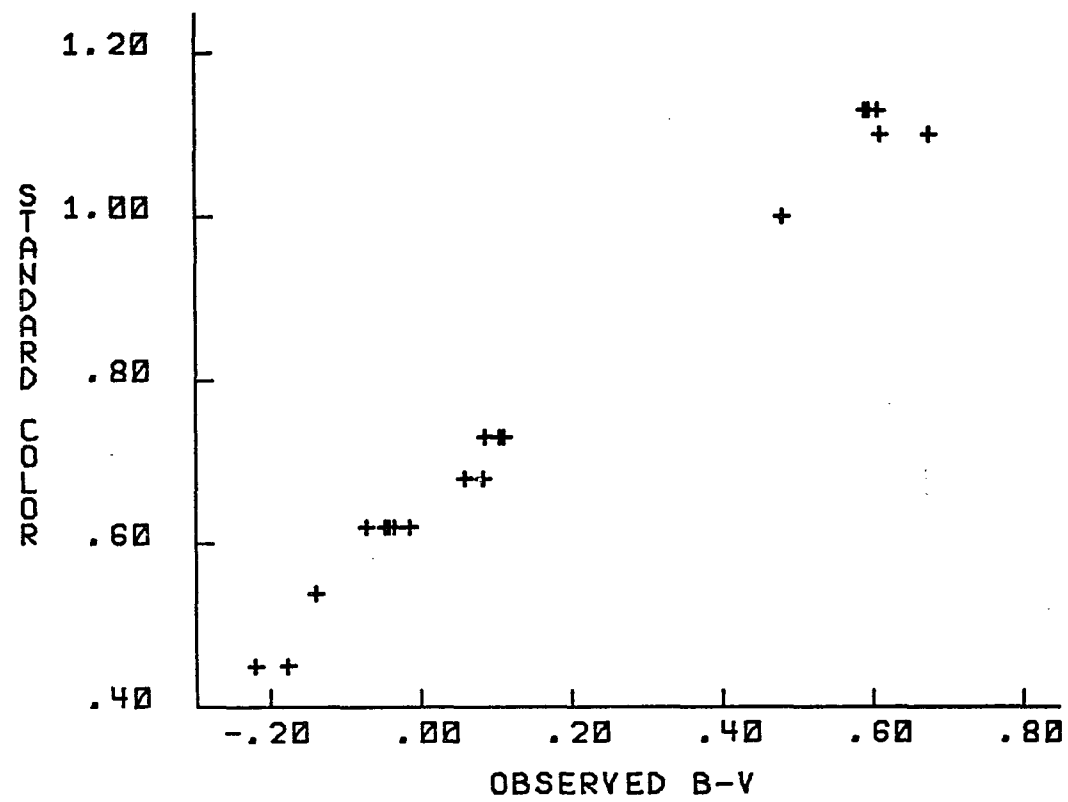tion from the slope of 0.933. The colors of the calibration objects are
listed in Table 5.

Figure 29. Transformation curve for calibration photometry.

The Interacting Galaxies

The systems observed are shown in Figures 30 to 32. NGC 2648 (Arp 89) was selected because it is fairly bright and it shows both a bridge and a tail. While the interaction is obvious, it is not terribly extreme. The primary is a fairly normal looking Sb galaxy showing the distortion of interaction primarily in the two spiral arms at the edge of its disk, one of which seems to connect it to its companion. The elongated form of the companion suggests that it has planar symmetry and is seen edge-on. Dust is clearly visible in good photographs. Short exposure photographs and digicon scans show it to have a small bright nucleus. Long exposure photographs show the very faint tail being several times longer than the main body of the companion.

NGC 4676 (Arp 242) was chosen because it is one of the best known interacting systems and shows some remarkably bright features. It has been modeled by Toomre and Toomre (1972) and observed spectroscopically as was recounted in chapter I. When viewed through the telescope the eastern galaxy shows a distinct nucleus while the western member has a granular appearance showing no prominent nucleus. Both members show tails, one very narrow and bright, the other broad, diffuse and enormously long. The extent of this tail is 8 or 10 times the size of its primary. The northern galaxy shows a great deal of dust, while the other member shows little morphological structure.

Arp 174 was chosen because it shows a very large faint plume, yet evidently neither galaxy is a spiral. This is very interesting because it is difficult to see how a system with no planar symmetry could produce a tail by the mechanism described in chapter II. The nuclei of
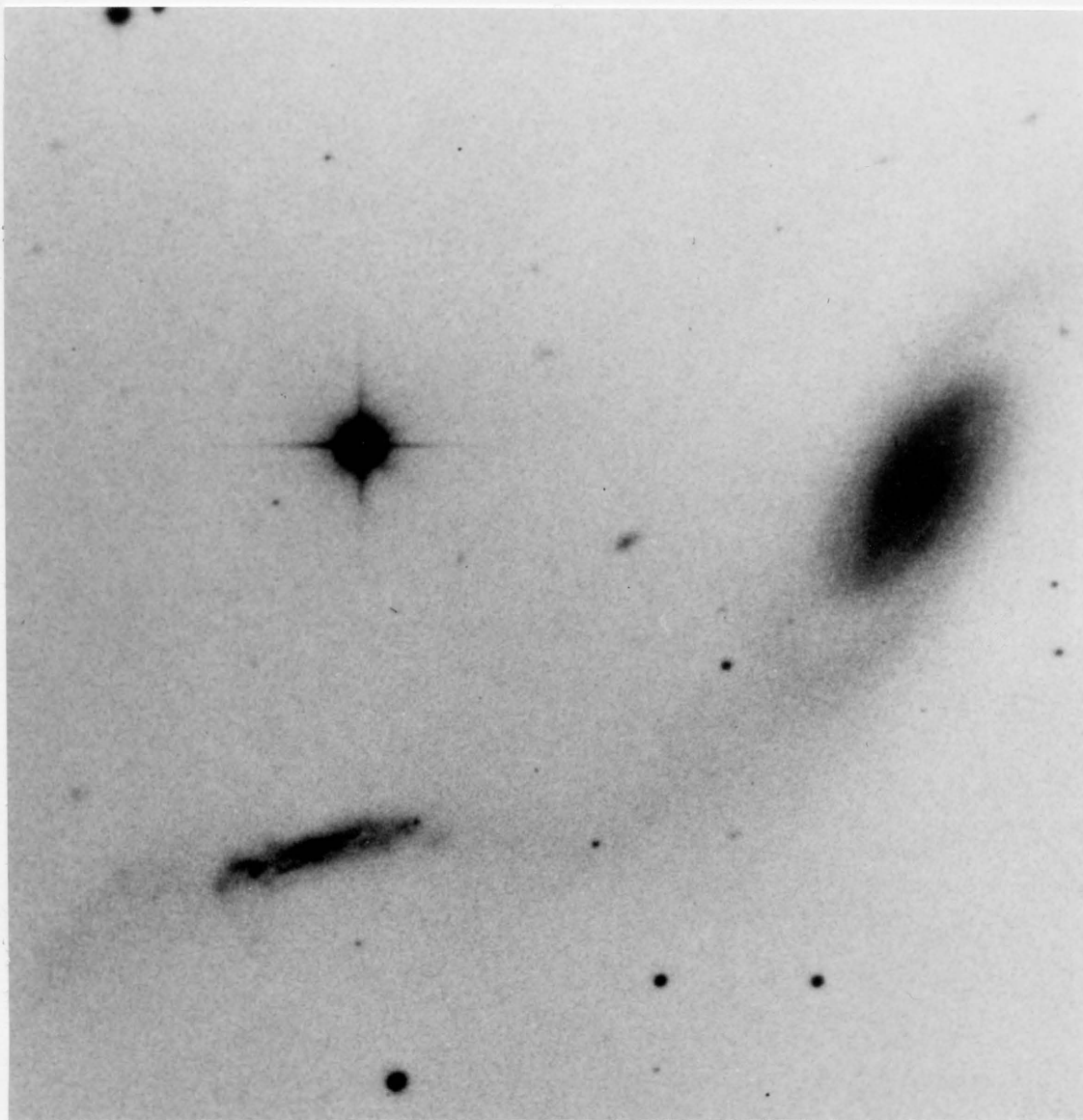
Figure 30. NGC 2648.
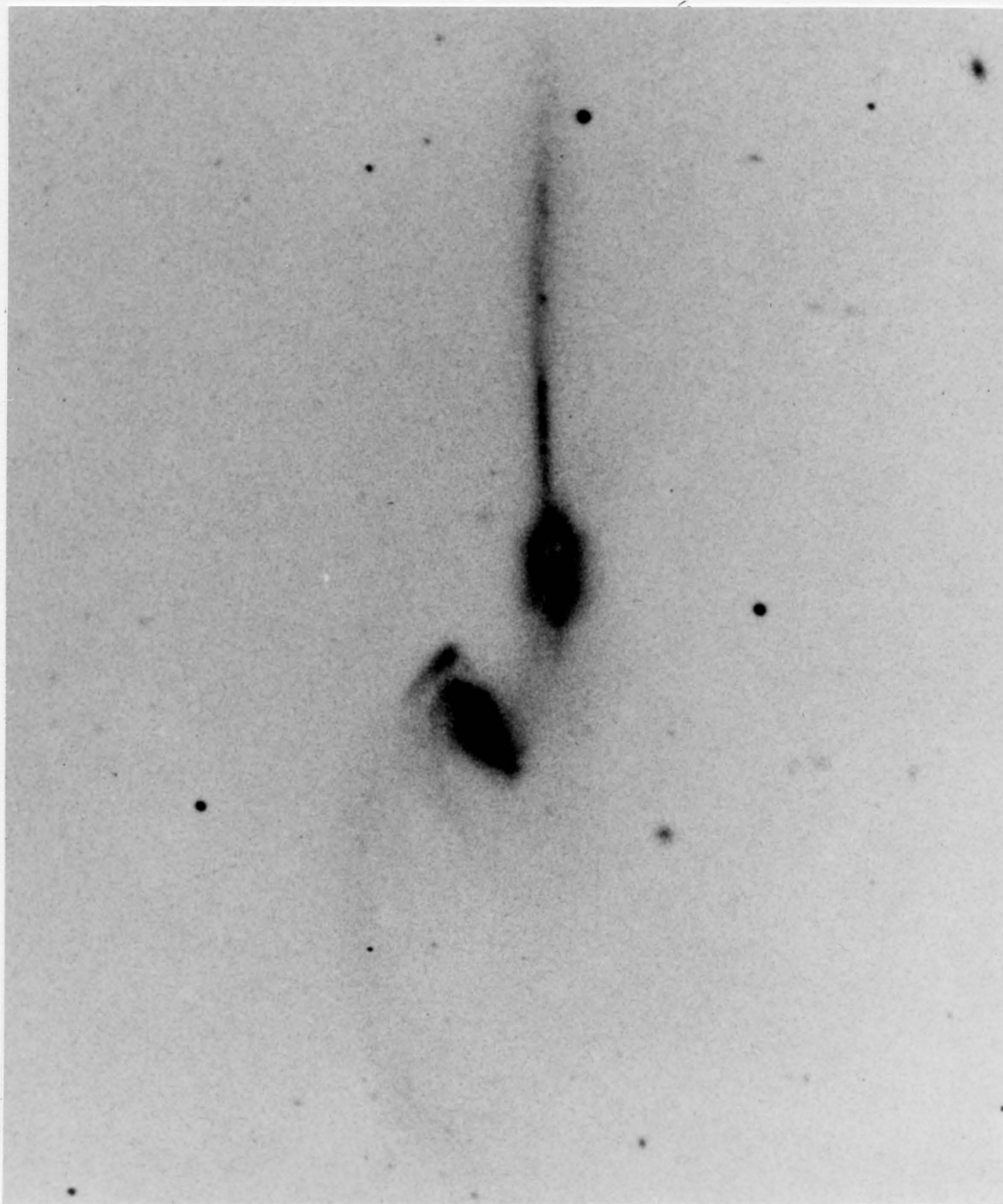
North is up. From Arp (1966).

Figure 31. NGC 4676 (Arp 242).
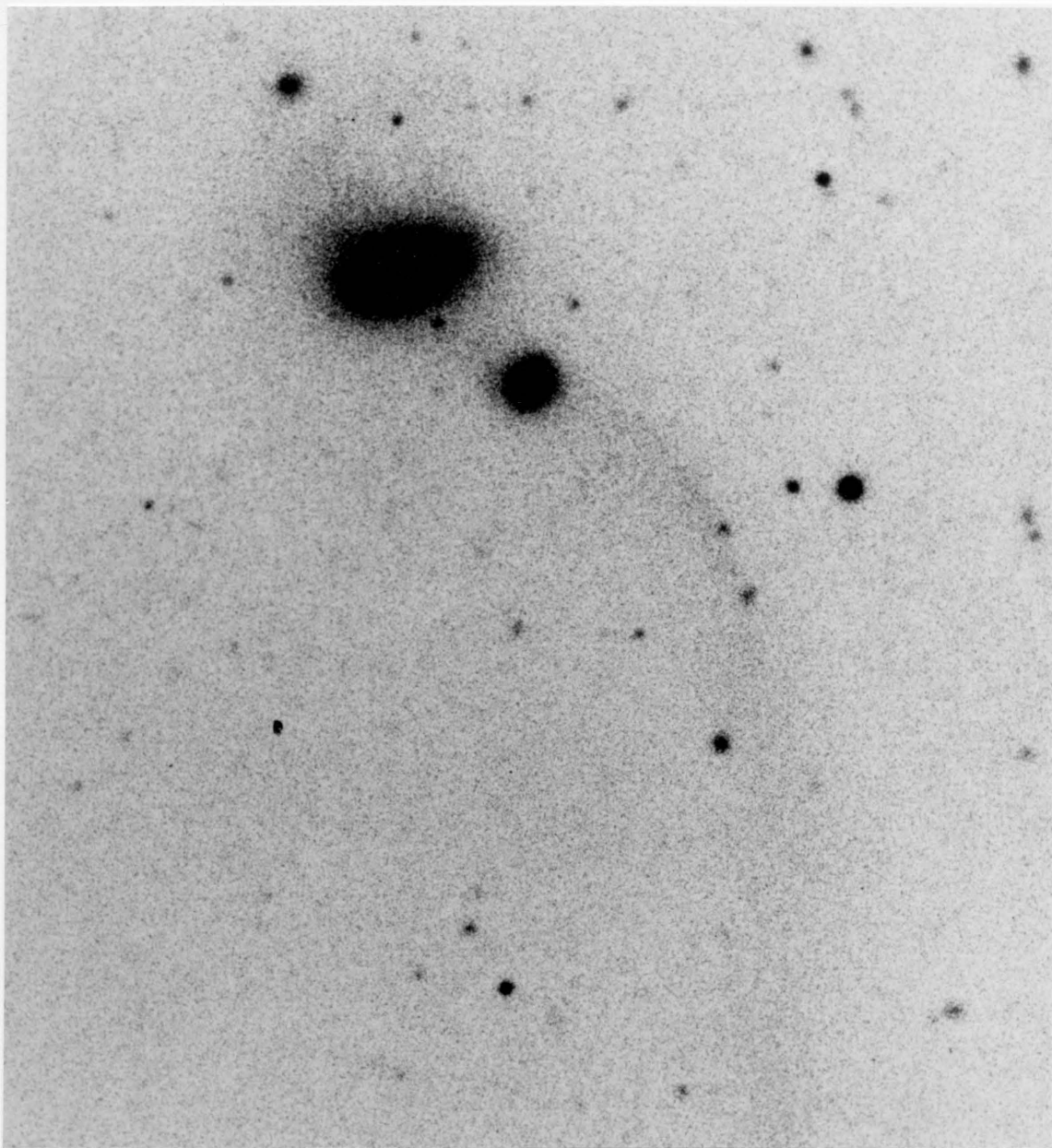
North is up. From Arp (1966).

Figure 32. Arp 174.

North is up. From Arp (1966).

the two galaxies are rather bright and provide good color calibration. The photograph of this system in Arp's Atlas shows faint patches of luminosity east of the larger galaxy.

The sketches in Figures 33 to 35 identify all the slit positions used and all the calibration objects. The exact position angles are listed in Table 4 and the apparent colors of the calibration objects in Table 5. Figure 34 shows a bifurcation of the faint tail of the southern galaxy. This is just barely visible in good photographs and is not shown in Stockton's (1974) sketch of this system. The digicon scans taken along slit position E clearly show 3 maxima however, so this tail is a bit larger than was previously thought.

Scans taken at slit position A used the bright stellar nucleus of the galaxy as a calibration object. Its color was determined from the scans taken at slit position C. Similarly, scans made at slit position F were calibrated by slit position G. The nuclei of the Arp 174 system were measured directly with the stellar photometer.

Results of the Observations

In all the data discussed below the errors quoted are random errors derived from the square root of the counts. Errors quoted for colors are derived from the square root of the sum of the squares for the blue and the visual scans.

Analysis of the raw data shows that the random error of a single measure is evidently entirely accounted for by counting statistics. Significant systematic errors may be present. An obvious source of systematic errors is the photometry of the calibration objects. This is

Table 4. Identification of slit positions.

Object	Slit Position	Slit Position Angle (degrees)	Calibration Object	Number of Scan Pairs
NGC 2648	A	105	Nucleus	1
NGC 2648	B	75	Star No. 1	2
NGC 2648	C	21	Star No. 1	1
NGC 2648	D	138	Star No. 1	1
NGC 4676	E	51	Star No. 2	1
NGC 4676	F	4	Scan G	1
NGC 4676	G	45	Star No. 3	2
Arp 174	H	51	Nuclei	1

Table 5. Colors of calibration objects.

Object	Standard B–V
Star No. 1	1.10 ± .06
Star No. 2	0.98 ± .05
Star No. 3	1.46 ± .08
Nucleus	0.85 ± .04
Arp 174A Nucleus	1.53 ± .02
Arp 174B Nucleus	1.42 ± .03
Scan G	1.14 ± .1

Figure 33. Sketch of NGC 2648.

The lines indicate the slit positions used. Star number 1 served as the calibration object in this system.
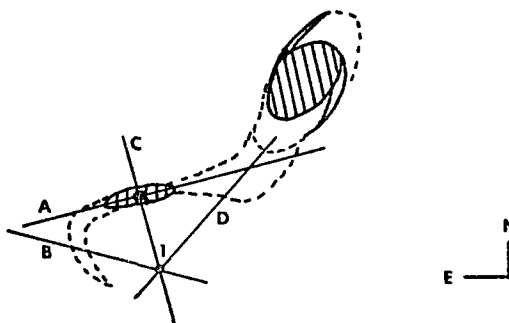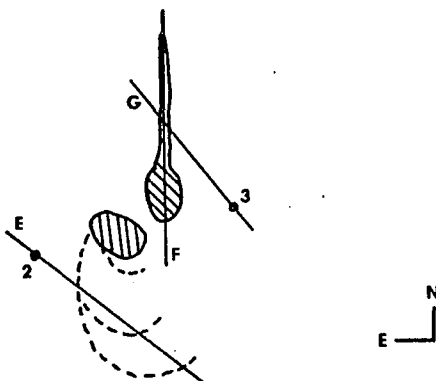

Figure 34. Sketch of NGC 4676.

The lines indicate the slit positions used. Star numbers 2 and 3 are the calibration objects for this system.
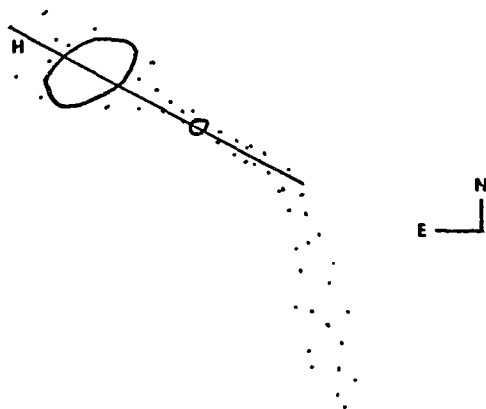
Figure 35. Sketch of Arp 174.

The line indicates the slit position used. The nuclei of the two galaxies served as the calibration objects.

probably not serious since they are generally bright (except for star number 2). Further, it affects all scans using that calibration object in the same way so that relative colors are not affected. Guiding errors and poor seeing are a more serious source of systematic error because they can disturb the measurement of the calibration star differently than they do the diffuse image of the galaxy. Their effects are also variable from scan to scan. Guiding errors in the direction along the slit would be seen as a flattening (blurring) of the star profiles. No such effects were observed. Guiding errors perpendicular to the slit will not affect the profile of the star as much and cannot be detected so easily.

The photometry of NGC 2648 is best represented by Figure 36 which shows the color along the length of the small companion (slit position A). Table 6 summarizes the colors in this system. The larger variations seen in Figure 36 are probably real. Scans taken at slit position B (very faint part of the tail) have a signal level about equal to the noise and are extremely uncertain. Considering this their agreement with the color in the brighter part of the tail is surprising. The measurement of the nucleus of the companion is the most certain one since the nucleus is so bright. It is interesting that scans A and D overlap at a point between the two galaxies. At the point in common scan D shows a color of about 1.3 and scan A shows a color of about 1.0. The expected random errors are large enough to account for perhaps half of this discrepancy. One would expect some disagreement since scan A uses a secondary calibration object, yet the difference is still difficult to explain. It is likely that scan D has suffered some sort of

Figure 36. B-V color in NGC 2648.

Standard B-V color corrected for redshift and galactic absorption. This data was taken
with slit position A. The vertical lines drawn through each point indicate the random
errors. Region 1 is the beginning of the faint tail – its brightest portion, region 2
is the main body of the galaxy, and region 3 is the bridge. The dot in region 2
indicates the position of the nucleus. Only points with random errors smaller than
0.15 in B-V are shown here.
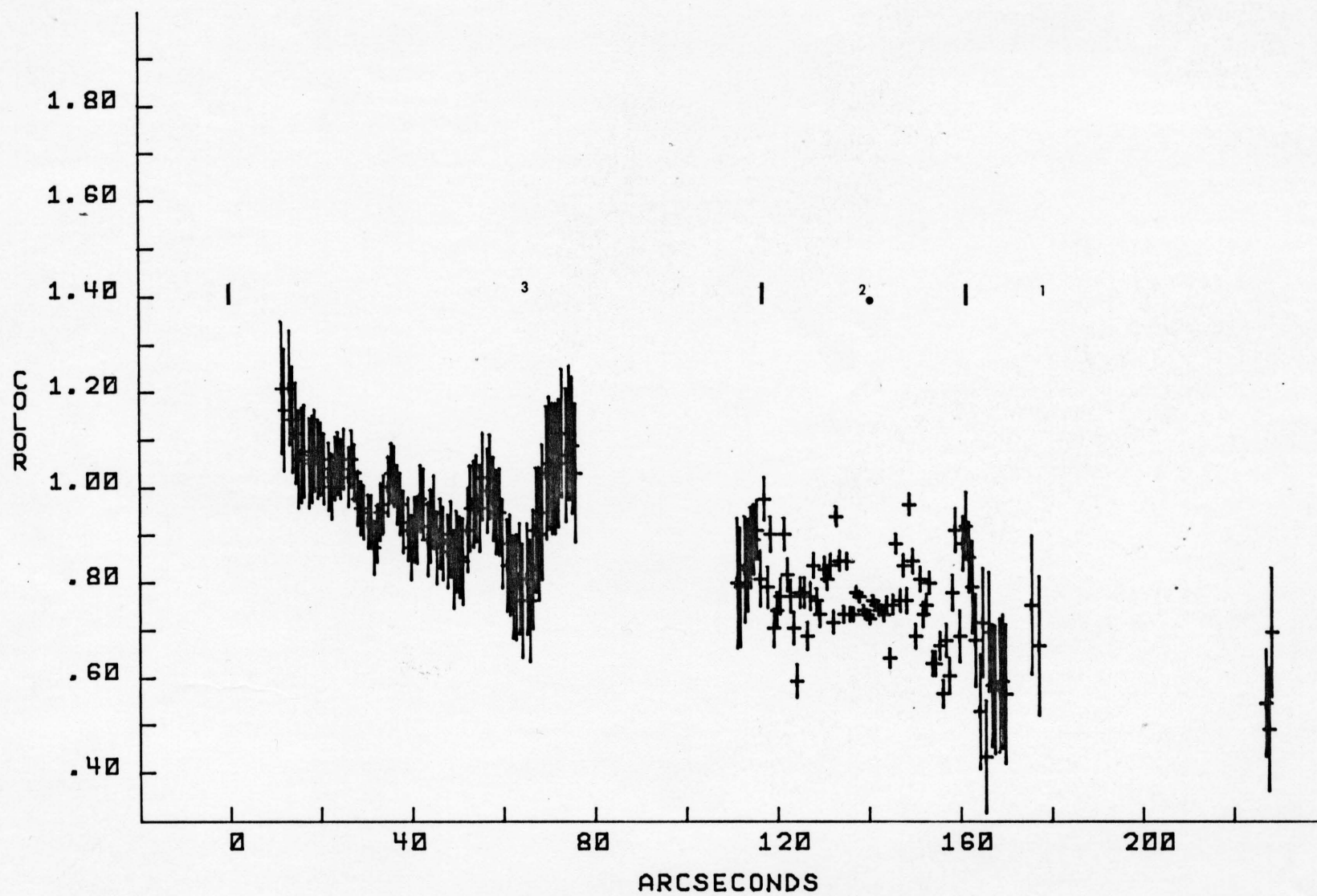
Figure 36.   B-V color in NGC 2648.

Table 6.   Mean colors in NGC 2648.

Area	Slit Position	Average B-V
Nucleus	C	0.75 ± .04
Along Companion	A	0.77 ± .02
Bridge	D	1.34 ± .04
Faint Tail	B	0.77 ± .56
	B	1.06 ± .47
Tail	A	0.70 ± .09

minor calibration error amounting to about 0.15 magnitudes. Poor seeing or guiding could account for this.

The integrated color of the main body of the companion is normal for an Sab or Sb galaxy (even allowing 0.1 mag for tilt correction), however there are some abnormalities here.

1. The nucleus of the companion is rather blue, especially considering that it is seen edge-on and that there is obviously dust present. Typical colors for the nuclei of spirals are about 1.0 in B-V, rarely redder. The latest types may be this blue however.

2. The outer parts of normal spirals are bluer than the inner parts by several tenths, yet the companion has a rather flat color profile.

3. The outer parts of the large spiral are surprisingly red. Even if there are substantial absolute calibration errors in this data it is clear that the bridge and the outer parts of the large spiral are at least 0.2 magnitude redder than the nucleus of the companion.

The photometry of NGC 4676 is summarized in Table 7. Figure 37 shows scan F along the western galaxy, the one with the very bright tail. This scan was calibrated by scan G which had a random error of about 0.06 determined from 2 separate scans. The very red color of all the features in Figure 37 is presumably due to the large amounts of dust present and the fact that the tail is probably an elongated disk seen edge-on. This profile is normal in the sense that the nucleus is the reddest feature. There are two bright spots in the disk of this galaxy. The one which is marked as the nucleus is the one which is centrally located. It is also the redder of the two. The variations in color in the faint part of the tail are probably real since they are significantly

larger than the random errors. The value of 0.92 ± .27 listed in Table 7 for the faint tail refers only to its brightest portion and represents an average over 56 points. This is an extremely faint feature. The two other points where the slit crossed the tails have very large uncertainties, yet fortuitously are within 0.15 of the 0.92 value.

The digicon scans of Arp 174 are unfortunately not very useful as far as faint features are concerned because it is extremely difficult to set a sky level for them. The extent of the faint parts of this system is evidently considerably larger than the photograph implies. Little can be said except about the brighter parts. The calibration photometry done with the stellar photometry (with a 12 arcsecond diaphragm) shows the nucleus of the larger galaxy to have an apparent B-V of 1.53 and the smaller one to be 1.42. These colors are unusually red but it is unlikely that they are seriously in error. Both galaxies are roughly 15th magnitude or brighter. The standard stars observed on the same night went from 10th to 15th magnitude and the transformation (Figure 29) looks rather good. Only two measures of each galaxy were made, but each pair agrees within 0.04 magnitude. Furthermore, the digicon scans which constitute a completely independent measure of the color difference between the two galaxies, verify that it is 0.10 in B-V.

Galactic absorption is negligible for this system and a redshift correction would not account for a significant part of the anomaly. Neither ellipticals nor spirals are observed to have colors redder than about 1.0 and most ellipticals are about 0.9 at their nucleus. About all that can be said about the color profile of this system is that in the larger galaxy the color becomes bluer further from the nucleus. It

Figure 37. B-V color in NGC 4676.

Standard B-V color corrected for redshift and galactic absorption. This data was taken
at slit position F. Region 2 is the disk of the galaxy, region 3 is the bright portion
of the northern tail (see Figure 35). Region 1 contains the faint material south of the
galaxy. The dot in region 2 indicates the presumed position of the nucleus. Only
points with random error less than 0.15 in B-V are shown here.
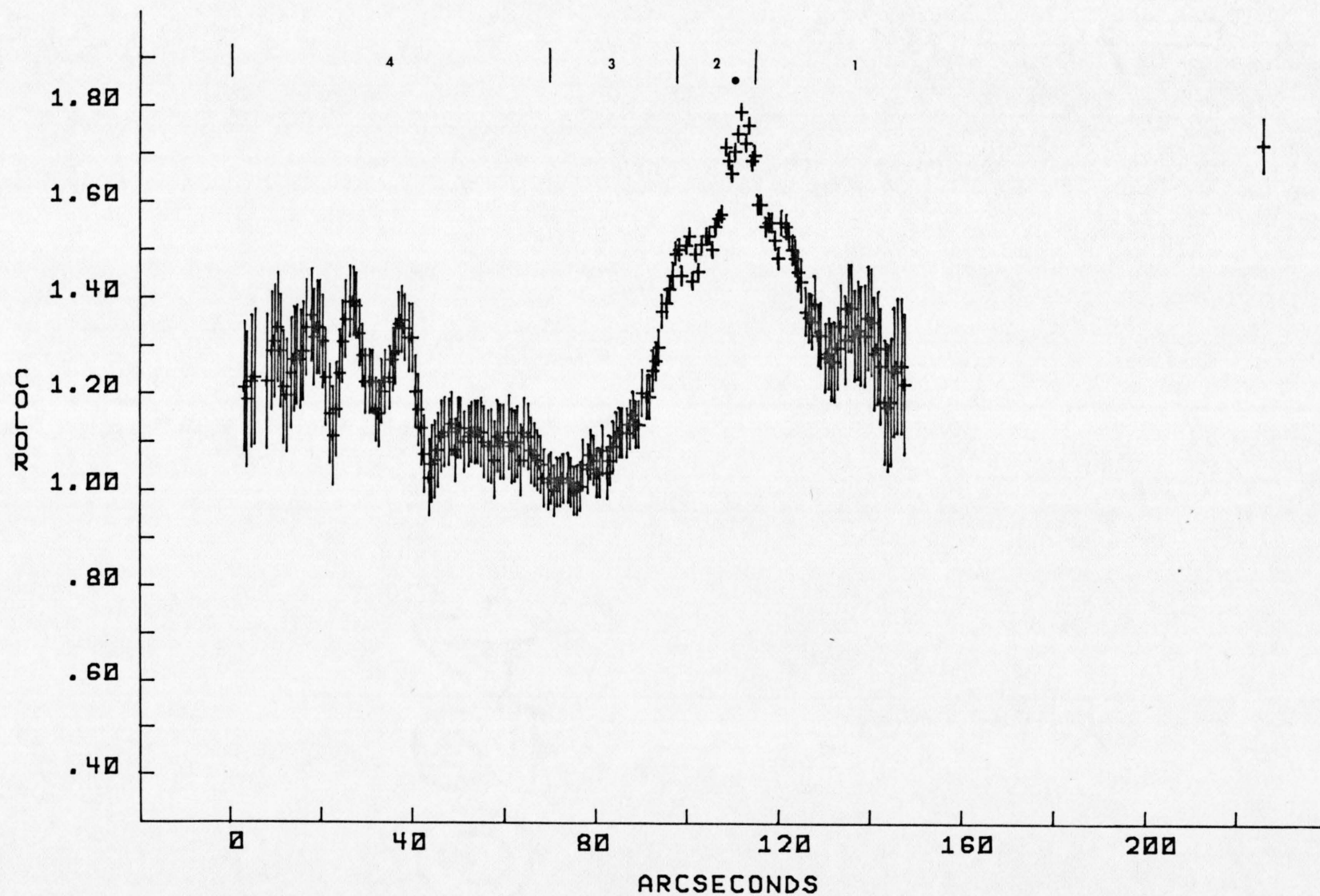
Figure 37.   B-V color in NGC 4676.

Table 7. Mean Colors in NGC 4676.

Area (Figure 38)	Slit Position	Mean Color
Region 3 (tail)	F	1.11 ± .05
Region 1	F	1.28 ± .12
Region 4 (tail)	E	0.92 ± .27

appears to be 0.3 or 0.4 bluer than the nucleus at a point some 20 arc-seconds east of the galaxy. The smaller galaxy has a nearly stellar profile and nothing can be said about the color in its outer parts.

It is interesting to note Sandage's (1963) photometry of VV117 and VV123. Each of these interacting systems appears to be an elliptical with a very badly disrupted spiral or irregular companion. In each case the elliptical's nuclear region has B-V of about 0.9 to 1.03. The nuclei of the "spiral" components have B-V of 0.81 in one case and 0.45 in the other. These two systems have many HII regions clearly visible and show much more severe interaction than the 3 systems observed here. The digicon photometry of Arp 295 done by Beaver, Harms, Tifft, and Sargent (1974) found the very faint narrow bridge in that system to have a B-V of 1.0, which is more in agreement with these results.

The next chapter will discuss the possible interpretations of these observations and their impact on the modeling of chapter II.

CHAPTER IV

CONCLUSIONS

This chapter offers some brief interpretation of the results described in the preceeding two chapters. Some suggested observations and their anticipated results are given. Since the foregoing chapters have neglected any discussion of the interstellar medium, some discussion of that subject is also in order here.

The Interstellar Medium

The behavior of the interstellar medium in the course of the interaction is probably important in determining the observable features of a system. The most important question is whether the formation of large numbers of stars can be stimulated in this way. The models in chapter II can give only a very general indication of the behavior of the interstellar medium because of the complete absence of viscosity or inelasticity in those models. They imply that most of the disturbance suffered by the interstellar material will be smooth flow resulting in continuous compression or expansion of the gas rather than inducing much mixing or "head on" collisions, maximum compression occuring around perigalacticon. However, some models, especially the 1/4 mass models, show some outer orbits being distorted into a figure eight, so some high speed collisions may occur.

Assuming the interstellar medium has a density of one hydrogen atom per cubic centimeter it is obvious that the mean free path of a

hydrogen atom cannot exceed a tiny fraction of the cloud dimension (less than 0.0001 pc). If two clouds collide at a relative velocity of only 5 km/sec, which the point mass models indicate is not at all unlikely, then it is clear that the collision will be completely inelastic and that much of the energy will be thermalized. If the initial temperature is 10° K, then the atomic velocity is only 0.5 km/sec so the collision energy is the dominant component. If all the kinetic energy were converted uniformly to heat the resulting temperature would be 1000° K (for a 16 km/sec collision this value is 10,000° K). But this is a great oversimplification. The collision would be an asymmetric non-equilibrium process possibly producing locally very high densities. The mean free path at the interface would decrease rapidly with time as the density increases. The temperature depends on the efficiency of the radiative mechanisms which are present to radiate the heat of compression away during the 10^8 to 10^9 year time scale of the collision. If the temperature rises too quickly the cloud will not collapse. These cooling mechanisms are the subject of some speculation by those who compute models for protostar formation. McCrea (1957) and Larson (1969, 1974) and others have studied the gravitational collapse of a cold interstellar cloud. These models require an initial density of at least 10 hydrogen atoms/cm, a temperature of from 10° K to something less than 100° K, that all the hydrogen present be in molecular form, and of course there is a critical relationship between density and temperature which must be met if contraction of the nebula is to be possible. They show that the dust component of the interstellar medium can be effective in absorbing the kinetic energy of the compressing gas and radiating it

away from the cloud. This can be so effective that the cold initial temperature of the cloud can be preserved everywhere (except at the very core) for a very long time despite the contraction at a free fall rate. It is surely possible that stellar formation on a large scale could result during the gravitational interaction, but the question of how likely that is must await a careful modeling of the interstellar medium in such an encounter. This is a very difficult problem.

What would one expect to observe spectrographically and photometrically if there was much star formation within a short period of time? This depends on the time at which the system is observed and on the mass spectrum of the stars which are produced in this (presumably) abnormal method of star formation. Stockton's (1974) spectroscopy of NGC 4676 showed the composite spectrum of the bright tail in this system to be predominantly that of an A star. The Balmer series was seen in absorption down to H11. Stockton comments that a period of wide spread star formation some 5×10^7 years ago would account for this. The models in chapter II indicate that this system is being viewed some 6×10^8 years after perigalacticon. The disagreement in time scales here is not really so large as it seems. The time scale of the model can be changed quite a bit by altering initial conditions and one could call the dominant spectral type late A and early F in order to bring the time scales into better accord. Invoking an abnormal mass spectrum for the stars would also help. In any case it is probably significant that there is a dominant stellar type and that it is more prominent than in normal spiral galaxies.

It is interesting that Stockton reported no features of G or K giants even though his spectra extended to 6500 Å. These stars are evidently not important contributors to the luminosity, although they are in normal spiral galaxies. If there were many evolved massive stars, one would expect a prominent red giant contribution. The stellar population must not be old enough for late A and F stars to have evolved this far.

It is possible that there is some selection effect present in the predominant stellar type observed for a given interacting system. If gravitational interaction does stimulate star formation, then it is unlikely that one would find a strongly interacting galaxy with an extremely young population because the period of maximum shock to the interstellar medium occurs near perigalacticon and at that time the galaxies are often not recognizable (morphologically) as interacting galaxies but more likely as one peculiar galaxy. The models of chapter II were dealt with as end results and the course of a single model interaction over 10^9 years was not detailed (see Toomre and Toomre, 1972). If it had been however, it would have been seen that virtually every model shows enormous confusion at perigalacticon and only a few hundred million years later develops fine structure. So there may be a selection effect present which would make A and F type composite spectra predominate in strongly interacting galaxies. Obtaining low dispersion spectra of the filamentary structures in 5 or 6 systems might considerably strengthen the case for induced star formation in strongly interacting systems.

Photometry

The spectra of NGC 4676 indicate an A star spectrum yet the photometry for this galaxy (and for the other two systems as well) reported in chapter III showed anomalously red colors in at least some regions. Given the spectroscopic evidence for NGC 4676 the only likely explanation is that large amounts of dust are causing considerable reddening. If the major portion of the light comes from A and F stars, then the reddening in the tail is more than one magnitude. Since this tail is probably being seen edge-on, it is plausible that there may be a dust lane at its edge which is roughly one kpc thick and has 2 or 3 times more dust than is the mean in the Milky Way. Photographs show a great deal of dust present and Stockton (1974) reports what he assumes are interstellar H and K lines, so this is a plausible explanation.

It is interesting to note that M82, generally regarded as an exploding galaxy, is similar spectrographically and photometrically to NGC 4676. It is a very dusty system with an integrated color of $B - V = 0.91$ and an integrated spectral type of A5. Perhaps much of the interstellar medium in M82 has experienced some sort of disturbance similar to that found in interacting galaxies.

The NGC 2648 system shows rather red colors in the bridge and disk of the larger galaxy. The small companion is a relatively normal color (except possibly for the nucleus). Dust is clearly visible in the companion. In the bridge and disk the surface brightness is so low that it is difficult to judge the presence of dust from a photograph. The digicon scans suggest the presence of dust lanes defining spiral

structure in the outer parts of the companion however. It is reasonable to ascribe the color here to dust reddening also.

The very red nuclear colors found for the Arp 174 system are quite difficult to explain. Neither spirals nor ellipticals are known to have colors as red as 1.42 (for Arp 174b) or 1.53 (for Arp 174a) in their nuclei. These galaxies are apparently ellipticals, although the primary is a bit irregular in outline and shows very faint patches of luminosity around its perimeter. The companion is quite compact. The U-B colors of these two galaxies were also measured with the stellar photometer as 0.40 (Arp 174b) and 0.55 (Arp 174a). These are less certain than the B-V measures because the U-B transformation for that night is not as good as that for the B-V. Allowing a tenth or so error in U-B and assuming no reddening at all, these colors agree with those reported by Becker (1963) for Population II stars in globular clusters. It is impossible to draw any real conclusions from such meager evidence, however.

These photometric results are extremely intriguing but are badly in need of confirming observations. It is plausible that NGC 4676 and NGC 2648 are coincidentally dusty systems and that the fact that they show interaction is completely unrelated to any reddening which is present. However, it is inviting to speculate that the interaction somehow affects the interstellar medium so as to produce dust in great quantities. It is encouraging that Beaver et al. (1974) found a B-V of 1.0 for the long narrow filament in Arp 295. Photometry and spectroscopy on only a few other similar systems would be sufficient to substantiate these unusual colors as a normal part of the interaction

phenomenon. It would be especially interesting to, on the basis of the evolution of the simulations, attempt to select systems which appear to be at perigalacticon for observation. This would shed light on the question of star formation as a result of interaction.

The detailed results of the models are summarized in chapter II and need not be recounted here. This interpretation of the results is offered. The results of the simulations done here and elsewhere are very strong circumstantial evidence that this simple gravitational model is indeed the explanation of the appearance of interacting galaxies. The general modeling scheme as described in the literature to date has withstood withdrawal of some of its very idealistic features very well. Clutton-Brock (1972) has demonstrated that velocity dispersions a few times those observed in the solar neighborhood are completely destructive of fine structure. This work has shown that typical velocity dispersions do not produce serious observable morphological damage (except in the case of true bridges) and have virtually no detectable effect on photometry of those fine structures. This derives from the result that only those stars significantly more energetic than the mean are significantly dispersed, while those less energetic than the mean are not. Finally, there is evidently some quantitative value in trying to model certain particular systems as is shown by the NGC 4676 models.

The next step in the theory of interacting galaxies is the treatment of the interstellar medium. This would surely suggest processes whose observation is within the grasp of modern photon counting devices such as the digicon. With the advent of computer modeling and

this new instrumentation this subject, which for so long was handled

only with conjecture and supposition, can now be approached

quantitatively.

LIST OF REFERENCES

Alladin, S. M., 1965, Ap. J., <u>141</u>, 768.

Allen, R. J., Ekers, R. D., Burke, B. F., and Miley, G. K., 1973, Nature, <u>241</u>, 260.

Ambartsumian, V. A., 1958, Solvay Conference Report, Brussels, 241.

Arp, H. C., 1962, Ap. J., <u>136</u>, 1148.

Arp, H. C., 1966, Atlas of Peculiar Galaxies, Pasadena, California Institute of Technology.

Arp, H. C., 1970a, Nature, <u>225</u>, 1033.

Arp, H. C., 1970b, Ap. J. Lett., <u>5</u>, 257.

Arp, H. C., 1971, Nature Phys. Sci., <u>231</u>, 103.

Beaver, E. A., Harms, R. J., Tifft, W. G., and Sargent, T. A., 1974, P.A.S.P., <u>86</u>, 639.

Beaver, E. A., and McIlwain, C., 1971, Rev. Sci. Inst., <u>42</u>, 1321.

Becker, W., 1963, Basic Astronomical Data, Ed. K. Strand, University of Chicago Press.

Bottinelli, L., and Gouguenheim, I., 1973, A. Ap., <u>26</u>, 85.

Burbidge, E. M., and Burbidge, G. R., 1961, Ap. J., <u>133</u>, 726.

Burbidge, E. M., and Burbidge, G. R., 1963, Ap. J., <u>138</u>, 1306.

Burbidge, E. M., and Burbidge, G. R., 1964, Ap. J., <u>140</u>, 1617.

Burbidge, E. M., and Sargent, W. L. W., 1971, Nuclei of Galaxies Conference, Ed. O. Connel, 351.

Chandrasekhar, S., 1948, Principles of Stellar Dynamics, Dover Pub.

Clutton-Brock, M., 1972, Ap. Space Sci., <u>17</u>, 292.

Contopoulos, G., and Bozis, G., 1964, Ap. J., <u>139</u>, 1239.

D'Ordico, S., 1970, Ap. J., <u>160</u>, 3.

Eenev, T. M., Kozlov, N. N., and Sunyaev, R. A., 1973, A. and Ap., 22, 41.

Faber, S. M., 1973, Ap. J., 179, 423.

Freeman, K. S., 1970, Ap. J., 160, 811.

Gorbachev, B. I., 1970, Sov. A. J., 14, no. 5, 781.

Graham, J. A., and Rubin, V. C., 1973, Ap. J., 183, 19.

Hardie, R. H., 1962, Astronomical Techniques, Ed. W. A. Hiltner, University of Chicago Press.

Hohl, F., 1971, Ap. Space Sci., 14, 91.

Holmberg, E., 1937, Ann. Obs. Lund, no. 6.

Holmberg, E., 1940, Ap. J., 92, 200.

Holmberg, E., 1956, Lund Medd. Ser. 1, nr. 186, 10.

Holmberg, E., 1958, Medd. Lund. Astr. Obs. II, no. 136.

Holmberg, E., 1962, I.A.U. Symp. No. 15, 187.

Holmberg, E., 1969, Uppsalla Astr. Obs. Medd. No. 166.

Hoyle, F., and Harwit, M., 1962, P.A.S.P., 74, 202.

Karachentsev, I. D., 1970, Sov. A. J., 14, 407.

Karachentsev, I. D., 1972, Catalogue of Pairs of Galaxies, Soobsch. Spec. Astrofiz. Obs. Acad. Nauk SSSR, 7, 3.

Karachentsev, I. D., 1974, Comm. Spec. Ap. Obs., no. 11.

King, I. R., 1972, A. J., 71, 64.

King, I. R., 1973, Ap. J., 181, 27.

King, I. R., and Kiser, J., 1973, Ap. J., 181, 27.

Larson, R. B., 1969, M.N.R.A.S., 145, 271.

Larson, R. B., 1974, M.N.R.A.S., 166, 585.

Lewis, B. M., 1971, Nature Phys. Sci., 230, 13.

McCrea, W. H., 1957, M.N.R.A.S., 117, 562.

McCuskey, S. W., 1965, Galactic Structure, Ed. A. Blaauw, University of Chicago Press.

Oort, J., 1928, B.A.N., no. 159, 269.

Oort, J., 1965, Galactic Structure, Ed. A. Blaauw, University of Chicago Press.

Ostriker, J. P., and Peebles, P. J. E., 1973, Ap. J., 186, 467.

Page, T., 1952, Ap. J., 116, 63.

Page, T., 1960, Ap. J., 132, 910.

Page, T., 1961, Fourth Berkeley Symp. Math. Prob. Stat., 3, 277.

Page, T., 1962, Ap. J., 136, 685.

Page, T., 1970, Ap. J., 159, 791.

Page, T., Dahn, C., and Morrison, F., 1961, A. J., 66, 614.

Pfliederer, J., 1963, Zeit. Fur Astrof., 58, 12.

Pfliederer, J., and Seidentopf, H., 1961, Zeit. Fur Astrof., 51, 201.

Purton, C. R., and Wright, A. E., 1972, M.N.R.A.S., 159, 150.

Roberts, M. S., and Warren, J. L., 1968, A. and Ap., 6, 165.

Rood, H. J., 1965, A. J., 70, 689.

Rubin, V. C., and Ford, W. K., 1968, Ap. J., 154, 431.

Rubin, V. C., Ford, W. K., and D'Ordico, S., 1970, Ap. J., 160, 801.

Sandage, A. R., 1963, Ap. J., 138, 863.

Sandage, A. R., 1972, 178, 1.

Sastry, K. S., and Alladin, S. M., 1970, A. Space Sci., 7, 261.

Schaefer, M. M., Lecar, M., and Rybicki, G., 1973, Ap. and Space Sci., 25, 357.

Stockton, A., 1974, Ap. J., 187, 219.

Tashpulatov, N., 1970, Sov. A. J., 13, 968.

Theys, J. C., Spiegel, E. A., and Toomre, J., 1972, P.A.S.P., 84, 851.

Toomre, A., 1964, Ap. J., 139, 1217.

Toomre, A., 1970, I.A.U. Symp. No. 38, Ed. W. Becker, 344, Reidel Pub.

Toomre, A., and Toomre, J., 1971, Bull. A.A.S., 3, 390.

Toomre, A., and Toomre, J., 1972, Ap. J., 178, 623.

Vaucouleurs, G. H. de, 1961, Ap. J. Suppl., 5, 233.

Vaucouleurs, G. H. de, and Vaucouleurs, A. de, 1964, Austin, University of Texas Press.

Vorontsov-Velyaminov, B. A., 1957, Sov. A. J., 2, 805.

Vorontsov-Velyaminov, B. A., 1959, Atlas and Catalogue of Interacting Galaxies, Moscow Govt. Ast. Inst. and Govt. University of Moscow.

Vorontsov-Velyaminov, B. A., 1960, Ann. D. Ap., 23, 379.

Vorontsov-Velyaminov, B. A., 1962, I.A.U. Symp. No. 15, Ed. G. C. McVittie.

Weistrop, D., 1972, A. J., 77, 849.

Wright, A. E., 1972, M.N.R.A.S., 157, 309.

Yabushita, S., 1971, M.N.R.A.S., 153, 97.

Zwicky, F., 1956, Ergeb. Der Exakt Naturwiss., 29, 344.

Zwicky, F., 1957, Morphological Astronomy, Berlin, Springer-Verlag.

Zwicky, F., and Humason, M. L., 1964, Ap. J., 139, 269.